(Semi) Leptonic rare decays of B mesons as probes of the Standard model and beyond

A thesis submitted in partial fulfilment of

the requirements for the degree of

Doctor of Philosophy

by

Bharti Kindra

(Roll No. 14330004)

Under the guidance of

Dr. Namit Mahajan

Professor

Theoretical Physics Division

Physical Research Laboratory, Ahmedabad, India.

DEPARTMENT OF PHYSICS

INDIAN INSTITUTE OF TECHNOLOGY GANDHINAGAR

2019

Declaration

I declare that this written submission represents my ideas in my own words and where others' ideas or words have been included, I have adequately cited and referenced the original sources. I also declare that I have adhered to all principles of academic honesty and integrity and have not misrepresented or fabricated or falsified any idea/data/fact/source in my submission. I understand that any violation of the above will be cause for disciplinary action by the Institute and can also evoke penal action from the sources which have thus not been properly cited or from whom proper permission has not been taken when needed.

(Signature)

(Name: Bharti Kindra)

(Roll No: 14330004)

Date: July 22, 2019

CERTIFICATE

It is certified that the work contained in the thesis titled **“ (Semi) Leptonic rare decays of B mesons as probes of the Standard model and beyond ”** by Ms. Bharti Kindra (Roll No. 14330004), has been carried out under my supervision and that this work has not been submitted elsewhere for a degree.

Prof. Namit Mahajan
Professor
Theoretical Physics Division,
Physical Research Laboratory,
Ahmedabad, India.

(Thesis Supervisor)

Date:

Acknowledgements

I would like to express my sincere gratitude to my supervisor Prof. Namit Mahajan for the constant support during my Ph.D. I am truly grateful for his willingness and effort to help me in academical as well as non-academical issues. I respect him for his vast knowledge on any subject of physics and life. I could not have imagined having a better advisor and mentor for my Ph.D. I am honored to have worked under his supervision.

I would also like to thank the rest of my DSC committee: Prof. Subhendra Mohanty and Prof. Hiranmaya Mishra for their insightful comments, encouragement, and guidance during the last four years. I am grateful to my collaborator Dr. Aiofe Bharucha for the discussions and providing me opportunity to discuss my work on an international platform. My sincere thanks also goes to other members of THEPH division Prof. Srubabati Goswami, Prof. Dilip Angom, Dr. Partha Konar, Dr. Navinder Singh, and Dr. Ketan Patel from whom I have learnt a lot.

I am also grateful to my colleague, collaborator, and friend Bhavesh Chauhan for countless stimulating discussions. I acknowledge the other two Coffee Club members Ashish and Priyank for their support, careful reading of this thesis, and for all the fun we have had over the years. I specially thank Aman and Balbeer for all the tea outings. I am also grateful to my other colleagues Kaustav, Soumik, Vishnu, and Akanksha for making my stay at PRL enjoyable. I thank my seniors and collaborators Dr. Girish Kumar and Dr. Diganta Das for useful discussions. A special thanks to my friends Naveen Kumar, Ankit Jivrajani, and Prakhar Kulshrestha for the moral and emotional support.

I reserve my most special gratitude for my family. Without their support and love, I would have been able to dedicate myself to physics.

Last but not the least, I would like to acknowledge the various departments of PRL administration for their help and support.

(Bharti Kindra)

Abstract

In particle physics, *flavor* refers to a generation of an elementary particle. Within standard model, there are six flavors of quarks and three flavors of leptons. Study of these elementary particles and their interactions is referred to as *flavor physics*. Historically, it has played a crucial role in development of Standard Model (SM) of particle physics. At present, there are compelling indications that the framework of Standard Model is not complete. However, there are no direct hints of any new particle from collider experiments. Flavor physics plays an important role here as it provides indirect probe to study new physics. Specially, the loop induced decay modes are sensitive to both SM and heavy new physics particles. Thus, dedicated efforts have been made to study flavor interactions both experimentally and theoretically. On experimental side, a paramount data on flavor physics has been accumulated which has improved the understanding of flavor interactions. However, some recent measurement of flavor changing decays of B mesons show some deviations from SM predictions. In particular, the angular observables of decay modes based on $b \to s\ell^+\ell^-$ and $b \to c\ell\nu_\ell$ transitions have shown consistent anomalies. Global fits of all these observables suggest the presence of new physics but the solution is not unique. Due to lack of enough data and large uncertainties in SM calculations, the source of the deviations is not clear. In this thesis, we have studied more decays in Standard model and new physics scenarios suggested by the present data. The aim of the thesis is to have SM expectations values for the leptonic and semileptonic decay modes with contributions of QCD corrections included.

In Chapter 3, predictions of angular observables for semileptonic decays,

$B \to \rho\mu^+\mu^-$ and $B_s \to \bar{K}^*\mu^+\mu^-$ and their CP conjugate modes are given. It is found that the SM expectation for $B_s \to \bar{K}^*\mu^+\mu^-$ is in agreement with the recent LHCb results. For $B \to \rho\mu^+\mu^-$ analysis is more involved as ρ is a CP conjugate state and the flavor of the decaying B meosn can not be tagged. We consider the impact of $B - \bar{B}$ mixing on the angular observables systematically and give predictions separately for LHCb and B factories.

In Chapter 4, we give predictions for angular observables corresponding to $B \to K_2^*\mu^+\mu^-$ with SM and other new physics scenarios. It has been shown that this mode is important as it is induced by $b \to s\ell\ell$ transition at the quark level. However, because K_2^* is a tensor particle, hadronic inputs are much different in comparison to other $b \to s\ell\ell$ processes. Thus, the study of this mode can be important to isolate the source of the deviations observed. Moreover, it has been shown that this channel can be used to lift the degeneracy in the solutions of global fits.

In Chapter 5, we have studied four-lepton decay of charged B meson. This channel is important as it can provide constraints on one of the most important hadronic parameters. The calculation for this channel is same as that of radiative decay with one difference. The photon is this case is not on-shell and hence the momentum squared of photon (q^2) is not zero. We have systematically retained q^2 terms in the calculation of form factors and given predictions for the four-lepton decays where final state can have electrons and muons.

In Chapter 6 we summarize the work done and discuss some future directions that can be pursued following the work done in this thesis.

Keywords: flavor physics, semileptonic B decays, effective field theory, four-lepton decays, Wilson coefficients, form factors.

Contents

List of Figures

List of Tables

Chapter 1

Introduction

The Glashow-Weinberg-Salam model of particle physics [1–3], also known as the Standard Model (SM) is the most successful model describing almost all of the physical phenomena observed in experiments. The particle content of the SM consists of four spin-1 particles called *Gauge bosons*, one spin-0 particle, *Higgs*, and twelve spin$-1/2$ particles, called *fermions*. The SM Lagrangian is based on the gauge group:

$$\mathcal{G}_{SM} \equiv SU(3)_C \otimes SU(2)_L \otimes U(1)_Y. \tag{1.1}$$

$SU(3)_C$ refers to the 'color' symmetry. All the particles which carry color charge transform under $SU(3)_C$ as,

$$\psi \to e^{ig_s \lambda^a G^a} \psi \tag{1.2}$$

where, ψ represents a particle field, g_s is the coupling strength of strong force, λ^a are Gell-Mann matrices which are the generators of $SU(3)_C$ group and G^a are the gluon fields. $SU(2)_L$ represents the symmetry under which only fermions with left chirality transform:

$$\psi_L \to e^{ig_2 \tau^i W^i} \psi_L, \tag{1.3}$$

$$\psi_R \to \psi_R, \tag{1.4}$$

where, ψ represents any fermion, g_2 is the coupling strength corresponding to the $SU(2)_L$ group, τ^i are the Pauli matrices which are generator of the symmetry group and W^i are the three weak gauge bosons. Lastly, $U(1)_Y$ represents the quantum number, *weak hypercharge*. A field with hypercharge equal to Y transforms under $U(1)_Y$ as,

$$\psi \to e^{iY}\psi. \tag{1.5}$$

All elementary particles are representations of the gauge symmetry, shown in tables 1.1 and 1.2. The fermions are in the fundamental representation. There are three copies of each representation of fermions which are called *generations*. Most of the observed matter is made up of first generation of fermions only, i.e., up-quark, down-quark, and electron. The gauge bosons are the force carriers and are given by adjoint representation. The Higgs field is responsible for the mass of all the particles and transform as $(\mathbf{1},\ \mathbf{2}, 1/2)$ under $\mathcal{G}_{\mathrm{SM}}$.

Matter	Generation	Representation
$Q^\alpha \equiv \begin{pmatrix} u_L^\alpha \\ d_L^\alpha \end{pmatrix}$	$\begin{pmatrix} u_L \\ d_L \end{pmatrix}, \begin{pmatrix} c_L \\ s_L \end{pmatrix}, \begin{pmatrix} t_L \\ b_L \end{pmatrix}$	(**3, 2**, 1/6)
u_R^α	u_R, c_R, t_R	(**3, 1**, 2/3)
d_R^α	d_R, s_R, b_R	(**3, 1**, -1/3)
$L^\alpha \equiv \begin{pmatrix} \nu_L^\alpha \\ l_L^\alpha \end{pmatrix}$	$\begin{pmatrix} \nu_{eL} \\ e_L \end{pmatrix}, \begin{pmatrix} \nu_{\mu L} \\ \mu_L \end{pmatrix}, \begin{pmatrix} \nu_{\tau L} \\ \tau_L \end{pmatrix}$	(**1, 2**, -1/2)
e_R^α	e_R, μ_R, τ_R	(**1, 1**, -1)

Table 1.1: Matter content of Standard Model

Gauge bosons	Symmetry group	Representation
G^a	$SU(3)_C$	(**8, 1**, 0)
W^i	$SU(2)_L$	(**1, 3**, 0)
B	$U(1)_Y$	(**1, 1**, 0)

Table 1.2: Gauge bosons in Standard Model

The interactions between the particles are given by the Lagrangian which has following properties: It should be scalar under the Lorentz group; It should be invariant under $\mathcal{G}_{\rm SM}$; It should be renormalizable. With these conditions in mind, the most general gauge invariant SM Lagrangian can be written as,

$$\mathcal{L}_{SM} = \mathcal{L}_{\rm Gauge} + \mathcal{L}_{\rm Fermion} + \mathcal{L}_{\rm Yukawa} + \mathcal{L}_{\rm Higgs} + \mathcal{L}_{\rm gf} + \mathcal{L}_{\rm FP} \tag{1.6}$$

The first term describes the gauge kinetic term and is given by:

$$\mathcal{L}_{\rm Gauge} = -\frac{1}{4}G_a^{\mu\nu}G^a_{\mu\nu} - \frac{1}{4}F_i^{\mu\nu}F^i_{\mu\nu} - \frac{1}{4}B^{\mu\nu}B_{\mu\nu} \tag{1.7}$$

where $G_a^{\mu\nu}$, $F_i^{\mu\nu}$, and $B^{\mu\nu}$ are the field strengths corresponding to $SU(3)_C$, $SU(2)_L$, and $U(1)_Y$ respectively. These are defined in terms of the corresponding gauge boson fields as,

$$G^a_{\mu\nu} = \partial_\mu G^a_\nu - \partial_\nu G^a_\mu + g_s f^{abc} G^b_\mu G^c_\nu, \tag{1.8}$$

$$F^i_{\mu\nu} = \partial_\mu W^i_\nu - \partial_\nu W^i_\mu + g_2 \epsilon^{ijk} W^j_\mu W^k_\nu, \tag{1.9}$$

$$B_{\mu\nu} = \partial_\mu B_\nu - \partial_\nu B_\mu, \tag{1.10}$$

where, G^a_μ are the gluon fields corresponding to the group $SU(3)_C$, W^i_μ are the three weak gauge fields corresponding to the group $SU(2)_L$, and B_μ is the gauge boson corresponding to the group $U(1)_Y$. The symbols $\{a, b, c\}$ are color indices, $\{i, j, k\}$ are $SU(2)$ indices, g_s and g_2 are the interaction strengths.

The second term in Eq. (1.6) describes the kinetic term of fermions in the theory which also includes the interaction between fermions and gauge bosons,

$$\mathcal{L}_{\rm Fermion} = \bar{\psi} i \gamma^\mu \mathcal{D}_\mu \psi^i \tag{1.11}$$

where the covariant derivative is defined as,

$$\mathcal{D}_\mu = \partial_\mu - i g_S G^a_\mu \frac{\lambda^a}{2} - i g_2 W^i_\mu \frac{\tau^i}{2} - i g_1 \frac{Y}{2} B_\mu \tag{1.12}$$

ψ is a fermion field which can be either a quark or lepton. Along with ordinary derivative, covariant derivative also contains gauge boson fields. Since leptons do not carry any color charge, second term in Eq. (1.12) is absent in their case. Similarly, for all right handed fermions, the term with τ^i does not appear in the definition of covariant derivative as they are singlet under $SU(2)_L$ symmetry.

The third term, $\mathcal{L}_{\text{Yukawa}}$ describes the interactions between fermions and the scalar field, Higgs (Φ) doublet,

$$\mathcal{L}_{\text{Yukawa}} = -Y^d_{ij}\bar{q}_{i,L}\Phi d'_{j,R} - Y^u_{ij}\bar{q}_{i,L}\tilde{\Phi}u'_{j,R} - Y^e_{ij}\bar{l}_{i,L}\Phi e_{j,R} + h.c., \tag{1.13}$$

where Y^d_{ij}, Y^u_{ij}, and Y^e_{ij} are the Yukawa couplings. In terms of $SU(2)$ components Φ can be written as,

$$\Phi \equiv \begin{pmatrix} \phi^+ \\ \phi^0 \end{pmatrix}. \tag{1.14}$$

Since Φ and $\bar{q}_L$ are $SU(2)$ doublets, their combination can be an $SU(2)$ singlet and first term (and similarly third) of Eq. (1.13) is invariant under $SU(2)$ symmetry. Also, since sum of hypercharges of the particles in both first and third term adds to zero, these terms are also invariant under $U(1)_Y$. For second term of Eq. (1.13) to exist, Φ has to be replaced by its charged conjugate field $\tilde{\Phi}$, which is defined as,

$$\tilde{\Phi} \equiv i\tau_2\Phi^* = \begin{pmatrix} \phi_0^* \\ -\phi^- \end{pmatrix}. \tag{1.15}$$

For any $SU(2)$ doublet Φ, $i\tau_2\Phi^*$ also transforms as a doublet, and thus the second term is invariant under $SU(2)_L$. $\tilde{\Phi}$ transforms under SM gauge group as, $(1, 2, -1/2)$, thus second term is also invariant under $U(1)_Y$ as well.

The term $\mathcal{L}_{\text{Higgs}}$ of Eq. (1.6) defines the potential of the Higgs field and interactions between Higgs doublet and the gauge bosons,

$$\mathcal{L}_{\text{Higgs}} = (\mathcal{D}_\mu\Phi)^\dagger(\mathcal{D}^\mu\Phi) - V(\Phi), \tag{1.16}$$

where $V(\Phi)$ is the Higgs potential and is given by,

$$V(\Phi) = -\mu^2\Phi^+\Phi + \lambda(\Phi^\dagger\Phi)^2. \tag{1.17}$$

λ is a positive number such that the potential is always bounded from below. This part of Lagrangian is responsible for masses of all the particles. The mass generation is achieved through the spontaneous symmetry breaking (SSB) of $SU(2)_Y \times U(1)_Y$ to $U(1)_Q$ and this mechanism is called the *Higgs mechanism*

[4]. Minimization of Higgs potential demands vacuum expectation value (v) to be,

$$v \equiv \sqrt{\langle \Phi^\dagger \Phi \rangle} = \sqrt{\mu^2/2\lambda}. \tag{1.18}$$

This corresponds to degenerate solutions of Φ. Choosing a particular direction in the field space will break the symmetry. Without loss of generality we choose,

$$\langle \Phi \rangle_0 = \frac{1}{\sqrt{2}} \begin{pmatrix} 0 \\ v \end{pmatrix} \tag{1.19}$$

The vacuum state defined in Eq. (1.19) has a non-zero lower component with eigenvalue $t_3 = -1/2$ corresponding to the T_3 generator of $SU(2)_L$. Also, it has a non-zero value correponding to $U(1)_Y$ which is +1. This implies that this choice of vacuum breaks $SU(2)_L$ as well as $U(1)_Y$ symmetry. However, a residual symmetry is inevitable as there exists a linear combination of the two charges which remains unbroken, and given by Eq. (1.22).

$$\frac{T_3}{2} \langle \Phi \rangle_0 \neq 0 \tag{1.20}$$

$$\frac{Y}{2} \langle \Phi \rangle_0 \neq 0 \tag{1.21}$$

$$(\frac{T_3}{2} + \frac{Y}{2}) \langle \Phi \rangle_0 = 0 \tag{1.22}$$

This unbroken symmetry is recognized as electromagnetic charge with the value of charge given by,

$$Q = T_3 + Y. \tag{1.23}$$

After SSB, the Higgs field can be rewritten in a basis where only the physical components are present. This is known as unitary gauge and the scalar doublet is given by,

$$\Phi = \begin{pmatrix} 0 \\ \frac{v+h}{\sqrt{2}} \end{pmatrix} \tag{1.24}$$

In this gauge, kinetic term of $\mathcal{L}_{\text{Higgs}}$ yields the following mass terms for $SU(2)_L$ and $U(1)_Y$ gauge bosons,

$$\mathcal{L}_{\text{mass}} = \frac{1}{4} g_2^2 v^2 W^{+\mu} W^-_\mu + \frac{1}{8} v^2 \begin{pmatrix} W^3_\mu & B_\mu \end{pmatrix} \begin{pmatrix} g_2^2 & -g_2 g_1 \\ -g_2 g_1 & g_1^2 \end{pmatrix} \begin{pmatrix} W^3_\mu \\ B_\mu \end{pmatrix}, \tag{1.25}$$

where $W^{\pm}_{\mu} = \frac{1}{\sqrt{2}}(W^1_{\mu} \pm W^2_{\mu})$. It is evident from Eq. (1.25), that $M_{W^{\pm}} = gv/2$. Also, one of the linear combination of the neutral gauge bosons, W^3_{μ} and B_{μ}, given by,

$$Z_{\mu} = \frac{g_1 B_{\mu} + g_2 W^3_{\mu}}{\sqrt{g_1^2 + g_2^2}} \tag{1.26}$$

acquires mass, $M_Z = \frac{v}{2}\sqrt{g_1^2 + g_2^2}$ while the other orthogonal combination A_{μ} remains massless and is identified with the photon field which is the gauge boson corresponding to the residual symmetry after SSB, $U(1)_{\rm em}$

$$A_{\mu} = \frac{g_2 B_{\mu} + g_1 W^3_{\mu}}{\sqrt{g_1^2 + g_2^2}} \tag{1.27}$$

The SM Lagrangian defined in Eq. (1.6) also contains two additional terms: the gauge fixing term ($\mathcal{L}_{\rm gf}$) and Faddeev-Popov term ($\mathcal{L}_{\rm FP}$). These two terms are important to build a complete and consistent model.

1.1 Flavor in the Standard Model

There are six flavors of quarks in the SM, which are, up(u), down(d), charm(c), strange(s), bottom(b), and top(t); three charged leptons, which are, electron (e), muon (μ), and tau (τ) and a neutrino associated with each of these charged leptons. There is rich landscape of phenomenology associated with these. Within the SM, the interactions governing the dynamics of fermions are contained in $\mathcal{L}_{\rm Fermion}$ and $\mathcal{L}_{\rm Yukawa}$. Looking at the mass terms, which is contained in $\mathcal{L}_{Yukawa}$,

$$\mathcal{L}^{\rm mass}_{\rm Yukawa} = -\frac{v}{\sqrt{2}} M^u_{ij} \bar{u'}_{iL} u'_{jR} - \frac{v}{\sqrt{2}} M^d_{ij} \bar{d'}_{iL} d'_{jR} - \frac{v}{\sqrt{2}} M^e_{ij} \bar{e}'_{iL} e'_{jR} + h.c., \tag{1.28}$$

where the fields, u'_i, d'_i, and e'_i are flavor eigenstates. Since, there are no constraints over $M^{u,d,e}$, these matrices are complex as well as off-diagonal. The off-diagonal elements can lead to flavor violating transitions. To write the Lagrangian in terms of physical fields, the Yukawa matrices are diagonalized by means of biunitary transformations defined as,

$$u'_{iL,R} = (V^u_{L,R})_{ij} u_{jL,R},$$
$$d'_{iL,R} = (V^d_{L,R})_{ij} d_{jL,R}$$

$$e'_{iL,R} = (V^e_{L,R})_{ij} e_{jL,R} \tag{1.29}$$

where u_i, d_i, and e_i are mass eigenstates. Using Eq. (1.29), mass terms in mass basis is written as,

$$\mathcal{L}^{\text{mass}}_{\text{Yukawa}} = -\frac{v}{\sqrt{2}} M^{u,\text{diag}}_{ij} \bar{u}_{iL} u_{jR} - \frac{v}{\sqrt{2}} M^{d,\text{diag}}_{ij} \bar{d}_{iL} d_{jR} - \frac{v}{\sqrt{2}} M^{e,\text{diag}}_{ij} \bar{e}_{iL} e_{jR} + h.c., \tag{1.30}$$

with

$$M^{(u,d,e),\text{diag}} = V_L^{(u,d,e)\dagger} M^{(u,d,e)} V_R^{u,d,e}, \tag{1.31}$$

where $M^{(u,d),diag}$ are diagonal 3×3 matrices. Within SM, neutrinos are massless. However, for an extension of SM where neutrinos have non-zero mass, mass matrix of neutrino is also diagonalised again using biunitary transformation,

$$\nu'_{iL,R} = (V^\nu_{L,R})_{ij} \nu_{jL,R}. \tag{1.32}$$

The interactions of fermions with gauge bosons $W^\pm$ can also be written in the mass basis of fermions.

$$\mathcal{L}^{CC}_{int} = -\frac{g_2}{\sqrt{2}} \begin{pmatrix} \bar{d}_L & \bar{s}_L & \bar{b}_L \end{pmatrix} \gamma^\mu V_{CKM} \begin{pmatrix} u_L \\ c_L \\ t_L \end{pmatrix} W^-_\mu \tag{1.33}$$

$$-\frac{g_2}{\sqrt{2}} \begin{pmatrix} \bar{e}_L & \bar{\mu}_L & \bar{\tau}_L \end{pmatrix} \gamma^\mu U_{PMNS} \begin{pmatrix} \nu_{eL} \\ \nu_{\mu L} \\ \nu_{\tau L} \end{pmatrix} W^-_\mu + \text{h.c.}, \tag{1.34}$$

where $V_{\text{CKM}}(\equiv V_L^{u\dagger} V_L^d)$ and $U_{\text{PMNS}}(\equiv V_L^{e\dagger} V_L^\nu)$ are 3×3 unitary matrix. Hence, charged current couples an up type quark to a down type quark of any generation weighted by V_{CKM}. This phenomenon is called *quark mixing*. First suggested by Cabbibo and later by Kobayashi and Masakawa, the mixing matrix is called *CKM matrix* [5, 6]. Similarly, in the lepton sector, charged current interactions lead to *neutrino mixing* defined by U_{PMNS} (Pontecorvo-Maki-Nakagawa-Sakata) matrix [7]. In the work done for this thesis, neutrinos have been considered massless. Thus, the corresponding observables are not sensitive to U_{PMNS} matrix.

However, study of CKM matrix is essential to study quark transitions. The CKM matrix is a result of change of basis (rotation) of quarks, which implies that the matrix is unitary i.e., $V^\dagger V = VV^\dagger = 1$. In general, for a $N \times N$ unitary matrix, the number of real-valued parameters are N^2. However, not all of them are independent. Out of N^2, $N(N-1)/2$ are the Euler angles while the remaining $N(N+1)/2$ elements are phases. Some of these phases are spurious as one has the freedom to redefine the fermion fields as,

$$\psi_\alpha \to exp(i\alpha)\psi_\alpha; \quad \alpha = 1, 2, ..., N. \tag{1.35}$$

Number of such phases which can be redefined is $(2N-1)$. Thus, the total number of independent phases is $(N-1)(N-2)/2$. For three generations, the CKM matrix has three angles and one phase. Within the Standard Model, this phase is the only source of CP Violation (CPV). Different for the CKM matrix have been suggested using four parameters . One of the parameterization suggested by Particle Data Group (PDG) is [7],

$$\begin{align} V_{\text{CKM}} &= R_1(\theta_{23})\Gamma(\delta)R_2(\theta_{13})\Gamma(-\delta)R_3(\theta_{12}) \tag{1.36}\\ &= \begin{pmatrix} c_{12}c_{13} & s_{12}c_{13} & s_{13}e^{-i\delta} \\ -s_{12}c_{23} - c_{12}s_{23}s_{13}e^{i\delta} & c_{12}c_{23} - s_{12}s_{23}s_{13}e^{i\delta} & s_{23}c_{13} \\ s_{12}s_{23} - c_{12}c_{23}s_{13}e^{i\delta} & -c_{12}s_{23} - s_{12}c_{23}s_{13}e^{i\delta} & c_{23}c_{13} \end{pmatrix} \tag{1.37} \end{align}$$

where $c_{ij} = \cos\theta_{ij}$, $s_{ij} = \sin\theta_{ij}$. The three angles θ_{12}, θ_{13}, and θ_{23} are the real mixing parameters and δ is the phase. In the limit of two generations, θ_{12} is the Cabbibo angle [5]. Another commonly used parameterization of CKM matrix is the *Wolfenstein parameterization* [8]. It is defined in terms of four parameters: λ, A, ρ, η which are related to the parameters defined in Eq. (1.36) through the relations,

$$s_{12} = \lambda, \qquad s_{23} = A\lambda^2, \qquad s_{13}e^{-i\delta} = A\lambda^3(\rho - i\eta) \tag{1.38}$$

Using these relations, the Wolfenstein parameterization is given by,

$$V_{\text{CKM}} = \begin{pmatrix} 1-\lambda^2/2 & \lambda & A\lambda^3(\rho - i\eta) \\ -\lambda & 1-\lambda^2/2 & A\lambda^2 \\ A\lambda^3(1-\rho-i\eta) & -A\lambda^2 & 1 \end{pmatrix} + \mathcal{O}(\lambda^4). \tag{1.39}$$

It is an approximation based on the experimentally measured values of CKM elements. The parameter λ is used as an expansion parameter and related to the Cabbibo angle as $\lambda = sin\theta_{12} \sim 0.22$. The interesting feature is that the complex parameters show up in only two of the elements upto $\mathcal{O}(\lambda^3)$. This is due to the fact that CP violation is significant only when there is an interaction between first and third generation quarks. In principle, the complex parameter will show up in other elements if terms in higher order of λ are included but CP violation will still be suppressed. Theoretically, there is no constraint on the values of CKM elements except the CKM matrix has to be unitary. Thus, the values have to be experimentally measured. The current status of the parameters in Wolfenstein parameters is [7]:

$$\lambda = 0.22453 \pm 0.00044 \qquad A = 0.836 \pm 0.015$$

$$\bar{\rho} = 0.122^{+0.018}_{-0.017} \qquad \bar{\eta} = 0.355^{+0.012}_{-0.011}$$

where, $\bar{\rho} = \rho(1 - \lambda^2/2)$ and $\bar{\eta} = \eta(1 - \lambda^2/2)$.

Since different parameterization accommodate the physical phase of CKM matrix in different fashion, the CP-violation should be quantified in a way such that it is basis-independent. Such a basis-invariant quantity is *Jarlskog invariant* which is given by $J = Im[V_{ij}V_{kl}V^*_{il}V^*_{kj}]$ [9]. It is evident from the construction that all the spurious phases are cancelled within J. In terms of the CKM parameterizations discussed above,

$$J = c_{12}c_{23}c^2_{13}s_{12}s_{23}s_{13}sin\partial_{CKM} \sim \lambda^6 A^2 \eta. \tag{1.40}$$

Since J depends on all the mixing angles, it implies that a minimum of three number of generations are needed to have CP violation. Also, within SM, the value of CP violation is very small as J depends of sixth power of λ.

1.1.1 Unitarity triangle

Another interesting way of representing the CKM matrix is through the *unitarity triangles*. The unitarity of the matrix implies following relations between the elements:

$$\text{Column Orthogonality:} \quad \sum_i V_{ij}V^*_{ik} = \delta_{jk}$$
$$\text{Row Orthogonality:} \quad \sum_i V_{ij}V^*_{ki} = \delta_{jk} \tag{1.41}$$

Since the elements are in general complex numbers, these relations can be expressed as triangles in the complex plane, or $\rho - \eta$ *plane*. There are six such triangles, however, the most popular triangle is given by the scalar product of first and third column,

$$V_{ud}V^*_{ub} + V_{cd}V^*_{cb} + V_{td}V^*_{tb} = 0 \tag{1.42}$$

which is shown in Figure 1.1. The sides of the triangle are normalized as,

$$\frac{V_{ud}V^*_{ub}}{V_{cd}V^*_{cb}} + 1 + \frac{V_{td}V^*_{tb}}{V_{cd}V^*_{cb}} = 0 \tag{1.43}$$

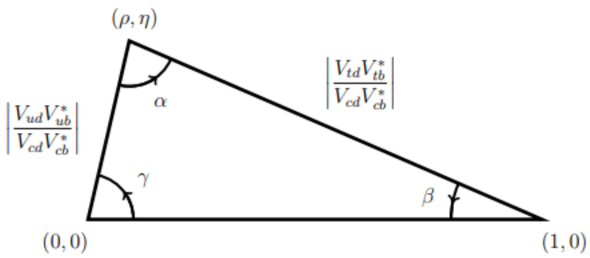

Figure 1.1: The Unitarity Triangle (UT).

In terms of Wolfenstein parameters, lengths of the sides of the unitarity triangle are given by,

$$\left|\frac{V_{ud}V^*_{ub}}{V_{cd}V^*_{cb}}\right| = \sqrt{\rho^2 + \eta^2} \qquad \left|\frac{V_{td}V^*_{tb}}{V_{cd}V^*_{cb}}\right| = \sqrt{(1-\rho)^2 + \eta^2} \tag{1.44}$$

while the remaining one side is of unit length, by normalization. The angles of the unitarity triangle are defined as,

$$\alpha = \phi_2 = arg\left(-\frac{V_{td}V^*_{tb}}{V_{ud}V^*_{ub}}\right) \quad \beta = \phi_1 = arg\left(-\frac{V_{cd}V^*_{cb}}{V_{td}V^*_{tb}}\right) \quad \gamma = \phi_3 = arg\left(-\frac{V_{ud}V^*_{ub}}{V_{cd}V^*_{cb}}\right) \tag{1.45}$$

The reason that this particular triangle is important is because all the three terms on the left hand side of Eq. (1.42) are of the same order in λ ($\mathcal{O}(\lambda^3)$) while other triangles are *squashed*. Another important feature of all UTs is that the area of the UTs is proportional to the Jarlskog invariant,

$$\text{Area of UTs} = \frac{1}{2}|J| \tag{1.46}$$

The values of elements of CKM matrix are measured through flavor decays. The present status of unitarity triangle is shown in Figure 1.2 where important constraints from B and K decays have been taken into account.

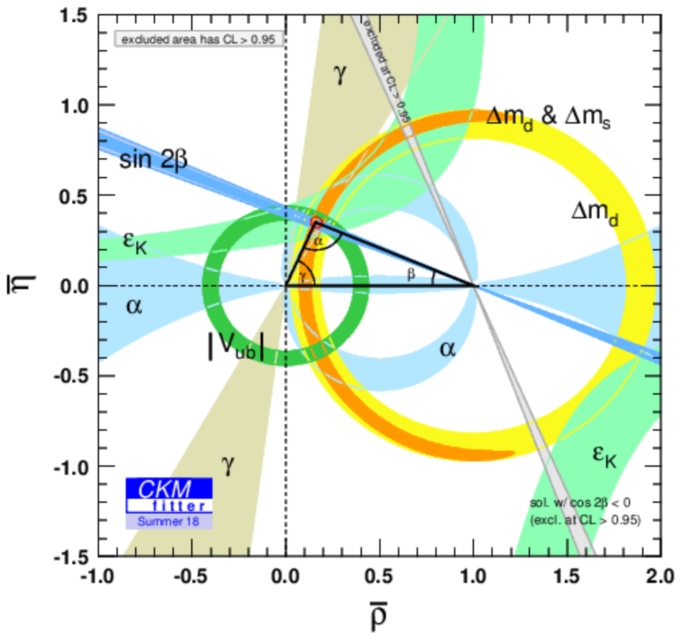

Figure 1.2: The SM CKM fit and individual constraints (colored regions show 95% CL.)[10]

1.2 Current Excitements in B physics

Given the historical importance and theoretical motivation to discover new particles and unravel the underlying physics, dedicated and extensive work is being done on the experimental side as well. Within LHC, apart from ATLAS and CMS collaborations, the LHCb collaboration is dedicated to the precision study of flavor physics, in particular B decays. Other such experimental facility is Belle II located at KEK, Japan where the electron-positron beams are collided with energies chosen as to produce a large number of $B-\bar{B}$ meson pairs and hence this is known as a *B factory*. Both the experiments are dedicated to find signals of New Physics (NP) through indirect searches.

These experiments have provided important constraints on the parameters of CKM matrix through measurements of various modes. Some of the deviations have been found in the observables related to the semileptonic B decays. These decays can be induced by Flavor Changing Neutral Currents (FCNCs) at quark level, e.g., $B \to K^{(*)}\ell^+\ell^-$ or CCs, e.g., $B \to D^{(*)}\ell^+\nu_\ell$. The amplitudes of loop suppressed decays, $b \to s(d)$ transitions are ideal to look for NP as the new contribution can be sizeable in comparison to SM contribution. Some such decays, which includes, $B^+ \to K^+\mu^+\mu^-$ [11], $B^0 \to K^{*0}\mu^+\mu^-$ [12–17, 19, 20], $B_s^0 \to \phi\mu^+\mu^-$ [21, 22], and $\Lambda_b^0 \to \Lambda^0\mu^+\mu^-$ [23] have been measured and interestingly, SM expectations of the branching ratio exceeds the measured value for all the modes. Other than the branching ratio, many angular observables also show some discrepancy. Another set of interesting observables are R_K, R_{K^*} defined as [11],

$$R_K = \frac{\mathcal{BR}(B^+ \to K^+\mu^+\mu^-)}{\mathcal{BR}(B^+ \to K^+e^+e^-)} \tag{1.47}$$

$$R_{K^*} = \frac{\mathcal{BR}(B \to K^*\mu^+\mu^-)}{\mathcal{BR}(B \to K^*e^+e^-)}, \tag{1.48}$$

mainly because the uncertainties in the hadronic form factors, cancel to a very large extent in the SM predictions. The expected value of $R_{K^{(*)}}$ is predicted to be 1 within SM [18]. However, the measured value for R_K is,

$$R_K^{\rm LHCb} = 0.745^{+0.090}_{-0.074} \pm 0.036 \qquad \text{for } 1.1 < q^2 < 6.0 \text{ GeV}^2 \tag{1.49}$$

which is 2.6σ below the SM prediction. The ratio R_{K^*} has been measured in two q^2 bins [19] (where q^2 is the invariant mass squared of the lepton pair), finding,

$$R_{K^*}^{\rm LHCb} = 0.66^{+0.11}_{-0.07} \pm 0.03 \qquad \text{for } 0.045 < q^2 < 1.1 \text{ GeV}^2, \tag{1.50}$$

$$R_{K^*}^{\rm LHCb} = 0.69^{+0.11}_{-0.07} \pm 0.05 \qquad \text{for } 1.1 < q^2 < 6.0 \text{ GeV}^2, \tag{1.51}$$

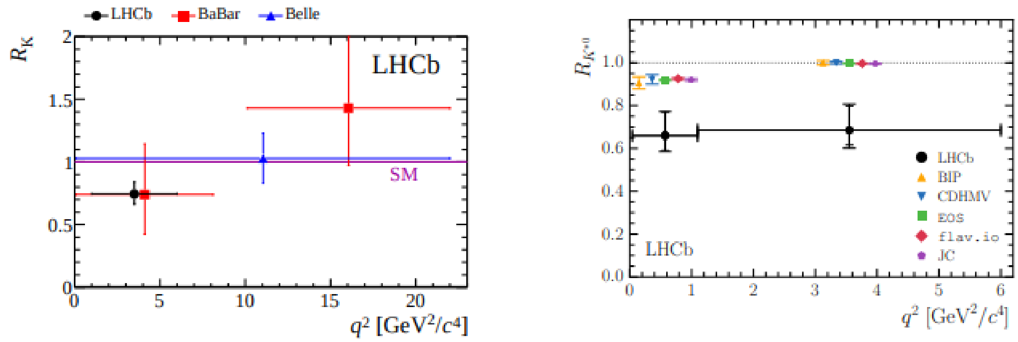

Figure 1.3: LHCb, Belle, and BaBar measurements of R_K and LHCb measurement of R_{K^*} (right). SM predictions are taken from [18].

The R_K and R_K^* measurements from various experiments are shown in Figure 1.3.

A notable deviation is in the angular observable, P_5', corresponding to the decay $B^0 \to K^*\mu^+\mu^-$ [17]. The sources of the anomalies in $b \to s\ell\ell$ are unclear. One of the obvious sources can be a NP. The global fits to the experimental data strongly suggest new couplings of vector or axial vector nature [24–26]. Another suggested possibility is an incorrect evaluation of the long-distance effects contribution to the decay process, which is due to the charm resonance region [27].

Charged current transitions are also a good probe to study Lepton Flavor Universality (LFU). The two such observables that have been studied are:

$$R_{D^{(*)}} = \frac{\mathcal{BR}(B \to D^{(*)}\tau\bar{\nu}_{\tau)}}{\mathcal{BR}(B \to D^{(*)}\ell\bar{\nu}_{\ell)}} \tag{1.52}$$

with $\ell = e, \mu$. The experimental value of R_D and R_{D^*} consistently exceeds the SM expectation [28, 29], as measured at BaBar [31, 32], Belle [33, 34], and LHCb [35]. However, the latest measurement of Belle [36] and LHCb [37] are consistent with SM value. The averages are given as,

The experimental values of R_D and R_{D^*} exceed the SM expectations by 2.0σ and 2.3σ respectively. Even though the deviation is small, it has been observed both at LHCb and B-factories, which corroborates the importance of this result. Another channel which has been tested for Lepton Flavor Universality Violation (LFUV) is $B_c^+ \to J/\psi\tau^+\nu_\tau$. Since B-factories have been operating on $\Upsilon(4S)$

Observable	SM value	Experimental Average
R_D	0.299 ± 0.003	$0.407 \pm 0.039 \pm 0.024$
R_{D^*}	0.258 ± 0.005	$0.306 \pm 0.013 \pm 0.007$

Table 1.3: SM expectation value and experimental average for R_{D^*} [30]

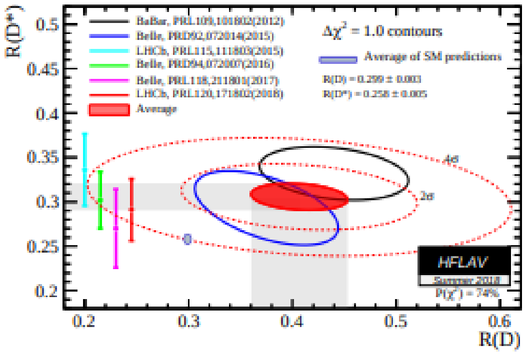

Figure 1.4: Average of $R_{D^{(*)}}$ ratios [30]

which decays mainly into B meson system, the branching ratio of B_c has been studied at LHCb only. The ratio measured by LHCb is [38],

$$R_{J/\psi} \equiv \frac{\mathcal{BR}(B_c^+ \to J/\psi \tau^+ \nu_\tau)}{\mathcal{BR}(B_c^+ \to J/\psi \mu^+ \nu_\mu)} = 0.71 \pm 0.17 \pm 0.18 \tag{1.53}$$

The theoretical uncertainties in the predictions for this observable are large due to the uncertainty in the values of form factors. The central value corresponding to various predictions lies in the range $[0.25, 0.28]$ [39–42]. The observed values of $R_{J/\psi}$ exceeds the SM prediction but the result is compatible with the SM within about 2σ.

Individually, each of the above mentioned measurements is not very significant at the moment but the tensions observed are coherent. Global fits to $b \to s\ell\ell$ decays suggest new physics such that it contributes to the Wilson coefficient C_9 with or without additional contributions to $C_{10}^{(\prime)}$ and C_9'. Another possible source of these anomalies can be incorrect evaluation of the long-distance effects from vector charmonium region. To settle the discrepancies, more data is needed.

Measurements from Belle 2 and LHC run 3 are expected to shed some light on it [43].

In the work done for the thesis I have studied semileptonic B decay modes i.e., $B \to \rho\mu^+\mu^-$, $B_s \to \bar{K}^*\mu^+\mu^-$, and $B \to K_2^*\mu^+\mu^-$. Since these processes are also based on $b \to s(d)\ell\ell$ transition at the quark level, their measurements can provide complementary information about the present anomalies. To interpret the data it is necessary to have SM predictions to compare with. I have given the first set of SM expectation values of all the angular observables corresponding to the aforementioned decay modes.

Chapter 2

Effective Hamiltonian

The effective field theory (EFT) approach is generally followed when there are disparate energy scales present in the theory. Hence it is quite natural to study heavy meson decays in the framework of EFT. In the case of K , D, or B meson decays, the two important energy scales include the mass of the decaying meson ($E \sim \mathcal{O}(1)$ GeV) and the electroweak scale ($m_W \sim \mathcal{O}(100)$ GeV). The principle of effective theory is to keep only relevant degrees of freedom at a given scale while heavy degrees of freedom are integrated out. To describe the phenomenon at energy E, the knowledge of the theory at heavy scale Λ is not required. Therefore, the effective theory can also be considered as a low-energy limit of a full theory. There are many advantages of studying K, D, and B decays in effective theory since the irrelevant degrees of freedom do not enter the Lagrangian and the physics becomes simple. Also, the long-distance physics and short-distance physics can be treated independently.

2.1 Operator Product Expansion

Hadrons decay through weak currents at quark level. The weak decays, specially B decays, are governed by processes involving W bosons, Z boson, or top quarks as propagators which describe the short-distance physics at scales m_W ,m_Z, and m_t respectively. However, the quarks exist within hadrons in a bound state with typical binding energy $\sim \mathcal{O}(1)$ GeV which is much lower than the weak scale. Thus, the actual picture of a decaying meson is described at scale $\mathcal{O}(m_B, m_D, m_K)$ in case of B, D, and K meson respectively.

The separation of physics at these two disparate scales can be achieved using *Operator Product Expansion* (OPE) [44–46]. It parameterizes the low-energy effects of the full theory as an expansion in $1/m_W^2$, where m_W is the mass of W boson. As the heavy degrees of freedom are integrated out, it generates a series of local operators where higher dimensional operators are suppressed by powers of (q^2/m_W^2). This series of local operators is called OPE. The main idea of OPE is that the physical effects at high energy scale appear local when probed at low energy. Consider two local operators with spacetime coordinates x and y. The product of these two operators is not local and the energy scale corresponding to the separation being $\sim 1/(x-y)$. However, if the energy used to probe the system is much smaller than $1/(x-y)$, that corresponds to the limit $x-y \to 0$. In this limit, the product can be expressed in term of a local operator as,

$$\mathcal{O}(x)\mathcal{O}(y) \sim \sum_i \mathcal{C}_i(x-y)\mathcal{O}_i\left(\frac{x+y}{2}\right) \tag{2.1}$$

where $\mathcal{C}_i$ are the Wilson coefficients and contain the short-distance effects i.e., physical information when $x \to y$. The effects at the intrinsic scale of theory $(x+y)/2$ are captured by the local operators O_i. Thus, in OPE, the Hamiltonian is written as a series of local operators O_i multiplied by effective coupling constants $\mathcal{C}_i$,

$$\mathcal{H}_{\text{eff}} = \frac{G_F}{\sqrt{2}} \sum_i \mathcal{C}_i(\mu)\mathcal{O}_i(\mu). \tag{2.2}$$

where G_F is the Fermi constant:

$$\frac{G_F}{\sqrt{2}} = \frac{g^2}{8m_W^2} \tag{2.3}$$

As a general convention, the effective Hamiltonian relevant for B decays is written by redefining the Wilson coefficients such that,

$$\mathcal{H}_{\text{eff}} = \frac{G_F}{\sqrt{2}} \sum_i \lambda_i^{\text{CKM}}\mathcal{C}_i(\mu)\mathcal{O}_i(\mu) \tag{2.4}$$

where, λ_i^{CKM} carries the relevant CKM factors, $\mathcal{C}_i(\mu)$ are the Wilson coefficients, and $\mathcal{O}(\mu)$ are the effective operators, and μ is the factorization scale. The object of interest here is the hadron decay amplitude which is given by,

$$A(P \to F) = \langle F|\mathcal{H}_{\text{eff}}|P\rangle = \frac{G_F}{\sqrt{2}} \sum_i \lambda_i^{\text{CKM}} \mathcal{C}_i(\mu) \langle F|\mathcal{O}_i|P\rangle \tag{2.5}$$

where, P and F are hadrons in initial and final state respectively. The scale μ separates the short distance contributions $\mathcal{C}_i$ from long distance part $\mathcal{O}_i$, with $\mathcal{C}_i$ carrying the information above μ while all the contributions below μ belong to long-distance effects are contained in $\langle\mathcal{O}_i\rangle$ ($\equiv \langle F|\mathcal{O}_i|P\rangle$). The value of μ is arbitrary but it is customary to choose it as the mass of the decaying meson and thus large logarithms $\ln(m_W/\mu)$ can compensate for the small value of QCD coupling constant, α_s and breaks the perturbation series. This problem is tackled by resumming the large logarithms to all orders in α_s. This is done using the renormalization group (RG) improved perturbation theory. The summation of the terms $(\alpha_s)^n \ln(m_W/\mu)^n$ to all orders in n is called the leading-logarithmic approximation (LO). In order to achieve sufficient precision, it is desirable to include next-to-leading logarithmic order terms (NLO) which is obtained by resumming $\alpha_s^n(\ln m_W/\mu)^{n-1}$ series. For proper matching of $\mathcal{C}_i$ and O_i, it is actually important to consider atleast NLO terms. Moreover, it can be evolved down from one scale to other. In doing so, only the physics contribution above the final μ is transformed, hence changing only the value of $\mathcal{C}_i$. Since μ is not a physical scale, the μ-dependence of the WCs should cancel the μ-dependence of the matrix elements.

The general expression of WCs as a function of the scale at which it is computed is given by,

$$\mathcal{C}(\mu) = U(\mu, m_W)\mathcal{C}(m_W) \tag{2.6}$$

where $\mathcal{C}(m_W)$ are the values at the initial scale m_W and $U(\mu, m_W)$ is the evolution matrix. The evolution matrix is determined by solving the RG equation,

$$\frac{d}{d\ln\mu}\mathcal{C}_i(\mu) = \gamma_{ij}^T \mathcal{C}_j(\mu) \tag{2.7}$$

where γ is the anomalous dimension matrix. Eq. (2.7) follows from the fact that the physical amplitude should not depend on the scale μ. Solving the RG equation gives,

$$U(\mu, m_W) = 1 + \int_{g_s(m_W)}^{g_s(\mu)} dg \frac{\gamma^T(g)}{\beta(g)} + \int_{g_s(m_W)}^{g_s(\mu)} dg \int_{g_s(m_W)}^{g_s(g)} dg' \frac{\gamma^T(g)}{\beta(g)} \frac{\gamma^T(g')}{\beta(g')} + \ldots \tag{2.8}$$

where g_s is the QCD coupling and

$$\beta(g_s) = \frac{d}{d\ln\mu} g_s(\mu) \tag{2.9}$$

is the beta-function which governs evolution of the coupling as a function of scale μ. This implies that μ dependence should be cancelled by that of hadronic matrix elements.

The concept of OPE can be understood by a simple example of $K^0 \to \pi^+\pi^-$. It is based on $s \to u\bar{u}d$ transition, which is a weak charged-current transition at tree level, as shown in Figure 2.1. Similarly, another example is $D \to K\pi$ based on $c \to su\bar{d}$ transition explained in [47]. The amplitude in the unitary gauge of the process at tree-level in full theory is given by,

$$A_{\text{full}} = \frac{g_2^2}{2} V_{us} V_{ud}^* (\bar{s}\gamma^\mu P_L u) \frac{1}{q^2 - m_W^2} \left(-g_{\mu\nu} + \frac{q_\mu q_\nu}{m_W^2} \right) (\bar{u}\gamma^\nu P_L d) \tag{2.10}$$

where $P_L = (1-\gamma_5)/2$, V_{us} and V_{ud} are the CKM elements, and q^2 is the four-momentum square of the propagator. In the rest frame of decaying meson, maximum value of momentum transfer can be m_K and the conditions $q^2/m_W^2 \ll 1$ and $\frac{q_\mu q_\nu}{m_W^2} \ll 1$ are always true. Because of this,

$$\frac{1}{q^2 - m_W^2} = -\frac{1}{m_W^2}\left(1 + \frac{q^2}{m_W^2}\right) \approx -\frac{1}{m_W^2}. \tag{2.11}$$

To find the value of Wilson coefficients, the amplitude in the full theory is equated to the effective amplitude (Eq. (2.5)) in OPE. This process is called *matching*. Thus, at the leading order, the only operator which contributes to the process is

$$O_2 = (\bar{s}_i \gamma^\mu P_L u_i)(\bar{u}_j \gamma^\mu P_L d_j), \tag{2.12}$$

where i, j are color indices. The corresponding Feynman diagram in shown in Figure 2.1. O_2 is a dimension-six operator. The higher dimensional operators (i.e. greater than six) appear with q^2/m_W^2 term and hence are generally suppressed. At $\mathcal{O}(\alpha_s^0)$, the only operator which contributes is O_2 with $\mathcal{C}_2 = 1$. When QCD corrections are considered at order α_s, additional operator with the same flavour structure as O_2 but different color structure starts contributing,

$$O_1 = (\bar{s}_i \gamma^\mu P_L u_j)(\bar{u}_j \gamma^\mu P_L d_i) \tag{2.13}$$

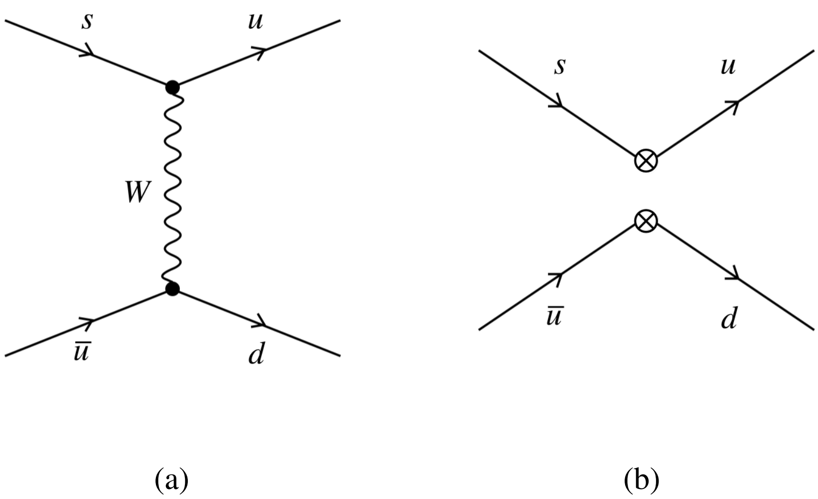

Figure 2.1: (a) $s \to u\bar{u}d$ at tree level in the full theory, (b) $s \to u\bar{u}d$ at tree level in the effective theory

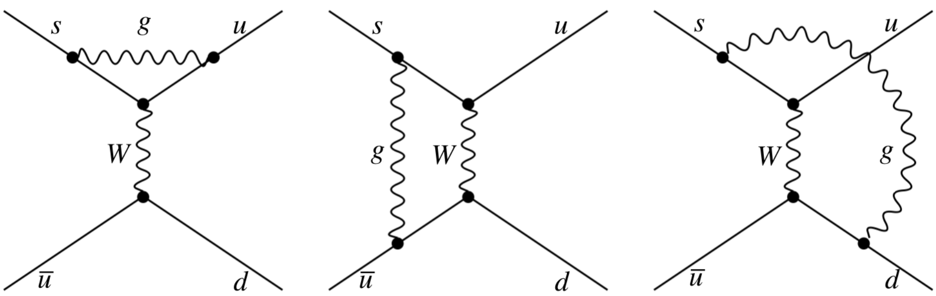

Figure 2.2: α_s correction to $s \to u\bar{u}d$ in the full theory

The Feynman diagrams corresponding to the α_s corrections are given in Figure 2.2. The Feynman rule for gluon-fermion interactions includes generators of $SU(3)_C$ group, which using the color algebra are rewritten as,

$$T^a_{ij}T^a_{kl} = -\frac{1}{2N}\delta_{ij}\delta_{kl} + \frac{1}{2}\delta_{il}\delta_{jk} \tag{2.14}$$

where $N = 3$ is number of colors. The first term in (2.14) corresponds to the original operator O_2 while the second term generates the additional operator O_1. To find the Wilson coefficients at order α_s the amplitude including QCD

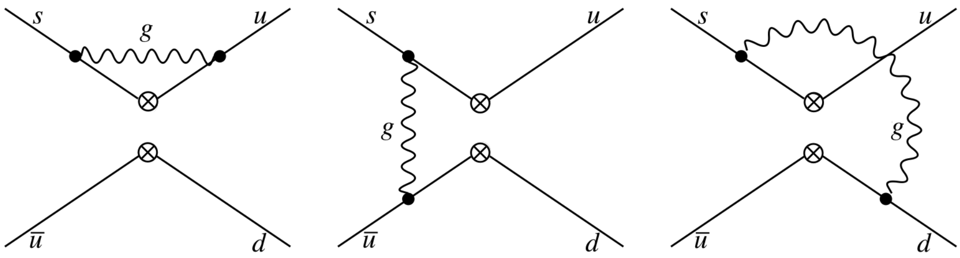

Figure 2.3: α_s correction to $s \to u\bar{u}d$ in the effective theory

corrections should first be evaluated in full theory. It is then matched with the effective theory as,

$$A_{\text{full}} = A_{\text{eff}} = \frac{G_F}{\sqrt{2}} V_{us} V_{ud}^* (\mathcal{C}_1 \langle O_1 \rangle + \mathcal{C}_2 \langle O_2 \rangle) \tag{2.15}$$

The full amplitude corresponding to diagrams in Figure 2.2 and their symmetric counterparts, at order α_s is,

$$\begin{aligned} A_{\text{full}} = \frac{G_F}{\sqrt{2}} V_{us} V_{ud}^* [&\left(1 + 2C_F \frac{\alpha_s}{4\pi} (\frac{1}{\epsilon} + \ln \frac{\mu^2}{-p^2}) + \frac{3}{N} \frac{\alpha_s}{4\pi} \ln \frac{m_W^2}{-p^2}\right) \langle O_2 \rangle \\ &- 3 \frac{\alpha_s}{4\pi} \ln \frac{m_W^2}{-p^2} \langle O_1 \rangle] \end{aligned} \tag{2.16}$$

where $C_F = 4/3$ is the relevant color factor. The singularity in Eq. (2.16), $1/\epsilon$, is removed by quark field renormalization. The matrix elements are calculated by solving the corresponding Feynman diagrams in effective theory which are given in Figure 2.3.

$$\begin{aligned} \langle Q_1 \rangle^0 = &\left(1 + 2C_F \frac{\alpha_s}{4\pi} (\frac{1}{\epsilon} + \ln \frac{\mu^2}{-p^2}) + \frac{3}{N} \frac{\alpha_s}{4\pi} (\frac{1}{\epsilon} + \ln \frac{\mu^2}{-p^2})\right) \langle O_1 \rangle \\ &- 3 \frac{\alpha_s}{4\pi} (\frac{1}{\epsilon} + \ln \frac{\mu^2}{-p^2}) \langle O_2 \rangle \end{aligned} \tag{2.17}$$

$$\begin{aligned} \langle Q_2 \rangle^0 = &\left(1 + 2C_F \frac{\alpha_s}{4\pi} (\frac{1}{\epsilon} + \ln \frac{\mu^2}{-p^2}) + \frac{3}{N} \frac{\alpha_s}{4\pi} (\frac{1}{\epsilon} + \ln \frac{\mu^2}{-p^2})\right) \langle O_2 \rangle \\ &- 3 \frac{\alpha_s}{4\pi} (\frac{1}{\epsilon} + \ln \frac{\mu^2}{-p^2}) \langle O_1 \rangle \end{aligned} \tag{2.18}$$

where Q_1^0 and Q_2^0 are the operators before renormalization. Some of the divergences in Eq. (2.17) can be eliminated through the quark field renormalization. The additional divergences can be removed by operator renormalization. As given in Eq. (2.17), $\langle Q_1 \rangle$ is proportional to not just $\langle O_1 \rangle$ but also O_2 and similarly for

Q_2. This feature is called *operator mixing*. Due to this, the operator renormalization constant in this case is a 2×2 matrix, which is given by,

$$Q_i^0 = Z_{ij} Q_j, \tag{2.19}$$

where,

$$Z = 1 + \frac{\alpha_s}{4\pi}\frac{1}{\epsilon}\begin{pmatrix} 3/N & -3 \\ -3 & 3/N \end{pmatrix} \tag{2.20}$$

The matching condition given in Eq. (2.15) gives,

$$\mathcal{C}_1(\mu) = -3\frac{\alpha_s}{4\pi}\ln\frac{m_W^2}{\mu^2} \qquad\qquad \mathcal{C}_2(\mu) = 1 + 3\frac{\alpha_s}{4\pi}\ln\frac{m_W^2}{\mu^2} \tag{2.21}$$

This explains the important feature of OPE which is to disentangle the short-distance and long-distance contributions. It is also clear from the structure in Eq. (2.16) which contains the following factor,

$$\left(1 + C\alpha_s\ln\frac{m_W^2}{-p^2}\right) = \left(1 + C\alpha_s\ln\frac{m_W^2}{\mu^2}\right) \times \left(1 + C\alpha_s\ln\frac{\mu^2}{-p^2}\right) \tag{2.22}$$

where $C = 3/(4\pi N)$. From Eqs. (2.17) and (2.21) it can be seen that the contribution of loop corrections from scale μ to m_W is absorbed in Wilson coefficients while the contribution due to scale below μ is absorbed in the definition of operators.

2.2 Effective Hamiltonian for semileptonic transition

In this chapter I have studied various decay modes based on the transition $b \to q_d \ell^+ \ell^-$. Here q_d refers to either a down-quark or strange-quark. Also, both the transitions considered here are based on FCNCs. The only difference arises because of the CKM factors. In this section, the effective Hamiltonian for $b \to q_d \ell^+ \ell^-$ transition is discussed.

The Feynman diagrams which contribute at the leading order are shown in Figure 2.4. The effective Hamiltonian is derived by integrating out the heavy particles which include $W-$boson, $Z-$ boson, and $t-$ quark. The Higgs' field, h, does not play a role since its coupling to light particles is proportional to their mass and thus the effects are negligible. In terms of effective theory, the Hamiltonian can be written as,

$$\mathcal{H}_{\rm eff} = \frac{4G_F}{\sqrt{2}}\left[\sum_{i=1}^{2}\mathcal{C}_i(\xi_c\mathcal{O}_i^c + \xi_u\mathcal{O}_i^u) - \xi_t\sum_{i=3}^{10}\mathcal{C}_i\mathcal{O}_i\right] \tag{2.23}$$

where $\xi_{u,c,t}$ are the CKM factors defined as, $\xi_i = V_{ib}V_{id}^*$. $O_i^{u,c}$ form the operator basis. Within Standard Model, the relevant set of operators for the process are,

$$\begin{aligned}
&\mathcal{O}_1^u = (\bar{d}_L\gamma_\mu T^a u_L)(\bar{u}_L\gamma^\mu T^a b_L) && \mathcal{O}_2^u = (\bar{d}_L\gamma_\mu u_L)(\bar{u}_L\gamma^\mu T^a b_L)\\
&\mathcal{O}_1^c = (\bar{d}_L\gamma_\mu T^a c_L)(\bar{c}_L\gamma^\mu T^a b_L) && \mathcal{O}_2^c = (\bar{d}_L\gamma_\mu c_L)(\bar{c}_L\gamma^\mu b_L)\\
&\mathcal{O}_3 = (\bar{s}_L\gamma_\mu b_L)\sum_q(\bar{q}\gamma^\mu q) && \mathcal{O}_4 = (\bar{s}_L\gamma_\mu T^a b_L)\sum_q(\bar{q}\gamma^\mu T^a q)\\
&\mathcal{O}_5 = (\bar{s}_L\gamma_{\mu_1}\gamma_{\mu_2}\gamma_{\mu_3} b_L)\sum_q(\bar{q}\gamma^{\mu_1}\gamma^{\mu_2}\gamma^{\mu_3} q) &&\\
&\mathcal{O}_6 = (\bar{s}_L\gamma_{\mu_1}\gamma_{\mu_2}\gamma_{\mu_3} T^a b_L)\sum_q(\bar{q}\gamma^{\mu_1}\gamma^{\mu_2}\gamma^{\mu_3} T^a q) &&\\
&\mathcal{O}_7 = \frac{e}{g_s^2}m_b(\bar{d}_L\sigma^{\mu\nu}b_R)F_{\mu\nu} && \mathcal{O}_{8g} = \frac{1}{g_s}m_b(\bar{d}_L\sigma^{\mu\nu}T^a b_R)G^a_{\mu\nu}\\
&\mathcal{O}_9 = \frac{e^2}{g_s^2}(\bar{d}_L\gamma_\mu b_L)(\bar{\ell}\gamma^\mu\ell) && \mathcal{O}_{10} = \frac{e^2}{g_s^2}(\bar{d}_L\gamma_\mu b_L)(\bar{\ell}\gamma^\mu\gamma_5\ell).
\end{aligned} \tag{2.24}$$

where the L(R) subscript refer to the left(right) handed component of the fermions. There can be operators other than defined in Eq. (2.24) in the extension of Standard Model. The full basis including beyond SM operators is given in Appendix A. The extra factors strong coupling constant (g_s) in the definition of the operators are included so that the Wilson coefficients can be written in a perturbative series. The $\mathcal{C}_i$ in Eq. (2.23) are the Wilson coefficients which encode short-distance physics. In terms of perturbation theory, WCs can be expanded as,

$$\mathcal{C}_i = \mathcal{C}_i^{(0)} + \frac{\alpha_s}{4\pi}\mathcal{C}_i^{(1)} + \left(\frac{\alpha_s}{4\pi}\right)^2\mathcal{C}_i^{(2)} + \mathcal{O}(\alpha_s^3) \tag{2.25}$$

Only $\mathcal{C}_i^{(0)}$ are needed for leading logarithm (LL) results. Similarly, for next-to leading logarithm results (NLL) $\mathcal{C}_i^{(1)}$ should also be computed and so on. In literature, the Wilson coefficient for $b \to q_d\ell^+\ell^-$ transitions have been computed

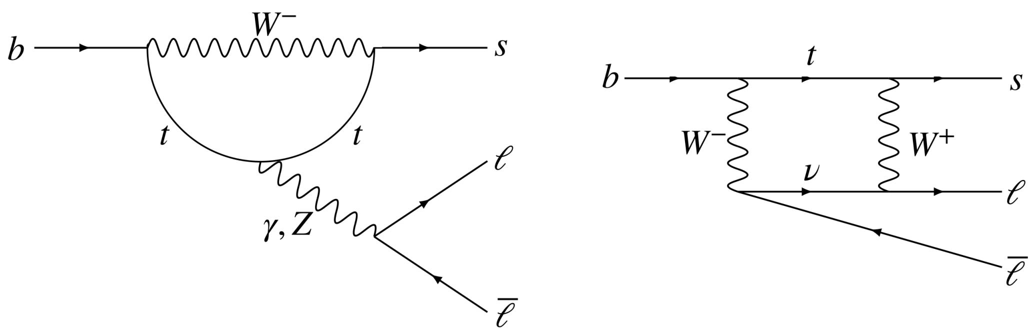

Figure 2.4: The Feynman diagrams corresponding to process $b \to d_i \ell^+ \ell^-$. left: penguin diagram, right: box diagram.

upto NNLL [48–52]. This requires the calculation of matching condition upto two-loop accuracy at scale $\mu = m_W$. To compute the corresponding values at scale $\mu = m_b$, anomalous dimensions in the renormalization-group equations is needed upto three-loop accuracy. As discussed in Section 2.1, the operators can mix during the evolution to a lower scale. They appear in a particular combination within matrix elements, thus for convenience *effective Wilson Coefficients* are defined as,

$$\begin{aligned}
\mathcal{C}_9^{\text{eff}} &= \left(1 + \frac{\alpha_s(\mu)}{\pi}\omega_9(\hat{s})\right)\Big(A_9 - \frac{\xi_c}{\xi_t}T_{9a}\ h(\hat{m_c}^2, \hat{s}) - \frac{\xi_u}{\xi_t}T_{9a}\ h(0, \hat{s}) \\
&\quad + T_{9b}\ h(\hat{m_c}^2, \hat{s}) + U_9\ h(1, \hat{s}) + W_9\ h(0, \hat{s})\Big) + \frac{\alpha_s(\mu)}{4\pi}\Big(\frac{\xi_u}{\xi_t}(\mathcal{C}_1^{(0)}F_{1,u}^{(9)} \\
&\quad + \mathcal{C}_2^{(0)}F_{2,u}^{(9)}) + \frac{\xi_c}{\xi_t}(\mathcal{C}_1^{(0)}F_{1,c}^{(9)} + \mathcal{C}_2^{(0)}F_{2,c}^{(9)}) - A_8^{(0)}F_8^{(9)}\Big), \qquad (2.26a)\\
\mathcal{C}_7^{\text{eff}} &= \left(1 + \frac{\alpha_s(\mu)}{\pi}\omega_7(s)\right)\ A_7 + \frac{\alpha_s(\mu)}{4\pi}\Big(\frac{\xi_u}{\xi_t}(\mathcal{C}_1^{(0)}F_{1,u}^{(7)} + \mathcal{C}_2^{(0)}F_{2,u}^{(7)}) \\
&\quad + \frac{\xi_c}{\xi_t}(\mathcal{C}_1^{(0)}F_{1,c}^{(7)} + \mathcal{C}_2^{(0)}F_{2,c}^{(7)}) - A_8^{(0)}F_8^{(7)}\Big) \qquad (2.26b)\\
\mathcal{C}_{10}^{\text{eff}} &= \left(1 + \frac{\alpha_s(\mu)}{\pi}\omega_9(\hat{s})\right)A_{10} \qquad (2.26c)
\end{aligned}$$

where $h(q^2, m_q)$ is the loop function given by,

$$h(q^2, m_q) = -\frac{4}{9}\left(\ln\frac{m_q^2}{\mu^2} - \frac{2}{3} - z\right) - \frac{4}{9}(2+z)\sqrt{|z-1|} \qquad (2.27)$$

$$\left(\theta(z-1)\tan^{-1}\frac{1}{\sqrt{z-1}} + \theta(1-z)(\ln\frac{1+\sqrt{1-z}}{\sqrt{z}} - \frac{i\pi}{2})\right) \qquad (2.28)$$

where $z = 4m_q^2/q^2$. The auxiliary quantities $A_7, A_9, A_{10}, T_{9a}, T_{9b}, U_9$, and W_9 are linear combinations of various Wilson coefficients and are given in the Appendix

B. In this case, the effective Wilson coefficients at scale $\mu = m_b$ are given as [49] The coefficient $\mathcal{C}_9^{\text{eff}}$ contain a weak phase in the form of CKM parameter and a strong phase is contained in the function $h(q^2, m_q)$. This is the necessary and sufficient condition to be able to study CP violation. However, CP violating observables are expected to be very small in comparison to the experimental sensitivity for $b \to s\ell\ell$ process while that is not the case for $b \to d\ell\ell$. This is because for $b \to s\ell\ell$ decay, $\xi^s_{c,t} \sim \lambda^2$ while the CKM element which are dominated by CKM phase i.e. $\xi_u \sim \lambda^4$. Since the term with CKM phase is suppressed, CP violating quantities are estimated to be small. In case of $b \to d\ell\ell$, $\xi_u \sim \xi_c \sim \xi_t \sim \lambda^4$, thus this transition is sensitive to CP violation.

Using the effective Hamiltonian in Eq. (2.23), the amplitude for the hadronic process $B \to V\ell^+\ell^-$ (where B in the B meson and V is a vector meson) is given by,

$$\mathcal{A}(B \to V\ell^+\ell^-) = \left\langle \ell^+\ell^- V|\mathcal{H}_{\text{eff}}|B\right\rangle \tag{2.29}$$

$$\begin{aligned} &= \left\langle \ell^+\ell^-|\bar{l}\Gamma_i l|0\right\rangle \langle V|\bar{q}_d\Gamma_i' b|B\rangle \\ &+ \frac{e^2}{q^2}\left\langle \ell^+\ell^-|\bar{\ell}\gamma^\mu\ell|0\right\rangle \times \left\langle V|T\left\{j^{had}_{\mu,em}(x)\mathcal{H}^{\text{had}}_{\text{eff}}(0)\right\}|B\right\rangle \end{aligned} \tag{2.30}$$

The first term in Eq. (2.30) includes contribution from operators $\mathcal{O}_{7,9,10}$. The matrix element corresponding to the other operators can not be naively factorized and are categorized as *non-factorizable* terms. The operators $\mathcal{O}_{1-6,8g}$ can contribute to the process only via an intermediate photon, thus amplitude can be written in terms of form factors as [53],

$$\begin{aligned} \mathcal{A}(B \to V\ell^+\ell^-) =& \frac{G_F\alpha}{\sqrt{2}\pi} V_{tb}V^*_{td}\Big[\left\{\left\langle V|\bar{d}\gamma^\mu(\mathcal{C}_9^{\text{eff}}P_L)b|B\right\rangle - \frac{2m_b}{q^2}\left\langle V|\bar{d}\; i\;\sigma^{\mu\nu}q_\nu(\mathcal{C}_7^{\text{eff}}P_R)b|B\right\rangle\right\} \\ & (\bar{\ell}\gamma_\mu\ell) + \left\langle V|\bar{d}\gamma^\mu(\mathcal{C}_{10}^{\text{eff}}P_L)b|B\right\rangle(\bar{\ell}\gamma_\mu\gamma_5\ell) - 16\pi^2\frac{\bar{\ell}\gamma^\mu\ell}{q^2}\mathcal{H}^{\text{non-fac}}_\mu\Big]. \end{aligned} \tag{2.31}$$

These hadronic matrix elements require non-perturbative calculations. For the case where energy of the final meson (V) is large i.e., low$-q^2$ region, Light Cone Sum Rules (LCSR) can be used [54, 55]. The approach depends on standard QCD sum rule technique combined with the information of distribution amplitudes of hadron. QCD factorization (QCDF) formalism [56, 57] suggests that the hadronic matrix elements at leading power in $1/m_b$ are computed in terms of B meson form factors and distribution amplitudes of hadrons involved. The hadronic matrix elements corresponding to the operators $\mathcal{O}_{7,9,10}$ can be expressed in terms of seven form factors, the most general parameterization of which is given by,

$$\langle V(p',\varepsilon^*)|\bar{q}\gamma^\mu b|\bar{B}(p)\rangle = \frac{2iV(q^2)}{m_B+m_V}\epsilon^{\mu\nu\rho\sigma}\varepsilon^*_\nu p'_\rho p_\sigma, \tag{2.32a}$$

$$\begin{aligned}\langle V(p',\varepsilon^*)|\bar{q}\gamma^\mu\gamma_5 b|\bar{B}(p)\rangle = {} & 2m_V A_0(q^2)\frac{\varepsilon^*.q}{q^2}q^\mu + (m_B+m_V)A_1(q^2)\left[\varepsilon^{*\mu} - \frac{\varepsilon^*.q}{q^2}q^\mu\right] \\ & - A_2(q^2)\frac{\varepsilon^*.q}{m_B+m_V}\left[p^\mu + p'^\mu - \frac{m_B^2-m_V^2}{q^2}q^\mu\right],\end{aligned} \tag{2.32b}$$

$$\langle V(p',\varepsilon^*)|\bar{q}\sigma^{\mu\nu}\gamma_\nu b|\bar{B}(p)\rangle = 2T_1(q^2)\epsilon^{\mu\nu\rho\sigma}\varepsilon^*_\nu p_\rho p'_\sigma, \tag{2.32c}$$

$$\begin{aligned}\langle V(p',\varepsilon^*)|\bar{q}\sigma^{\mu\nu}\gamma_5 q_\nu b|\bar{B}(p)\rangle = {} & (-i)T_2(q^2)\left[(m_B^2-m_V^2)\varepsilon^{*\mu} - (\varepsilon^*.q)(p^\mu + p'^\nu)\right] \\ & (-i)T_3(q^2)(\varepsilon^*.q)\left[q^\mu - \frac{q^2}{m_B^2-m_V^2}(p+p')^\mu\right],\end{aligned} \tag{2.32d}$$

where m_B is the mass of B meson, m_V is the mass of vector meson in the final state, and ε^* is the polarization vector of the vector meson. The seven form factors $\{V, A_0, A_1, A_2, T_1, T_2, T_3\}$ are functions of q^2 where, $q = p - p'$. These form factors are hadronic quantities and their computation involves non-perturbative calculations. In the large recoil region, i.e. low-q^2 region, the form factors are computed using light cone sum rules (LCSR) whereas in high-q^2 region the form factors are computed using lattice QCD. However, these calculations suffer from large uncertainties due to hadronic parameters and rely on many assumptions which introduces systematic uncertainties.

$\mathcal{H}_\mu^{\text{non-fac}}$ in Eq. (2.31) represents the non-factorizable contribution of non-local hadronic matrix element. This results from four quark and chromomagnetic operators combined with virtual photon emission which then decays to lepton pair. These corrections are given in terms of hard-scattering kernels ($\mathcal{T}_a^q s$), where $a \in \{\perp, \|\}$ and $q \in \{u, c\}$, which are convoluted with the meson distribution amplitudes [56, 57]. The non-factorizable corrections included in this work are

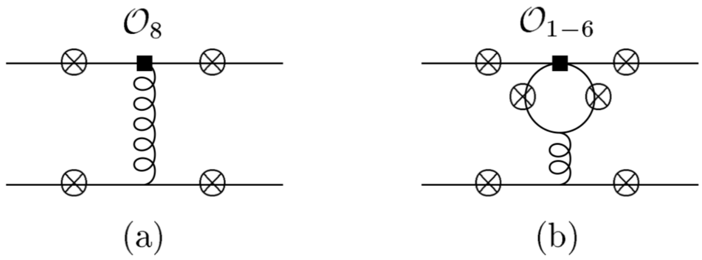

Figure 2.5: Non-factorizable contribution to $B \to V\ell^+\ell^-$ due to spectator scattering. The circled cross marks show the possible insertion of a virtual photon.

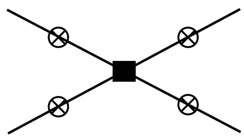

Figure 2.6: Non-factorizable contribution to $B \to V\ell^+\ell^-$ due to weak annihilation.

discussed below.

Spectator Scattering: The intermediate quark loop (up or charm) or chromomagnetic operator (O_{8g}) can emit a hard gluon which can be absorbed by the spectator quark. The Feynman diagrams corresponding to spectator scattering are given in Figure 2.5.

Weak Annihilation: The b quark in the B meson can annihilate with the spectator quark to give the meson in the final state. This contributes to the leading order term in α_s as the QCD correction to weak annihilation is highly suppressed.The Feynman diagrams corresponding to weak annihilation are given by Figure 2.6.

Soft-gluon correction: Quark in the intermediate loop can emit a soft gluon which contributes to non-factorizable correction. The contribution is proportional to $1/(4m_c^2 - q^2)$, and rises near the vector resonances. Hence, it can be calculated in the region $[2-6]$ GeV^2. In the region beyond that, hadronic dispersion relations

i	a^i	b^i	c^i
$\perp$	9.25	-0.5	9.35
$\|\|$	9.25	-0.5	9.35
0	33	-0.9	10.35

Table 2.1: Values of parameters defined for $\Delta C_9^{i,\text{soft}}$

are employed which systematically include the contribution of charm resonance [58]. For $B \to V\ell\ell$ based on $b \to s$ transition, the contribution of these two effects, i.e. soft-gluon emission and charmonium resonances, can be described by the parameterization defined in [26] which is valid in the q^2 region $[1-9]$ GeV^2. Such corrections have not been explicitly computed for process based on $b \to d$ transition. For $B \to K^*\ell\ell$ these corrections are parameterized as,

$$\Delta\mathcal{C}_{9,c}^{\perp,\text{soft}}(q^2) = \frac{a^\perp + b^\perp q^2(c^\perp - q^2)}{q^2(c^\perp - q^2)} \tag{2.33}$$

$$\Delta\mathcal{C}_{9,c}^{\|,\text{soft}}(q^2) = \frac{a^\| + b^\| q^2(c^\| - q^2)}{q^2(c^\| - q^2)} \tag{2.34}$$

$$\Delta\mathcal{C}_{9,c}^{0,\text{soft}}(q^2) = \frac{a^0 + b^0(q^2+1)(c^0 - q^2)}{(q^2+1)(c^0 - q^2)} \tag{2.35}$$

where, the mean values of parameters are given in Table 2.1. These non-factorizable corrections are very important while giving model-based predictions. For instance, it has been shown in [56] that the value of zero of forward-backward asymmetry significantly shifts when contribution of spectator scattering is included.

Λ/m_B *corrections*: One drawback of the QCDF discussed here is that the description works in the limit $m_b \to \infty$. The corresponding corrections form a part of non-factorizable terms as a series expansion in terms of Λ/m_B and are known as *non-factorizable power corrections*. There is no proper method to calculate its contribution, however, they are estimated to be roughly $\mathcal{O}(10\%)$ at amplitude level [58].

Another approach that is used to describe the hadronic matrix elements is based on large energy limit of the final state hadron. The energy of the hadron V is defined as,

$$2m_B E = m_B^2 + m_V^2 - q^2 \tag{2.36}$$

Here, large E implies low q^2 (< 6 GeV^2). There are two advantages of this approach. First, since this region is well below charmonium threshold, there is no interference with resonant contribution. Second, in this limit, the seven form factors (*full form factors*) are reduced to two independent form factors (*soft form factors*) denoted by $\xi_\perp(q^2)$ and $\xi_\|(q^2)$ where $\xi_\perp(q^2)$ contributes to the transverse polarization of the vector meson while $\xi_\|(q^2)$ contributes to the longitudinal polarization. At the leading order in $\mathcal{O}(\alpha_s)$ and $\mathcal{O}(1/m_b)$, the full form factors are related to these two soft-form factors as [59],

$$\xi_\perp(E) = \frac{m_B}{m_B + m_V} V(q^2) = \frac{m_B + m_V}{2E} A_1(q^2) = T_1(q^2) = \frac{m_B}{2E} T_2(q^2) \tag{2.37}$$

$$\begin{aligned} \xi_\|(E) &= \frac{m_V}{E} A_0(q^2) = \frac{m_B + m_V}{2E} A_1(q^2) = \frac{m_B - m_v}{m_B} A_2(q^2) \\ &= \frac{m_B}{2E} T_2(q^2) - T_3(q^2) \end{aligned} \tag{2.38}$$

Using the factorization approach mentioned above, several observables have been constructed with the idea that soft form factors cancel completely. However, in addition to the non-factorizable corrections discussed above, there are additional $\mathcal{O}(\alpha_s)$ and $\mathcal{O}(1/m_b)$ corrections which have been computed in [56, 57, 59]. In the work done for $b \to d\ell\ell$, I have used the full form factors which are available upto twist-5. While for the channel based on $b \to s\ell\ell$ i.e, $B \to K_2^*\ell\ell$, soft form factors have been used.

Chapter 3

$\mathbf{B \to \rho\mu^+\mu^-}$ and $\mathbf{B_s \to \overline{K}^*\mu^+\mu^-}$ decays in Standard Model

A lot of attention has been given to semileptonic decays of bottom hadrons as a result of increasing experimental evidence of new physics. Many decays have been observed involving the FCNC $b \to s\ell^+\ell^-$ and charged current $b \to c\ell\nu$. Most reliable measurements include $R_{K^{(*)}}$ [11, 19] and $R_{D^{(*)}}$ [31, 33, 35, 60, 61] which hint towards Lepton Flavor Universality (LFU) violation. These particular observables have very small theoretical uncertainties because some hadronic parameters cancel in the ratio. These measurements are important for precision tests of the standard model as well as for searches of new physics.

Albeit there exist rich data for $b \to s\ell^+\ell^-$ induced processes, the $b \to d$ counterpart of the weak decay, i.e. $b \to d\ell^+\ell^-$, has not caught much attention perhaps because of low branching ratio. At the quark level, the lowest order contribution arises at one loop level through diagrams similar to $b \to s\ell\ell$ which include box diagrams and electroweak penguin diagrams. The only difference in the two FCNC channels is due to the weak phases from CKM matrix elements $\xi_q^i = V_{qi}^* V_{qb}$, where $q \in \{u, c, t\}$ and $i \in \{s, d\}$. For $b \to s\ell\ell$ transition, $\xi_{c,t}^s \sim \lambda^2$ and $\xi_u^s \sim \lambda^4$ where $\lambda = 0.22$. Since $u\bar{u}$ contribution introduces CKM phase which is negligible for $b \to s\ell\ell$, CP violating quantities are very small in SM. On the other hand, since $\xi_u^d \sim \xi_c^d \sim \xi_t^d \sim \lambda^4$ for $b \to d\ell\ell$, the B decays mediated through this transition allow for large CP violating quantities. Also, leading order contribution in this case is smaller than the leading contribution in $b \to s\ell\ell$ which makes this channel more sensitive to new physics. Hence, it is desirable to study processes like $B \to \{\pi, \rho\}\,\ell^+\ell^-$ and $B_s \to \left\{\bar{K}, \bar{K}^*\right\}\ell^+\ell^-$ experimentally as well as theoretically. The first transition of this variety to be measured is $B \to \pi\ell^+\ell^-$ by LHCb with 5.2σ significance [62] which is in good agreement with the expected value in SM [63, 64]. Other than this $B^0(B_s^0) \to \pi^+\pi^-\mu^+\mu^-$ has also been observed by LHCb, where the muons in final state do not originate from a resonance [65]. In my work, two decay modes have been studied: $B \to \rho\mu^+\mu^-$ and $B_s \to \bar{K}^*\mu^+\mu^-$. Predicted value of branching ratio for $B^0 \to \rho^0\ell^+\ell^-$ is of the same order as $B \to \pi\ell^+\ell^-$, thus making it possible to be measured with upgraded experimental facilities. Since experiments already have good measurements of $B \to K^*\ell^+\ell^-$ mode, it is likely that $B_s \to \bar{K}^*\ell^+\ell^-$ mode may get early attention. The branching ratio of this mode is expected to be a factor of two more that $B^0 \to \rho^0\ell^+\ell^-$ owing to the factor of $1/\sqrt{2}$ in the definition of $\rho^0 \sim (u\bar{u} - d\bar{d})/\sqrt{2}$ as compared to $K^* \sim \bar{s}d$. Further, neglecting SU(3) breaking effects, one expects the branching fractions to be $\mathcal{O}(\lambda^2)$ smaller than those in $b \to s\ell^+\ell^-$ decays. Predictions for certain observables including branching ratio, direct CP asymmetry, and forward-backward asymmetry have been given for $B \to \rho\ell^+\ell^-$ [57, 66–69]. For $B_s \to \bar{K}^*\mu^+\mu^-$, only branching ratio has been studied based on relativistic quark model [70] and light cone sum rules (LCSR) based on heavy quark effective theory (HQET) approach [71]. However, a complete study of angular distribution is lacking.

Phenomenological analysis of the decays induced by this channel will provide complementary information about the nature of New Physics (NP). The most prevailing problem in the theoretical description is due to the long distance effects of $c\bar{c}$ and $u\bar{u}$ resonant states. In the q^2 region close to these resonances, only model dependent predictions are available which result in large uncertainty. To avoid these uncertainties, the study has been restricted to a region which is well below J/ψ resonance region ~ 6 GeV^2.

3.1 Theoretical Framework

B and B_s are pseudoscalar mesons while ρ and $\bar{K}^*$ are vector mesons. The general formalism of $B \to V\ell\ell$ process discussed in Section 2.2, applies here. The amplitude is given by Eq. (2.31)

$$\mathcal{M} = \frac{G_F \alpha}{\sqrt{2}\pi} V_{tb} V_{td}^* \Big[\Big\{ \langle V | \bar{d}\gamma^\mu (C_9^{\text{eff}} P_L) b | P \rangle - \frac{2m_b}{q^2} \langle V | \bar{d}\; i\; \sigma^{\mu\nu} q_\nu (C_7^{\text{eff}} P_R) b | P \rangle \Big\} (\bar{\ell}\gamma_\mu \ell) + \langle V | \bar{d}\gamma^\mu (C_{10}^{\text{eff}} P_L) b | P \rangle (\bar{\ell}\gamma_\mu \gamma_5 \ell) - 16\pi^2 \frac{\bar{\ell}\gamma^\mu \ell}{q^2} \mathcal{H}_\mu^{\text{non-fac}} \Big]. \quad (3.1)$$

The non-factorizable corrections that have been taken into account involves spectator scattering, weak annihilation, and soft-gluon correction as discussed in Section 2.2. he expressions for soft-gluon emission from the up loop are still absent and need to be computed properly. Though the corresponding expressions exist for $B \to \pi\ell\ell$ mode but they can not be naively used for the present purpose. For current study, we are assuming an uncertainty of $\sim 10\%$ in C_9 to account for this missing piece:

$$\delta C_{9,u}^{\text{soft}} = a e^{i\theta} \quad (3.2)$$

where, $|a| \in \{0, 0.5\}$ and $\theta \in \{0, \pi\}$. The evaluation, particularly the sign, of this correction requires a complete LCSR calculation which is beyond the present work. The impact of these contributions doesn't turn out to be very significant except for one or two observables. However, to be complete and to indicate possible effect of these corrections, we include them in our numerical study.

3.2 Transversity Amplitudes

The amplitude given in Eq.(3.1) can be written in terms of helicity amplitudes. Consider the decay of B meson as $B \to VV'$, where V is the usual final state vector meson and V' is the intermediate vector particle which decays into the lepton pair. The amplitude for the process can be written as,

$$\mathcal{M}(m,n)(B \to VV') = \varepsilon_V^\mu(m) \mathcal{M}_{\mu\nu} \varepsilon_{V'}^\nu(n) \quad (3.3)$$

Parameter	Value	Parameter	Value
f_B	200 ± 30 MeV [57]	f_{B_s}	230 ± 30MeV [72]
$f_{\rho,\perp}$	150 ± 25 MeV [57]	$f_{K^*,\perp}$	175 ± 25 MeV [72]
$f_{\rho,\parallel}$	209 ± 1 MeV [57]	$f_{K^*,\parallel}$	218 ± 4 MeV [72]
$a^{\parallel}_{1,K^*}$	0.17 ± 0.04 [73]	$a^{\perp}_{1,K^*}$	0.18 ± 0.05 [73]
$a^{\parallel}_{2,K^*}$	0.05 ± 0.05 [73]	$a^{\perp}_{2,K^*}$	0.03 ± 0.03 [73]
$a^{\parallel}_{1,\bar{K}^*}$	-0.17 ± 0.04 [73]	$a^{\perp}_{1,\bar{K}^*}$	-0.18 ± 0.05 [73]
$a^{\parallel}_{2,\bar{K}^*}$	0.05 ± 0.05 [73]	$a^{\perp}_{2,\bar{K}^*}$	0.05 ± 0.05 [73]

Table 3.1: The input parameters used to calculate non-factorizable corrections.

where, $\varepsilon^{\mu}_{V}(n)$ and $\varepsilon^{\mu}_{V'}(n)$ are the polarization vectors of V and V' respectively, and given by,

$$\varepsilon^{\mu}_{V}(\pm) = (0, 1, \pm i, 0)/\sqrt{2} \tag{3.4}$$

$$\varepsilon^{\mu}_{V}(0) = (k_z, 0, 0, k_0)/m_{K^*} \tag{3.5}$$

$$\varepsilon^{\mu}_{V'}(\pm) = (0, 1, \mp i, 0)/\sqrt{2} \tag{3.6}$$

$$\varepsilon^{\mu}_{V'}(0) = (-q_z, 0, 0, -q_0)/\sqrt{q^2} \tag{3.7}$$

$$\varepsilon^{\mu}_{V'}(t) = (q_0, 0, 0, q_z)/\sqrt{q^2} \tag{3.8}$$

where $q^{\mu} = (q_0, 0, 0, q_z)$ and $k^{\mu} = (k_0, 0, 0, k_z)$ are the four-momenta of V' and V respectively. The helicity amplitudes can now be written by contracting $\mathcal{M}_{\mu\nu}$ with specific polarization vectors. Using Eq. (3.3),

$$H_m = \mathcal{M}(m, m)(B \to VV') \tag{3.9}$$

where n can be $0, +, -$. Transversity amplitudes are defined as linear combinations of helicity amplitudes as,

$$A_{\perp,\parallel} = (H_+ \mp H_-)/\sqrt{2} \tag{3.10}$$

$$A_0 = H_0 \tag{3.11}$$

$$A_t = \mathcal{M}_{(0,t)}(B \to VV') \tag{3.12}$$

The full amplitude for the process $B \to V\ell^+\ell^-$ can now be written in terms of amplitude of $B \to VV'$ followed by the subsequent decay of V' in a lepton pair,

$$\mathcal{M}(B \to VV'(\to \mu^+\mu^-))(m) \propto \varepsilon_V^{*\mu}(m)\mathcal{M}_{\mu\nu} \sum_{n,n'} \varepsilon_{V'}^{*\nu}\varepsilon_{V'}^{\rho}(n')g_{n,n'}(\bar{\ell}\gamma_\rho P_{L,R}\ell) \tag{3.13}$$

where $g_{n,n'} = \mathrm{diag}(+,-,-,-)$ and $P_{L,R} = (1 \pm \gamma_5)/2$. The amplitude can be written in terms of three transversity amplitudes corresponding to the left chirality ($A^L_{\perp,\|,0}$) and three transversity amplitudes for the right chirality of the lepton pair($A^R_{\perp,\|,0}$), as well as A_t. The non-factorizable corrections discussed in Section can be added to transversity amplitudes or the Wilson coefficient C_9^{eff}. Following [56, 58], we add the corrections in the transversity amplitudes which are then given by,

$$\begin{aligned} A_{\perp L,R}(q^2) &= \sqrt{2\lambda}\; N\big[2\frac{m_b}{q^2}(C_7^{\text{eff}}T_1(q^2) + \Delta T_\perp) + (C_9^{\text{eff}} \mp C_{10} \\ &\quad + \Delta C_9^1(q^2))\frac{V(q^2)}{M_B + M_V}\big] \end{aligned} \tag{3.14a}$$

$$\begin{aligned} A_{\| L,R}(q^2) &= -\sqrt{2}N(M_B^2 - M_V^2)\big[2\frac{m_b}{q^2}(C_7^{\text{eff}}T_2(q^2) + 2\frac{E(q^2)}{M_B}\Delta T_\perp) \\ &\quad + (C_9^{\text{eff}} \mp C_{10} + \Delta C_9^2(q^2))\frac{A_1(q^2)}{M_B - M_V}\big] \end{aligned} \tag{3.14b}$$

$$\begin{aligned} A_{0L,R}(q^2) &= -\frac{N}{2M_V\sqrt{q^2}}\big[2m_b\big((M_B^2 + 3M_V^2 - q^2)(C_7^{\text{eff}}T_2(q^2)\big) \\ &\quad - \frac{\lambda}{M_B^2 - M_v^2}(C_7^{\text{eff}}T_3(q^2) + \Delta T_\|)) + (C_9^{\text{eff}} \mp C_{10} + \Delta C_9^3) \\ &\quad \big((M_B^2 + M_V^2 - q^2)(M_B + M_V)A_1(q^2) - \frac{\lambda}{M_B + M_V}A_2(q^2)\big)\big] \end{aligned} \tag{3.14c}$$

$$A_t(q^2) = \frac{N}{\sqrt{s}}\sqrt{\lambda}2C_{10}A_0(q^2) \tag{3.14d}$$

where,

$$\Delta T_\perp = \frac{\pi^2}{N_c}\frac{f_P f_{V,\perp}}{M_B}\frac{\alpha_s C_F}{4\pi}\int \frac{d\omega}{\omega}\Phi_{P,+}(\omega)\int_0^1 du\; \Phi_{V,\perp}(u)(T_\perp^{c,\text{spec}} + \frac{\xi_u}{\xi_t}(T_\perp^{u,\text{spec}})) \tag{3.15}$$

$$\begin{aligned} \Delta T_\| &= \frac{\pi^2}{N_c}\frac{f_P f_{V,\|}}{M_B}\frac{M_V}{E}\sum_\pm \int \frac{d\omega}{\omega}\Phi_P(\omega)\int_0^1 du\; \Phi_{V,\|}(u)\big[T_\|^{c,WA} + \frac{\xi_u}{\xi_t}T_\|^{u,WA} \\ &\quad \frac{\alpha_s C_F}{4\pi}(T_\|^{c,\text{spec}} + \frac{\xi_u}{\xi_t}T_\|^{,\text{spec}})\big] \end{aligned} \tag{3.16}$$

$$\Delta C_9^i = \Delta C_{9,c}^{i,soft} + \Delta C_{9,u}^{i,soft} \tag{3.17}$$

where $P \equiv \bar{B}, \bar{B}_s$ and $V \equiv \rho, K^*$. The values of input parameters used to calculate the corrections are given in Table 3.1.

3.3 Form Factors

The matrix elements corresponding to operators $\mathcal{O}_{7,9,10}$ are expressed in terms of seven form factors which are functions of q^2:

$$\begin{aligned}
c_V\langle V(k)|\bar{d}\gamma^\mu b|B(p)\rangle &= \frac{2V(q^2)}{m_B+m_V}\epsilon^{\mu\nu\rho\sigma}\epsilon^*_\nu p_\rho k_\sigma, \\
c_V\langle V(k)|\bar{d}\gamma^\mu\gamma_5 b|P(p)\rangle &= 2im_V A_0(q^2)\frac{\epsilon^*\cdot q}{q^2}q^\mu + i(m_B+m_V)A_1(q^2)\left[\epsilon^*_\mu - \frac{\epsilon^*\cdot q}{q^2}q^\mu\right] \\
&\quad - iA_2(q^2)\frac{\epsilon^*\cdot q}{m_B+m_V}\left[P^\mu - \frac{m_B^2-m_V^2}{q^2}q^\mu\right], \\
c_V\langle V(k)|\bar{d}q_\nu\sigma^{\mu\nu}b|P(p)\rangle &= 2iT_1(q^2)\epsilon^{\mu\nu\rho\sigma}\epsilon^*_\nu p_\rho k_\sigma, \\
c_V\langle V(k)|\bar{d}q_\nu\sigma^{\mu\nu}\gamma_5 b|P(p)\rangle &= T_2(q^2)\left[(m_B^2-m_V^2)\epsilon^*_\mu - \epsilon^*\cdot qP^\mu\right] \\
&\quad + T_3(q^2)\epsilon^*\cdot q\left[q^\mu - \frac{q^2(p+k)^\mu}{m_B^2-m_V^2}\right],
\end{aligned} \tag{3.18}$$

where $q_\mu = (p-k)_\mu$, $P_\mu = (p+k)_\mu$, and $c_V = 1/\sqrt{2}$ in the case of $\bar{B}^0 \to \rho^0\ell\ell$; 1 for $\bar{B}_s \to K^*\ell\ell$ and $\bar{B}^\pm \to \rho^\pm\ell\ell$. Form factors can be calculated using the method of QCD Sum Rules on Light-Cone (LCSRs) in the low-q^2 region. For semileptonic B decays, the method involves calculation of correlation function of the weak currents involving b quark, evaluated between the vacuum and light meson in the final state. The correlation function is factorized into non-perturbative and process-independent hadron distribution amplitudes (DAs), ϕ, convoluted with process-dependent amplitudes T.

$$\text{correlation function} \sim \sum_n T^{(n)} \otimes \phi^{(n)} \tag{3.19}$$

where, n represents twist. The contributions with increasing twist decreases by increasing powers of virtualities of the currents involved ($\sim m_b^2$ in the low q^2 range). We follow [55] for form factors of $B \to \rho$ and $B_s \to K^*$ hadronic decays, which provides an improved determination of $B \to V$ form factors compared to

Parameter	Value	Parameter	Value
M_B	5.27 GeV	M_ρ	0.775 $\pm$ 0.025 GeV
M_{B_s}	5.366 GeV	M_{K^*}	0.891 GeV
m_b	4.80 $\pm$ 0.06 GeV	m_c	1.4 $\pm$ 0.2 GeV
μ	5 GeV	α_s	0.215
G_F	1.16×10^{-5} GeV^{-2}	α_{em}	1/137
λ	0.22506 $\pm$ 0.00050	A	0.811 $\pm$ 0.026
$\bar{\rho}$	$0.124^{0.019}_{-0.018}$	$\bar{\eta}$	0.356 $\pm$ 0.011

Table 3.2: The inputs used to obtain numerical values of observables

those in [54]. In [55], updated values of hadronic parameters are used and contributions upto twist-5 in DAs have been systematically included. Further, making use of equations of motion, it is shown that the uncertainties in the ratios of form factors are reduced and so does the dependence on mass scheme. Another advantage is that the combined fits to sum rules and lattice calculations at low and high q^2 are given which provides form factors valid over the whole range. In this work, we call the updated form factors as BSZ (Bharucha-Straub-Zwicky) form factors while those in [54] as BZ (Ball-Zwicky) form factors.

The form factors are written as a series expansion in terms of the parameter [55],

$$z(t) = \frac{\sqrt{t_+ - t} - \sqrt{t_+ - t_0}}{\sqrt{t_+ - t} + \sqrt{t_+ - t_0}} \tag{3.20}$$

where, $t_\pm = (M_B \pm M_V)^2$ and $t_0 = t_+(1 - \sqrt{1 - t_-/t_+})$. Form factors are parametrized as:

$$F_i(q^2) = (1 - s/m_{R,i}^2)^{-1} \Sigma_k \alpha_k^i \left[z(s) - z(0)\right]^k . \tag{3.21}$$

where $m_{R,i}$ is the resonance mass which is equal to 5.279 GeV for $A_0(s)$, 5.325 GeV for $T_1(s)$ and $V(s)$, and 5.724 GeV for rest of the form factors.

Below, detailed SM predictions are provided employing BSZ form factors, computed using LCSRs, which is referred to as BSZ1 form factors in this chapter. To compare the numerical impact of the improved form factors, a direct comparison has been provided between results obtained using BSZ form factors with lattice and LCSR results combined together (referred as BSZ2 form factors in this chapter), and BZ form factors, in the case of $\bar{B}_s \to K^*\ell^+\ell^-$. While for $\bar{B}^0 \to \rho^0\ell^+\ell^-$, BSZ form factors (LCSR) have been used only, since combined fit with lattice results are not available for this mode.

3.4 Observables

In the experiments, $B \to K^*\ell^+\ell^-$ is treated as a four-body decay as resonant contribution from $K^* \to K\pi$ is considered. Similarly, the four-body decay under study here are $B_s \to \bar{K}^*(\to K^-\pi^+)\ell^+\ell^-$, $B \to \rho\ell^+\ell^-$ and their CP conjugates. For a four body decay, $B \to V(\to M_1M_2)\ell^+\ell^-$, the decay distribution can be completely described in terms of four kinematic variables; the lepton invariant mass squared (q^2) and three angles θ_V, θ_l, and ϕ. The angle θ_V is the angle between direction of flight of M_2 with respect to B meson in the rest frame of V, θ_ℓ is the angle made by ℓ^- with respect to the B meson in the dilepton rest frame and ϕ is the azimuthal angle between the two planes formed by dilepton and M_1M_2. The full angular decay distribution of $B \to V(\to M_1M_2)\ell^+\ell^-$ is given by [74],

$$\frac{d^4\Gamma}{dq^2\ dcos\theta_V\ d\theta_\ell\ d\phi} = \frac{9}{32\pi} I(q^2, \theta_V, \theta_\ell, \phi) \tag{3.22}$$

where,

$$\begin{aligned} I(q^2, \theta_V, \theta_\ell, \phi) = \Big(& I_1^s \sin^2\theta_V + I_1^c \cos^2\theta_V + (I_2^s \sin^2\theta_V + I_2^c \cos^2\theta_V)\cos 2\theta_\ell \\ & + I_3 \sin^2\theta_V \sin^2\theta_\ell \cos 2\phi + I_4 \sin 2\theta_V \sin 2\theta_\ell \cos\phi + I_5 \sin 2\theta_V \sin\theta_\ell \cos\phi \\ & + (I_6^s \sin^2\theta_V + I_6^c \cos^2\theta_V)\cos\theta_\ell + I_7 \sin 2\theta_V \sin\theta_\ell \sin\phi \\ & + I_8 \sin 2\theta_V \sin 2\theta_\ell \sin\phi + I_9 \sin^2\theta_V \sin^2\theta_\ell \sin 2\phi \Big). \end{aligned} \tag{3.23}$$

Here, V is an intermediate vector meson which decays to M_1 and M_2 whereas $\ell^+\ell^-$ can be any lepton pair. The corresponding angular decay distribution

$(d^4\bar{\Gamma}/(dq^2 dcos\theta_\pi d\theta_\ell d\phi))$ for the CP-conjugated process, $\bar{B} \to \bar{V}(\to \bar{M}_1\bar{M}_2)\ell^+\ell^-$, is obtained from Eq. (3.22) with the replacement, $I_i \to \tilde{I}_i \equiv \zeta_i \bar{I}_i$, where, $\zeta_i = 1$ for $i \in \{1,2,3,4,7\}$ and -1 for $i \in \{5,6,8,9\}$. $\bar{I}_i$ is equal to I_i with the weak phase (CKM phase here) conjugated. The functions I_i can be written in terms of transversity amplitudes [74]. In the $b \to s$ transition, since the Wilson coefficients are effectively real, modulo a small imaginary part coming due to function $h(m^2, s)$ in $C_9^{\rm eff}$, $\bar{I}_i$ are essentially I_i and observables sensitive to imaginary part of I_i are rather small within SM. This is not the case in $b \to d$ induced decays and we see this feature explicitly in the results below. Various observables are constructed from Eq. (3.22) by integrating over angles in various range. These observables are generally plagued with large uncertainties due to form factors. To avoid this, a lot of work has been done to construct observables which are theoretically clean in low-q^2 region [75–81]. Such observables are free from this dependence at the leading order and are called *form factor independent* (FFI) observables. Those which have a form factor dependence in the leading order are called *form factor dependent* (FFD) observables. We study both classes of observables as discussed below. We shall see below, SU(3) breaking effects are clearly visible in some of the observables.

FFD observables are (which have been experimentally studied in the context of $B \to \bar{K}^*\ell\ell$[71]):

$$\frac{d\Gamma}{dq^2} = \int_{-1}^{1} {\rm dcos}\theta_\ell \int_{-1}^{1} {\rm dcos}\theta_V \int_0^{2\pi} \phi \frac{d^4\Gamma}{dq^2 {\rm dcos}\theta_V {\rm dcos}\theta_\ell d\phi} = \frac{1}{4}(3I_1^c + 6I_1^s - I_2^c - 2I_2^s) \tag{3.24a}$$

$$A_{FB}(q^2) = \frac{1}{d\Gamma/dq^2}\left[\int_{-1}^{0} - \int_0^1\right] {\rm dcos}\theta_\ell \frac{d^4\Gamma}{dq^2 {\rm dcos}\theta_\ell} = \frac{-3I_6^s}{3I_1^c + 6I_1^s - I_2^c - 2I_2^s} \tag{3.24b}$$

$$F_L(q^2) = \frac{3I_1^c - I_2^c}{3I_1^c + 6I_1^s - I_2^c - 2I_2^s} \tag{3.24c}$$

where, $\frac{d\Gamma}{dq^2}$ is the dilepton spectrum distribution, $A_{FB}(q^2)$ is the forward-backward asymmetry and $F_L(q^2)$ is the fraction of longitudinal polarization of the intermediate vector meson. Similar observables are constructed for the CP-conjugate process using the decay distribution $d^4\bar{\Gamma}/(dq^2\ dcos\theta_\pi\ d\theta_\ell\ d\phi)$ discussed above.

FFI observables or "clean observables" are independent of form factors in the leading order of $1/m_b$ and α_s thus exhibiting low hadronic uncertainties and enhanced sensitivity to new physics. Much attention has been given to the construction of such observables and some of them have been measured experimentally [13, 15]. We consider following set of FFI observables here:

$$\begin{aligned} P_1 &= \frac{I_3}{2I_2^s},\ P_2 = \beta_l \frac{I_6^s}{8I_2^s},\ P_3 = \frac{I_9}{4I_2^s},\ P_4' = \frac{I_4}{\sqrt{-I_2^c I_2^s}} \\ P_5' &= \frac{I_5}{2\sqrt{-I_2^c I_2^s}},\ P_6' = -\frac{I_7}{2\sqrt{-I_2^c I_2^s}},\ P_8' = -\frac{I_8}{2\sqrt{-I_2^c I_2^s}} \end{aligned} \tag{3.25}$$

We also consider observables analogous to R_{K^*} for which the form factor dependence cancels exactly for $B_s \to \bar{K}^*\ell\ell$, defined as:

$$R_{K^*}^{B_s} = \frac{\left[\mathcal{BR}(B_s \to \bar{K}^*\mu^+\mu^-)\right]_{q^2 \in \left\{q_1^2, q_2^2\right\}}}{\left[\mathcal{BR}(B_s \to \bar{K}^* e^+ e^-\right]_{q^2 \in \left\{q_1^2, q_2^2\right\}}} \tag{3.26}$$

where, numerator and denominator are integrated over q^2 in the range $[q_1^2 - q_2^2]$ GeV^2. Observables defined in Eqs. (3.24,3.25,3.26) are valid for $B_s \to \bar{K}^*\ell^+\ell^-$ decay mode. It has been pointed out in literature that the zeroes (value of q^2 where observables is zero) are also clean observables [82, 83]. Also, the relation between zeroes of different observables provide crucial tests of Standard Model. Thus, we also provide values of zeroes of different observables. Observables for the CP-conjugate decay, $\bar{B}_s \to K^*\ell^+\ell^-$ are also defined in the same way, with the substitution $I_i \to \bar{I}_i \equiv \zeta_i \tilde{I}_i$. Results for $B_s(\bar{B}_s) \to \bar{K}^*(K^*)\mu^+\mu-$ are given in the next section which can be compared with data collected at LHCb as well as Belle.

However, for $B^0 \to \rho^0\ell^+\ell^-$, results corresponding to LHCb and Belle have to be computed separately. Since $\rho^0 \to \pi\pi$, which is not a flavor specific state, the observables are affected by $B^0 - \bar{B}^0$ oscillations and the expressions of angular coefficients (I_is) defined in Eq. ((3.22)), have to be modified.

3.4.1 Time dependence of angular coefficients

Consider the transversity amplitude of $B \to f_{CP}\ell^+\ell^-$ by $\mathcal{A}_i$. The transversity amplitude for the CP-conjugate process $\bar{B} \to f_{CP}\ell^+\ell^-$ is then given by, $\tilde{A}_i$. The time evolution of the amplitudes is given by,

$$A_i(t) = g_+(t)A_i(0) + \frac{q}{p}g_-(t)\tilde{A}_i(0) \tag{3.27}$$

$$\tilde{A}_i(t) = \frac{p}{q}g_-(t)A_i(0) + g_+(t)\tilde{A}_i(0) \tag{3.28}$$

where, the argument of the amplitude 't' stands for time. The amplitude at $t = 0$ implies amplitude before taking the meson oscillation into account. Considering that CP violation in $B - \bar{B}$ mixing is small,

$$\frac{q}{p} = e^{i\phi} \tag{3.29}$$

where ϕ is the mixing angle, given by $\phi_{B_d} = \tan^{-1}(-1)$ and $\phi_{B_s} = \tan^{-1}(0.04)$. $g_\pm(t)$ in Eq. (3.27) are the usual time-evolution functions and given by,

$$g_+(t) = e^{-imt}e^{-\Gamma t/2}\left[\cosh\frac{\Delta\Gamma t}{4}\cos\frac{\Delta m t}{2} - i\sinh\frac{\Delta\Gamma t}{4}\sin\frac{\Delta m t}{2}\right] \tag{3.30}$$

$$g_-(t) = e^{-imt}e^{-\Gamma t/2}\left[-\sinh\frac{\Delta\Gamma t}{4}\cos\frac{\Delta m t}{2} + i\cosh\frac{\Delta\Gamma t}{4}\sin\frac{\Delta m t}{2}\right] \tag{3.31}$$

where $\Delta\Gamma$ and Δm are the difference in decay width and mass of the two physical states respectively, and

$$x = \Delta m/\Gamma \qquad\qquad y = \Delta\Gamma/2\Gamma \tag{3.32}$$

Substituting the time-dependent amplitudes in the definitions of angular coefficients given in Appendix C, we get the angular coefficients as function of time [84],

$$J_i(t) + \tilde{J}_i(t) = e^{-\Gamma t}[(I_i + \tilde{I}_i)\cosh(y\Gamma t) - h_i \sinh(y\Gamma t)], \tag{3.33}$$

$$J_i(t) - \tilde{J}_i(t) = e^{-\Gamma t}[(I_i - \tilde{I}_i)\cos(x\Gamma t) - s_i \sin(x\Gamma t)], \tag{3.34}$$

Where $J_i(t)$ and $\tilde{J}_i(t)$ are the time-dependent angular coefficients corresponding to the process $\bar{B} \to f_{CP}\ell^+\ell^-$ and $B \to f_{CP}\ell^+\ell^-$ respectively. They are related by,

$$\tilde{J}_i = \xi_i \bar{J}_i \tag{3.35}$$

where $\bar{J}_i$ are obtained by changing sign of all the weak phases in J_i. The additional functions (h_i and s_i) arise because of the mixing in B^0 meson system and are given in Appendix. This leads to two types of quantities, time-dependent observables and time-integrated observables. In this work, we consider observables which include time-integrated angular coefficients over a range $t \in [0, \infty)$ in the case of LHCb and $t \in (-\infty, \infty)$(in addition to $\exp(-\Gamma t) \to \exp(-\Gamma|t|)$) at Belle [84, 85]. After time-integration, the modified angular coefficients are given by,

$$\left\langle J_i + \tilde{J}_i \right\rangle_{\text{LHCb}} = \frac{1}{\Gamma}\left[\frac{I_i + \tilde{I}_i}{1-y^2} - \frac{y}{1-y^2} \times h_i\right], \tag{3.36}$$

$$\left\langle J_i - \tilde{J}_i \right\rangle_{\text{LHCb}} = \frac{1}{\Gamma}\left[\frac{I_i - \tilde{I}_i}{1+x^2} - \frac{x}{1+x^2} \times s_i\right], \tag{3.37}$$

$$\left\langle J_i + \tilde{J}_i \right\rangle_{\text{Belle}} = \frac{2}{\Gamma}\left[\frac{1}{1-y^2} \times (I_i + \tilde{I}_i)\right], \tag{3.38}$$

$$\left\langle J_i - \tilde{J}_i \right\rangle_{\text{Belle}} = \frac{2}{\Gamma}\left[\frac{1}{1+x^2} \times (I_i - \tilde{I}_i)\right], \tag{3.39}$$

where, $\langle\ \rangle$ represents time-integrated quantity. Other difference at LHCb and Belle arises due to the fact that flavor of the meson can be tagged using flavor-specific decays at Belle. Thus, flavor of the meson decaying to the final state is known at time $t = 0$ and the appropriate angular coefficient (J_i or $\tilde{J}_i$) can be used. On the other hand, there is no method to determine the flavor of meson at $t = 0$ at LHCb. As a result, the measured quantity at LHCb is $d\Gamma(B^0 \to \rho^0\ell^+\ell^-) + d\bar{\Gamma}(\bar{B}^0 \to \rho^0\ell^+\ell^-)$ allowing the observation of $\left\langle J_i + \tilde{J}_i \right\rangle$ combination only, which is a CP-averaged quantity for $i \in \{1, 2, 3, 4, 7\}$ and CP-violating quantity for $i \in \{5, 6, 8, 9\}$. Due to the difference in the method of measurement, we consider different observables to be studied at LHCb and Belle. The distinction is made on the basis of whether the flavor of the B meson can be tagged or not.

3.4.2 Observables for tagged decays

In the case when flavor of the $B^0/\bar{B}^0$ meson can be tagged, the definition of observables (say, O) in Eqs. (3.24, 3.25, 3.26) are modified as, $I_i \to \langle J_i \rangle$ and are denoted by $\langle O\rangle^{\text{Tagged}}$. Similarly, for the CP conjugate process, the observables $\left\langle\tilde{O}\right\rangle^{\text{Tagged}}$ are obtained by modification $\bar{I}_i \to \tilde{J}_i$. Full set of observables is given in Eqs. (3.40) and (3.41).

$$\left\langle\frac{d\Gamma}{dq^2}\right\rangle^{\text{Tagged}} = \frac{1}{4}(3J_1^c + 6J_1^s - J_2^c - 2J_2^s) \tag{3.40a}$$

$$\left\langle A_{FB}(q^2)\right\rangle^{\text{Tagged}} = \frac{-3J_6^s}{3J_1^c + 6J_1^s - J_2^c - 2J_2^s} \tag{3.40b}$$

$$\left\langle F_L(q^2)\right\rangle^{\text{Tagged}} = \frac{3J_1^c - J_2^c}{3J_1^c + 6J_1^s - J_2^c - 2J_2^s} \tag{3.40c}$$

$$\left\langle R_\rho\right\rangle^{\text{Tagged}} = \frac{\int_{q_1^2}^{q_2^2} dq^2 \ \left\langle d\Gamma/dq^2\right\rangle^{\text{Tagged}}}{\int_{q1^2}^{q_2^2} dq^2 \ \left\langle d\Gamma/dq^2\right\rangle^{\text{Tagged}}} \tag{3.40d}$$

$$\left\langle P_1\right\rangle^{\text{Tagged}} = \frac{J_3}{2J_{2s}}, \qquad \left\langle P_2\right\rangle^{\text{Tagged}} = \beta_l \frac{J_6^s}{8J_2^s}, \tag{3.41a}$$

$$\left\langle P_3\right\rangle^{\text{Tagged}} = \frac{J_9}{4J_2^s}, \qquad \left\langle P_4'\right\rangle^{\text{Tagged}} = \frac{J_4}{\sqrt{-J_2^c J_2^s}}, \tag{3.41b}$$

$$\left\langle P_5'\right\rangle^{\text{Tagged}} = \frac{J_5}{2\sqrt{-J_2^c J_2^s}}, \qquad \left\langle P_6'\right\rangle^{\text{Tagged}} = \frac{-J_7}{2\sqrt{-J_2^c J_2^s}}, \tag{3.41c}$$

$$\left\langle P_8'\right\rangle^{\text{Tagged}} = \frac{-J_8}{2\sqrt{-J_2^c J_2^s}} \tag{3.41d}$$

the functions J_i and $\tilde{J}_i$ used are time integrated functions obtained from Eq. (3.36) and given as,

$$\begin{aligned} J_i &= \frac{1}{\Gamma}[I_i + \tilde{I}_i + \frac{1}{1+x^2} \times (I_i + \tilde{I}_i)] \\ \tilde{J}_i &= \frac{1}{\Gamma}[I_i + \tilde{I}_i - \frac{1}{1+x^2} \times (I_i + \tilde{I}_i)] \end{aligned} \tag{3.42}$$

The definition of observables for the CP-conjugate decay $\bar{B}^0 \to \rho\mu^+\mu^-$ are obtained by replacing J_i by $\tilde{J}_i (\equiv \zeta_i \bar{I}_i)$.

3.4.3 Untagged

For untagged events, the required modification in the definition of observables is $I_i \to \left\langle J_i + \tilde{J}_i\right\rangle$ and the observables are denoted as $\langle O\rangle^{\text{Untagged}}$. For untagged events, the observables for $B^0 \to \rho^0\mu^+\mu^-$ are defined as,

$$\left\langle\frac{d\Gamma}{dq^2}\right\rangle^{\text{Untagged}} = \frac{1}{2}\left\langle\frac{d\Gamma}{dq^2} + \frac{d\bar{\Gamma}}{dq^2}\right\rangle^{\text{Untagged}} \tag{3.43}$$

$$\left\langle A_{FB}(q^2)\right\rangle^{\text{Untagged}} = \frac{-3(J_6^s + \tilde{J}_6^s)}{4\left\langle d\Gamma/dq^2\right\rangle^{\text{Untagged}}} \tag{3.44}$$

$$\left\langle F_L(q^2)\right\rangle^{\text{Untagged}} = \frac{3(J_1^c + \tilde{J}_1^c) - (J_2^c + \tilde{J}_2^c)}{4\left\langle d\Gamma/dq^2\right\rangle^{\text{Untagged}}} \tag{3.45}$$

$$\langle R_\rho\rangle^{\text{Untagged}} = \frac{\int_{q_1^2}^{q_2^2} dq^2 \ \left\langle d\Gamma/dq^2\right\rangle^{\text{Untagged}} + \left\langle d\Gamma/dq^2\right\rangle^{\text{Untagged}}}{\int_{q1^2}^{q_2^2} dq^2 \ \left\langle d\Gamma/dq^2\right\rangle^{\text{Untagged}} + \left\langle d\Gamma/dq^2\right\rangle^{\text{Untagged}}} \tag{3.46}$$

$$\langle P_1\rangle^{\text{Untagged}} = \frac{J_3 + \tilde{J}_3}{2(J_{2s} + \tilde{J}_2^s)}, \tag{3.47}$$

$$\langle P_2\rangle^{\text{Untagged}} = \beta_l \frac{J_6^s + \tilde{J}_6^s}{8(J_2^s + \tilde{J}_2^s)}, \tag{3.48}$$

$$\langle P_3\rangle^{\text{Untagged}} = \frac{J_9 + \tilde{J}_9}{4(J_2^s + \tilde{J}_2^s}, \tag{3.49}$$

$$\langle P_4'\rangle^{\text{Untagged}} = \frac{J_4 + \tilde{J}_4}{\sqrt{-(J_2^c + \tilde{J}_2^c)(J_2^s + \tilde{J}_2^s)}}, \tag{3.50}$$

$$\langle P_5'\rangle^{\text{Untagged}} = \frac{J_5 + \tilde{J}_5}{2\sqrt{-(J_2^c + \tilde{J}_2^c)(J_2^s + \tilde{J}_2^s)}}, \tag{3.51}$$

$$\langle P_6'\rangle^{\text{Untagged}} = \frac{-(J_7 + \tilde{J}_7)}{2\sqrt{-(J_2^c + \tilde{J}_2^c)(J_2^s + \tilde{J}_2^s)}} \tag{3.52}$$

$$\langle P_8'\rangle^{\text{Untagged}} = \frac{-(J_8 + \tilde{J}_8)}{2\sqrt{-(J_2^c + \tilde{J}_2^c)(J_2^s + \tilde{J}_2^s)}}. \tag{3.53}$$

where,

$$\begin{aligned} J_i &= \frac{1}{2\Gamma}[I_i + \tilde{I}_i + \frac{1}{1+x^2} \times (I_i + \tilde{I}_i) - \frac{x}{1+x^2} \times s_i] \\ \tilde{J}_i &= \frac{1}{2\Gamma}[I_i + \tilde{I}_i - \frac{1}{1+x^2} \times (I_i + \tilde{I}_i) + \frac{x}{1+x^2} \times s_i] \end{aligned} \tag{3.54}$$

It is clear from the form of observables that, Belle allows a study of angular distribution of both $B^0 \to \rho^0\ell^+\ell^-$ and $\bar{B}^0 \to \rho^0\ell^+\ell^-$ decays, while at LHCb, only a CP-averaged or CP-asymmetric study is possible. For the decays considered in this chapter $y = 0$. Thus, observables $\langle O\rangle^{\text{Untagged}}$ are also measurable at Belle. Moreover, it can be noticed from Eq. (3.36), that the value of these observables ($\langle O\rangle^{\text{Untagged}}$), if measured at Belle, are expected to be same at the two experiments, except $\langle BR\rangle^{\text{LHCb}}$, which should be twice for Belle in comparison to LHCb.

Even though tagging power at LHCb is low, new algorithms have been suggested to improve the tagging power by 50% [86, 87]. Thus, for completion we also give predictions for observables which can be measured at LHCb using tagging of B mesons. The definition of these observables is again given by $\langle O\rangle^{\text{Tagged}}$. Moreover, having measurements of angular distribution with and without tagging can be of phenomenological importance.

3.5 Results

In this section, observables have been presented as a function of q^2 and their binned values over two q^2 ranges: [0.1-1] GeV^2 and [1-6] GeV^2 and consider the di-muon pair in the final state. For $\bar{B}_s \to K^*\mu^+\mu^-$, the results are obtained using three sets of form factors. As discussed earlier, the BSZ(LCSR) form factors have been used and the results are compared with the results obtained using BZ form factors and BSZ form factors (LCSR+Lattice results). For $B^0 \to \rho^0\mu^+\mu^-$, only the BSZ form factors have been used.

The values of observables have been given with and without the inclusion of non-factorizable contributions to study their impact. The factorizable corrections are already included in the definition of C_9^{eff} and C_7^{eff} to NNLO. The non-factorizable ones i.e., weak annihilation, spectator scattering, and soft gluon emission are systematically included for predictions in the bin $[1-6]\text{GeV}^2$[1]. As mentioned before, the contribution of soft gluon emission from the up quark loop is not available at present. A very rough estimate leads us to include 10% uncertainty in C_9^{eff} due to this particular correction. The crucial issue here is not just the rough magnitude but also the sign and thus without a proper LCSR based calculation, this is the best one can do. In Tables 3.4, 3.5, 3.10, 3.11, 3.12, we present the value of the observables with these corrections included. In these tables, the first error is due to the form factors while the second shows the spread due to soft gluon emission from the up quark loops. These are presented for

[1]Since the parameterization used to define $\Delta C_{9,c}^{\text{soft}}$ are not valid below 1GeV^2, contribution of soft gluon emission has not been included in the lower bin, $[0.1-1]\text{GeV}^2$.

the BSZ2 set of form factors. It is found that the inclusion of these corrections has significant impact on observables like P_5', branching ratio, and A_{FB}. This confirms the broad pattern observed in $B \to K^*\mu\mu$. Although the results are presented for $[0.1-1]\text{GeV}^2$ and $[1-6]\text{GeV}^2$, a comparison of results with and without these corrections is more meaningful and reliable for $[1-6]$ GeV^2 bin as for $q^2 < 1\text{GeV}^2$, the soft gluon contribution tend to be very large. The observables are also plotted as function of q^2 as shown in Figure 3.7, 3.1, and 3.2. The values of the zeroes are given in Table 3.6 and 3.13. Since the error due to soft gluon emission from up quark is very small, we only show the error due to form factors in the value of zeroes [2].

3.5.1 $B_s \to \overline{K}^* \mu^+\mu^-$

SM predictions of angular observables for $B_s \to \bar{K}^*\mu^+\mu^-$ and $\bar{B}_s \to K^*\mu^+\mu^-$ corresponding to the form factor set BSZ1, BSZ2, and BZ have been given in Table 3.3.

	$\bar{B}_s \to K^*\mu^+\mu^-$		$B_s \to \bar{K}^*\mu^+\mu^-$	
	[0.1-1] GeV^2	[1-6] GeV^2	[0.1-1] GeV^2	[1-6] GeV^2
P_1[BSZ1]	0.006 ± 0.132	-0.081 ± 0.129	0.005 ± 0.131	-0.071 ± 0.114
[BSZ2]	0.008 ± 0.131	-0.097 ± 0.128	0.007 ± 0.129	-0.082 ± 0.113
[BZ]	0.006	-0.084	0.005	-0.069
P_2[BSZ1]	0.124 ± 0.013	0.011 ± 0.078	0.111 ± 0.011	0.094 ± 0.076
[BSZ2]	0.117 ± 0.013	0.051 ± 0.081	0.104 ± 0.011	0.132 ± 0.075
[BZ]	0.127	-0.012	0.110	0.095
P_3[BSZ1]	0 ± 0.001	0.002 ± 0.005	0 ± 0	0.001 ± 0.002
[BSZ2]	0 ± 0.001	0.002 ± 0.005	0 ± 0	0.001 ± 0.002
[BZ]	-0.0	0.001	0	0
P_4'[BSZ1]	-0.488 ± 0.053	0.619 ± 0.151	-0.489 ± 0.051	0.526 ± 0.159
[BSZ2]	-0.506 ± 0.052	0.575 ± 0.161	-0.508 ± 0.049	0.473 ± 0.168

[2] Ignoring the effect of soft gluon emission and time evolution, our results for branching ratio of $B(\bar{B}) \to \rho\mu^+\mu^-$ in the bin $[1-6]\text{GeV}^2$ and zero of A_{FB} are consistent with [57]

[BZ]	-0.489	0.654	-0.481	0.537
P_5'[BSZ1]	0.633 ± 0.057	-0.424 ± 0.119	0.673 ± 0.057	-0.324 ± 0.125
[BSZ2]	0.635 ± 0.055	-0.365 ± 0.126	0.659 ± 0.053	-0.264 ± 0.130
[BZ]	0.632	-0.450	0.679	-0.328
P_6'[BSZ1]	-0.098 ± 0.006	-0.071 ± 0.009	0.004 ± 0.001	-0.012 ± 0.002
[BSZ2]	-0.096 ± 0.006	-0.075 ± 0.010	0.004 ± 0.001	-0.013 ± 0.002
[BZ]	-0.0982	-0.067	0.004	0.024
P_8'[BSZ1]	0.0234 ± 0.004	0.023 ± 0.005	0.003 ± 0.001	0.009 ± 0.002
[BSZ2]	0.023 ± 0.005	0.022 ± 0.005	0.003 ± 0.001	0.009 ± 0.002
[BZ]	0.019	0.017	-0.005	0.003
$R_{K^*}^{B_s}$[BSZ1]	0.939 ± 0.010	0.997 ± 0.004	0.935 ± 0.009	0.997 ± 0.004
[BSZ2]	0.944 ± 0.010	0.999 ± 0.004	0.939 ± 0.011	0.998 ± 0.040
[BZ]	0.929	0.995	0.932	0.995
$BR \times 10^9$[BSZ1]	2.647 ± 0.331	5.807 ± 1.418	3.159 ± 0.378	6.011 ± 1.452
[BSZ2]	3.019 ± 0.366	7.274 ± 1.642	3.526 ± 0.409	7.531 ± 1.685
[BZ]	3.117	7.107	3.712	7.329
A_{FB}[BSZ1]	-0.078 ± 0.009	-0.021 ± 0.028	-0.076 ± 0.009	-0.033 ± 0.029
[BSZ2]	-0.065 ± 0.008	-0.012 ± 0.021	-0.065 ± 0.001	-0.035 ± 0.021
[BZ]	-0.078	0.004	-0.071	-0.033
F_L[BSZ1]	0.343 ± 0.065	0.824 ± 0.050	0.276 ± 0.058	0.800 ± 0.053
[BSZ2]	0.414 ± 0.101	0.876 ± 0.356	0.345 ± 0.058	0.848 ± 0.038
[BZ]	0.341	0.841	0.273	0.815

Table 3.3: Prediction of angular observables for $B_s \to \bar{K}^* \mu^+ \mu^-$ and $\bar{B}_s \to K^* \mu^+ \mu^-$ in the SM

Full branching ratio of $\bar{B}_s \to K^* \mu^+ \mu^-$ in SM using BSZ form factors based on LCSR calculation is,

$$\begin{aligned} \mathcal{BR}(B_s \to \bar{K}^* \mu^+ \mu^-) &= (2.849 \pm 0.719) \times 10^{-8} \\ \mathcal{BR}(\bar{B}_s \to K^* \mu^+ \mu^-) &= (2.897 \pm 0.732) \times 10^{-8} \end{aligned} \tag{3.55}$$

However branching ratio in full kinematic range, form factors based on LCSR are not much reliable as they are valid in low-q^2 region only while the kinematic range extends upto ~ 20 GeV^2 $((M_{B_s} - M_{K^*})^2)$. Hence, we also give below values of branching ratio using form factors obtained from combined fits of lattice and LCSRs results.

$$\begin{aligned} \mathcal{BR}(B_s \to \bar{K}^*\mu^+\mu^-) &= (3.356 \pm 0.814) \times 10^{-8} \\ \mathcal{BR}(\bar{B}_s \to K^*\mu^+\mu^-) &= (3.419 \pm 0.827) \times 10^{-8} \end{aligned} \tag{3.56}$$

which is in agreement with recent LHCb results [88],

$$\mathcal{BR}(B_s \to \bar{K}^*\mu^+\mu^-) = (3.0 \pm 1.0 \pm 0.2 \pm 0.3) \times 10^{-8} \tag{3.57}$$

.

The SM predictions of angular observables for $\bar{B}_s \to K^*\mu^+\mu^-$ are given in Tables 3.4 and 3.5. The value of zeroes of observables are given in Table 3.6. For completion, the observables are also plotted as function of q^2 in Figure 3.7.

	$\bar{B}_s \to K^* \mu^+ \mu^-$	
Observable	[0.1-1] GeV^2	[1-6] GeV^2
P_1	$0.012 \pm 0.129 \pm 0.001$	$-0.081 \pm 0.111 \pm 0.005$
P_2	$0.118 \pm 0.013 \pm 0.001$	$0.112 \pm 0.072 \pm 0.036$
P_3	$0.001 \pm 0.002 \pm 0.0$	$0.004 \pm 0.010 \pm 0.002$
P_4'	$-0.593 \pm 0.057 \pm 0.009$	$0.464 \pm 0.164 \pm 0.014$
P_5'	$0.547 \pm 0.051 \pm 0.016$	$-0.286 \pm 0.125 \pm 0.046$
P_6'	$-0.104 \pm 0.006 \pm 0.016$	$-0.095 \pm 0.011 \pm 0.002$
P_8'	$0.015 \pm 0.003 \pm 0.016$	$0.040 \pm 0.004 \pm 0.017$
$R_{K^*}^{B_s}$	$0.940 \pm 0.009 \pm 0.001$	$0.998 \pm 0.004 \pm 0.0$
$BR \times 10^9$	$3.812 \pm 0.450 \pm 0.086$	$7.803 \pm 1.758 \pm 0.357$
A_{FB}	$-0.060 \pm 0.008 \pm 0.001$	$-0.029 \pm 0.020 \pm 0.009$
F_L	$0.453 \pm 0.067 \pm 0.014$	$0.853 \pm 0.038 \pm 0.007$

Table 3.4: Summary of observables for $\bar{B}_s \to K^* \mu^+ \mu^-$ using BSZ2 form factors. The first uncertainty is due to form factors and second is due to soft-gluon corrections with up quark in the loop.

	$B_s \to \bar{K}^*\mu^+\mu^-$	
Observable	[0.1-1] GeV^2	[1-6] GeV^2
P_1	$0.011 \pm 0.135 \pm 0.001$	$-0.075 \pm 0.108 \pm 0.005$
P_2	$0.112 \pm 0.013 \pm 0.001$	$0.142 \pm 0.071 \pm 0.034$
P_3	$0.001 \pm 0.007 \pm 0.0$	$0.003 \pm 0.010 \pm 0.002$
P_4'	$-0.650 \pm 0.060 \pm 0.008$	$0.379 \pm 0.171 \pm 0.016$
P_5'	$0.543 \pm 0.053 \pm 0.016$	$-0.273 \pm 0.132 \pm 0.047$
P_6'	$-0.069 \pm 0.005 \pm 0.001$	$-0.078 \pm 0.004 \pm 0.002$
P_8'	$0.044 \pm 0.003 \pm 0.016$	$0.034 \pm 0.002 \pm 0.019$
$R_{K^*}^{B_s}$	$0.942 \pm 0.008 \pm 0.001$	$0.998 \pm 0.004 \pm 0.0$
$BR \times 10^9$	$4.411 \pm 0.560 \pm 0.101$	$8.391 \pm 1.856 \pm 0.375$
A_{FB}	$-0.056 \pm 0.008 \pm 0.001$	$-0.036 \pm 0.020 \pm 0.009$
F_L	$0.464 \pm 0.064 \pm 0.014$	$0.851 \pm 0.038 \pm 0.007$

Table 3.5: The summary of observables for $B_s \to \bar{K}^*\mu^+\mu^-$ using BSZ2 form factors. The source of uncertainties are same as mentioned in Table 3.4.

Observable	$\bar{B}_s \to K^*\mu^+\mu^-$	$B_s \to \bar{K}^*\mu^+\mu^-$
P_2	4.137 ± 0.421	4.307 ± 0.441
P_4'	1.867 ± 0.300	2.067 ± 0.327
P_5'	2.223 ± 0.319	2.267 ± 0.343
A_{FB}	4.081 ± 0.453	4.250 ± 0.476

Table 3.6: The values of zeroes of angular observables for $\bar{B}_s \to K^*\mu^+\mu^-$ and $B_s \to \bar{K}^*\mu^+\mu^-$. The uncertainty is due to form factors and the mean values include contribution of the non-factorizable corrections.

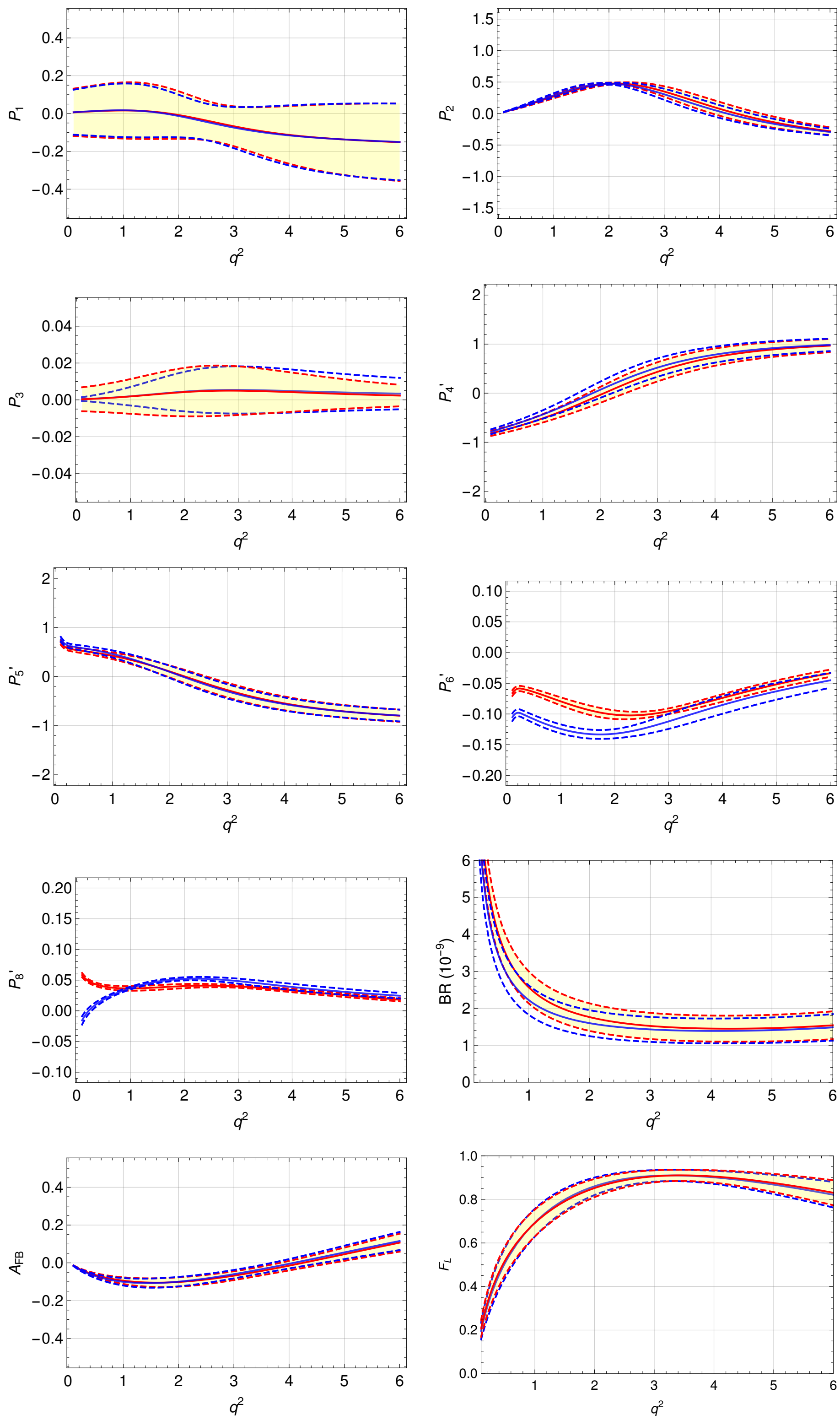

Table 3.7: The observables as functions of q^2. In these Figures, red solid curve shows the mean value of observable for $B_s \to \bar{K^*}\mu^+\mu^-$ and the blue solid curve show mean value of observables for $\bar{B}_s \to K^*\mu^+\mu^-$. The dashed curves show uncertainty in the values due to errors in determination of form factors only. The curves are obtained using BSZ2 form factors. The mean values include the contribution of non-factorizable corrections.

3.5.2 $B \to \rho\mu^+\mu^-$

	$B \to \rho\mu^+\mu^-$ (Belle)		$\bar{B} \to \rho\mu^+\mu^-$ (Belle)	
Observable	[0.1-1] GeV^2	[1-6] GeV^2	[0.1-1] GeV^2	[1-6] GeV^2
$\langle P_1 \rangle$	0 ± 0.178	-0.044 ± 0.119	0 ± 0.179	-0.048 ± 0.125
$\langle P_2 \rangle$	0.0772 ± 0.018	0.073 ± 0.071	0.071 ± 0.017	-0.016 ± 0.071
$\langle P_3 \rangle$	0 ± 0	0 ± 0.001	0 ± 0.001	0.001 ± -0.004
$\langle P_4' \rangle$	-0.501 ± 0.106	0.538 ± 0.169	-0.501 ± 0.104	0.597 ± 0.174
$\langle P_5' \rangle$	0.455 ± 0.095	-0.215 ± 0.099	0.368 ± 0.079	-0.308 ± 0.100
$\langle P_6' \rangle$	-0.0136 ± 0.003	-0.023 ± 0.005	-0.078 ± 0.015	-0.061 ± 0.014
$\langle P_8' \rangle$	0.006 ± 0.001	0.010 ± 0.002	0.019 ± 0.004	0.002 ± 0.004
$\langle R_\rho \rangle$	0.958 ± 0.181	1.128 ± 0.263	0.961 ± 0.174	1.124 ± 0.265
$\langle BR \rangle \times 10^9$	3.688 ± 0.515	7.052 ± 1.23	3.282 ± 0.451	6.892 ± 1.211
$\langle A_{FB} \rangle$	-0.053 ± 0.005	-0.027 ± 0.019	-0.046 ± 0.005	0.004 ± 0.018
$\langle F_L \rangle$	0.259 ± 0.064	0.734 ± 0.220	0.298 ± 0.073	0.749 ± 0.220

Table 3.8: Binned values of observables for $B \to \rho\mu^+\mu^-$ and $\bar{B} \to \rho\mu^+\mu^-$

As we mentioned above, due to ξ_u/ξ_t term in the present case, which is practically negligible in the case of $b \to s$ transition, the observable for the mode and the CP conjugated mode show clear differences and hence is a clear sign of CP violation. A precise measurement would determine whether the amount of CP violation is in conformity with the CKM picture or there are extra phases present. The observable P_6' is of particular interest in this regard as it is proportional to an imaginary part of Wilson coefficients. It can be noted that its value in low q^2 is significantly different for CP-conjugate modes, giving large value of CP asymmetry. For $B^0 \to \rho^0\mu^+\mu^-$, time-integrated branching ratio within SM is found out to be,

$$\begin{aligned}
\left\langle \mathcal{BR}(B \to \rho\mu^+\mu^-) \right\rangle^{\text{Belle}} &= (4.131 \pm 0.679) \times 10^{-8} \\
\left\langle \mathcal{BR}(\bar{B} \to \rho\mu^+\mu^-) \right\rangle^{\text{Belle}} &= (4.198 \pm 0.678) \times 10^{-8} \\
\langle BR \rangle^{\text{LHCb}} &= (4.164 \pm 0.678) \times 10^{-8}
\end{aligned} \tag{3.58}$$

	LHCb (untagged)	
Observable	[0.1-1] GeV^2	[1-6] GeV^2
$\langle P_1 \rangle$	0 ± 0.178	-0.046 ± 0.122
$\langle P_2 \rangle$	0.009 ± 0.009	0.045 ± 0.060
$\langle P_3 \rangle$	0 ± 0	0 ± 0.001
$\langle P_4' \rangle$	-0.500 ± 0.094	0.567 ± 0.151
$\langle P_5' \rangle$	0.058 ± 0.011	0.043 ± 0.009
$\langle P_6' \rangle$	-0.045 ± 0.009	-0.042 ± 0.009
$\langle P_8' \rangle$	0.012 ± 0.003	0.014 ± 0.003
$\langle R_\rho \rangle$	0.956 ± 0.165	1.116 ± 0.245
$\langle BR \rangle \times 10^9$	3.485 ± 0.483	6.972 ± 1.221
$\langle A_{FB} \rangle$	-0.006 ± 0.001	-0.016 ± 0.003
$\langle F_L \rangle$	0.278 ± 0.068	0.742 ± 0.218

Table 3.9: Binned values of observables for the process $B \to \rho\mu^+\mu^-$ to be measured LHCb for untagged events.

The tables for results corresponding to the decay $B \to \rho\mu^+\mu^-$ are given below. Tables 3.8 and 3.9 list the values without including the non-factorizable correction. The values with the corrections included are given in Tables 3.10, 3.11 and 3.12. The zeroes of the observables are given in Table 3.13.

3.6 Summary and Conclusions

Exclusive semileptonic decays mediated by $b \to s$ transitions have shown several deviations from SM expectations. This has attracted a lot of theoretical attention, attempting to explain these deviations. At present, it is not clear if the deviations are due to the physics beyond SM or just hadronic artefacts. An obvious solution is to study the analogous $b \to d$ transitions. Due to the complex phase involved, $b \to d$ transitions have a rich phenomenology and the CKM parameters ρ and η can be extracted from a dedicated study of angular

Observable	Experiment	$\bar{B} \to \rho\mu^+\mu^-$	
		[0.1-1] GeV^2	[1-6] GeV^2
$\langle P_1 \rangle$	Belle	$0.112 \pm 0.179 \pm 0.001$	$-0.063 \pm 0.113 \pm 0.003$
	LHCb	-0.034 ± 0.179	-0.061 ± 0.111
$\langle P_2 \rangle$	Belle	$0.008 \pm 0.009 \pm 0.0$	$0.0105 \pm 0.050 \pm 0.024$
	LHCb	0.078 ± 0.009	0.002 ± 0.050
$\langle P_3 \rangle$	Belle	$0 \pm 0.001 \pm 0.0$	$0.001 \pm 0.005 \pm 0.002$
	LHCb	0.261 ± 0.050	0.240 ± 0.030
$\langle P_4' \rangle$	Belle	$-0.586 \pm 0.076 \pm 0.046$	$0.529 \pm 0.155 \pm 0.017$
	LHCb	-0.616 ± 0.075	0.526 ± 0.155
$\langle P_5' \rangle$	Belle	$0.300 \pm 0.040 \pm 0.030$	$-0.263 \pm 0.075 \pm 0.098$
	LHCb	0.331 ± 0.039	-0.228 ± 0.075
$\langle P_6' \rangle$	Belle	$-0.088 \pm 0.006 \pm 0.001$	$-0.076 \pm 0.009 \pm 0.002$
	LHCb	-0.109 ± 0.008	-0.099 ± 0.010
$\langle P_8' \rangle$	Belle	$0.014 \pm 0.005 \pm 0.002$	$0.020 \pm 0.003 \pm 0.017$
	LHCb	-0.145 ± 0.024	0.124 ± 0.014
$\langle R_\rho \rangle$	Belle	$0.939 \pm 0.167 \pm 0.002$	$0.998 \pm 0.362 \pm 0.0$
	LHCb	0.954 ± 0.192	1.033 ± 0.289
$\langle BR \rangle \times 10^9$	Belle	$3.653 \pm 0.529 \pm 0.077$	$7.626 \pm 1.504 \pm 0.365$
	LHCb	1.977 ± 0.273	3.943 ± 0.756
$\langle A_{FB} \rangle$	Belle	$-0.041 \pm 0.005 \pm 0.001$	$-0.003 \pm 0.016 \pm 0.006$
	LHCb	-0.041 ± 0.001	-0.011 ± 0.002
$\langle F_L \rangle$	Belle	$0.431 \pm 0.069 \pm 0.014$	$0.832 \pm 0.038 \pm 0.006$
	LHCb	0.437 ± 0.068	0.832 ± 0.037

Table 3.10: Binned values of observables for the process $\bar{B} \to \rho\mu^+\mu^-$ using tagged events to be measured at Belle and LHCb. The mean values include non-factorizable corrections. The first uncertainty is due to form factors and second uncertainty is due to soft gluon emission with up quark in the loop.

Observable	Experiment	$B \to \rho\mu^+\mu^-$	
		[0.1-1] GeV^2	[1-6] GeV^2
$\langle P_1 \rangle$	Belle	$0.011 \pm 0.181 \pm 0.001$	$-0.059 \pm 0.110 \pm 0.003$
	LHCb	0.050 ± 0.181	-0.044 ± 0.110
$\langle P_2 \rangle$	Belle	$0.083 \pm 0.010 \pm 0.001$	$0.073 \pm 0.053 \pm 0.023$
	LHCb	0.083 ± 0.010	0.074 ± 0.053
$\langle P_3 \rangle$	Belle	$0 \pm 0.005 \pm 0.0$	$0.001 \pm 0.005 \pm 0.002$
	LHCb	-0.228 ± 0.044	-0.229 ± 0.028
$\langle P'_4 \rangle$	Belle	$-0.618 \pm 0.076 \pm 0.047$	$0.467 \pm 0.161 \pm 0.029$
	LHCb	-0.591 ± 0.077	0.470 ± 0.161
$\langle P'_5 \rangle$	Belle	$0.332 \pm 0.043 \pm 0.027$	$-0.211 \pm 0.084 \pm 0.085$
	LHCb	0.368 ± 0.043	-0.178 ± 0.084
$\langle P'_6 \rangle$	Belle	$-0.050 \pm 0.004 \pm 0.001$	$-0.064 \pm 0.004 \pm 0.002$
	LHCb	-0.030 ± 0.003	-0.042 ± 0.003
$\langle P'_8 \rangle$	Belle	$0.013 \pm 0.002 \pm 0.016$	$0.012 \pm 0.001 \pm 0.018$
	LHCb	-0.133 ± 0.021	0.113 ± 0.013
$\langle R_\rho \rangle$	Belle	$0.938 \pm 0.203 \pm 0.001$	$0.997 \pm 0.278 \pm 0.0$
	LHCb	0.955 ± 0.194	1.036 ± 0.289
$\langle BR \rangle \times 10^9$	Belle	$4.078 \pm 0.585 \pm 0.080$	$7.908 \pm 1.549 \pm 0.366$
	LHCb	2.165 ± 0.302	4.064 ± 0.778
$\langle A_{FB} \rangle$	Belle	$-0.045 \pm 0.005 \pm 0.001$	$-0.023 \pm 0.018 \pm 0.007$
	LHCb	-0.046 ± 0.005	-0.024 ± 0.018
$\langle F_L \rangle$	Belle	$0.414 \pm 0.067 \pm 0.014$	$0.822 \pm 0.039 \pm 0.007$
	LHCb	0.409 ± 0.067	0.822 ± 0.039

Table 3.11: Binned values of observables for the process $B \to \rho\mu^+\mu^-$ using tagged events to be measured at Belle and LHCb. The mean values include non-factorizable corrections. The first uncertainty is due to form factors and second uncertainty is due to soft gluon emission with up quark in the loop.

Observables	$B \to \rho\mu^+\mu^-$(LHCb)	
	[0.1-1] GeV^2	[1-6] GeV^2
$\langle P_1 \rangle$	$0.011 \pm 0.180 \pm 0.001$	$-0.061 \pm 0.111 \pm 0.003$
$\langle P_2 \rangle$	$0.008 \pm 0.001 \pm 0.0$	$0.033 \pm 0.003 \pm 0.001$
$\langle P_3 \rangle$	$0 \pm 0.002 \pm 0.0$	$0 \pm 0.001 \pm 0.0$
$\langle P_4' \rangle$	$-0.603 \pm 0.076 \pm 0.008$	$0.497 \pm 0.158 \pm 0.015$
$\langle P_5' \rangle$	$0.032 \pm 0.004 \pm 0.001$	$0.022 \pm 0.006 \pm 0.002$
$\langle P_6' \rangle$	$-0.068 \pm 0.005 \pm 0.001$	$-0.070 \pm 0.006 \pm 0.002$
$\langle P_8' \rangle$	$0 \pm 0.001 \pm 0.005$	$-0.003 \pm 0.002 \pm 0.006$
$\langle R_\rho \rangle$	$0.954 \pm 0.193 \pm 0.002$	$1.035 \pm 0.289 \pm 0.0$
$\langle BR \rangle \times 10^9$	$4.142 \pm 0.575 \pm 0.138$	$8.007 \pm 1.533 \pm 0.731$
$\langle A_{FB} \rangle$	$-0.046 \pm 0.005 \pm 0.0$	$-0.024 \pm 0.018 \pm 0.001$
$\langle F_L \rangle$	$0.422 \pm 0.068 \pm 0.032$	$0.827 \pm 0.0388 \pm 0.016$

Table 3.12: Binned values for observables for the process $B \to \rho\mu^+\mu^-$ using untagged events to be measured at LHCb. The results include non-factorizable corrections. The first uncertainty is due to form factors and second uncertainty is due to soft gluon emission with up quark in the loop.

Observables	Belle		LHCb	
	$B \to \rho\mu^+\mu^-$	$\bar{B} \to \rho\mu^+\mu^-$	$B \to \rho\mu^+\mu^-$	$\bar{B} \to \rho\mu^+\mu^-$
P_2	4.101 ± 0.441	3.593 ± 0.304	4.111 ± 0.443	3.604 ± 0.399
P_4'	1.869 ± 0.304	1.727 ± 0.282	1.851 ± 0.307	1.746 ± 0.279
P_5'	2.107 ± 0.344	1.842 ± 0.290	2.269 ± 0.353	1.860 ± 0.287
P_8'	-	-	1.827 ± 0.023	1.706 ± 0.036
A_{FB}	4.060 ± 0.462	3.560 ± 0.419	4.069 ± 0.462	3.571 ± 0.420

Table 3.13: Values of zeroes of angular observables for the process $B \to \rho\mu^+\mu^-$ and $\bar{B} \to \rho\mu^+\mu^-$ The uncertainty is due to form factors. Mean values include the contribution of non-factorizable corrections.

observables [57]. In this work the detailed predictions of angular observables for $\bar{B}^0 \to \bar{\rho}^0\mu^+\mu-$ and $\bar{B}_s \to K^*\mu^+\mu^-$ modes in the SM have been provided. It is found that the naive guess that branching ratio of $\bar{B}^0 \to \rho^0\mu^+\mu^-$ should be approximately half of the branching ratio of $\bar{B}_s \to K^*\mu^+\mu^-$ does not always work because of additional effects due to $B^0 - \bar{B}^0$ mixing. It may be worthwhile to mention that the values of observables for $B^\pm \to \rho^\pm\mu^+\mu^-$ are also expected to be same as that for $B_s(\bar{B}_s) \to \bar{K}^*(K^*)\mu^+\mu^-$ modulo strange quark mass and $SU(3)$ corrections. For the $\bar{B}_s \to K^*\mu + \mu^-$ mode, we have explicitly compared predictions of angular observables using different form factors. The results, provided in Table 3.3, clearly show a dependence on the form factors, even for the form factor independent observables, though the deviations in these observables are only marginal. Tables 3.4 and 3.5 contain the predicted values for BSZ2 form factors after including various non-factorizable corrections. These turn out to be important and should be included while comparing with data and to decipher any possible new physics.

A potentially important missing piece is the inclusion of finite width effects, especially relevant for $B \to \rho\ell\ell$ modes. Since, $\rho^0 \to \pi\pi$ width is large, it must be taken into account. In [89], an attempt is made to include these effects as a part of form factors. However, these effects are computed only for vector and axial vector form factors while no calculation exists for tensor form factors. These effects could be large and must be evaluated.

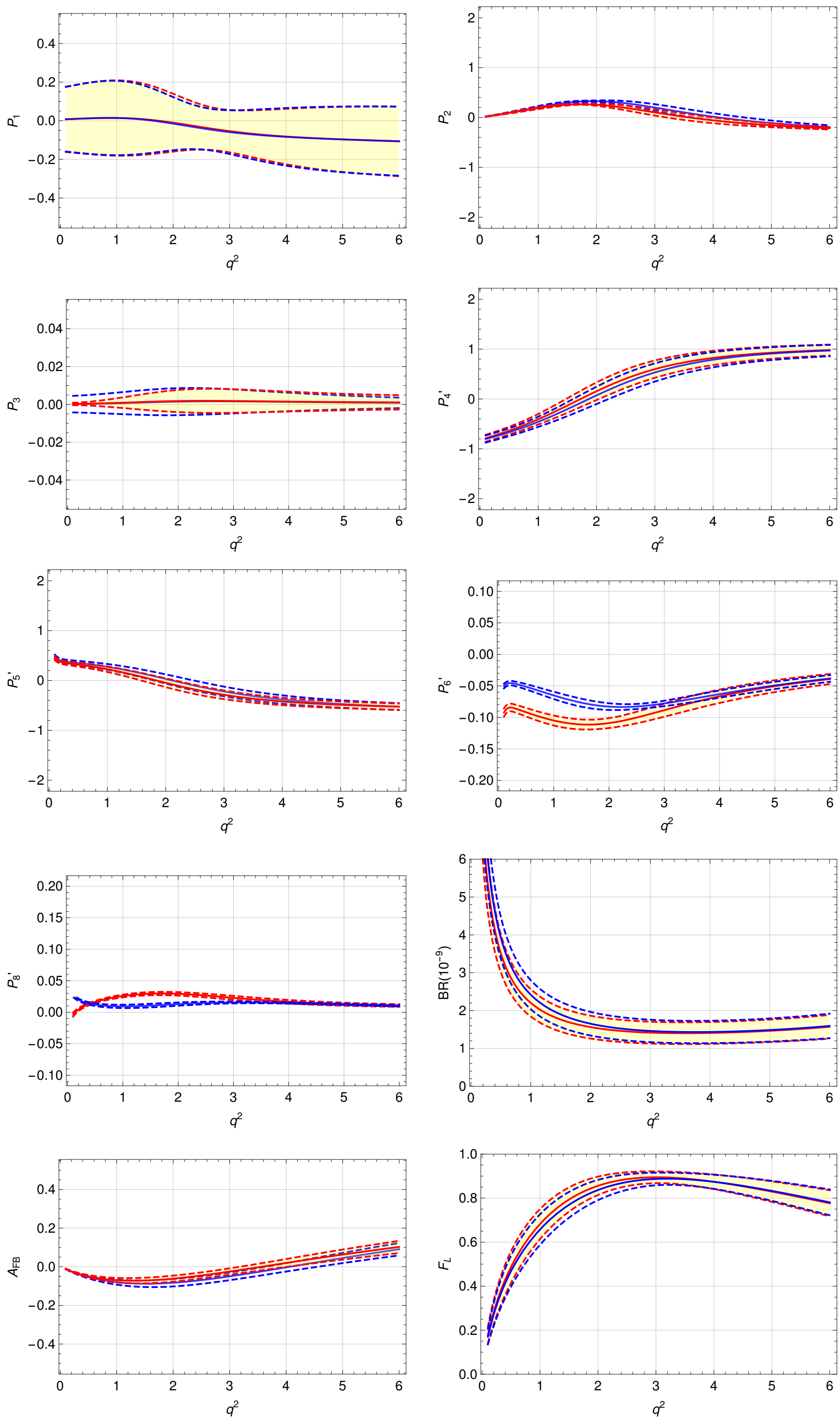

Figure 3.1: The observables as functions of q^2. The red (blue) solid curve shows the mean value of observable for $\bar{B}(B) \to \rho\mu^+\mu^-$. The dashed curve show uncertainty in the values due to errors in determination of form factors only. These plots are obtained using BZ form factors. The mean values include the contribution of non-factorizable corrections.

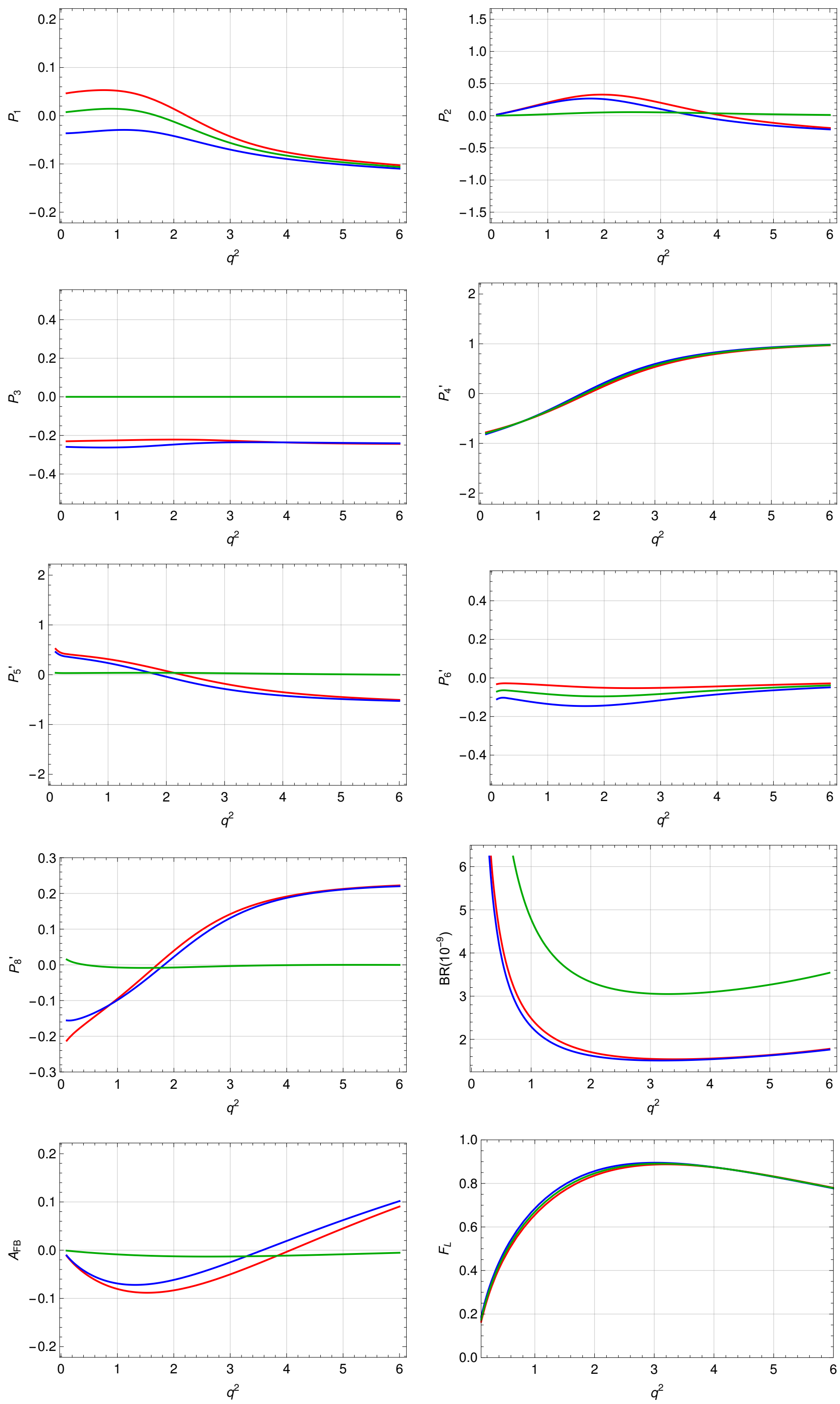

Figure 3.2: The values of observables to be measured at LHCb as functions of q^2. The red (blue) curve shows the values for $B\bar{B} \to \rho\mu^+\mu^-$. The green curve shows the values of observables defined for the untagged events. The plots are obtained using BZ form factors. The mean values include the contribution of non-factorizable corrections.

Chapter 4

$\mathbf{B \to K_2^* \ell^+ \ell^-}$ in Standard Model and beyond

Recent experiments have shown consistent deviations from SM predictions in the branching ratio of processes based on $b \to s$ transitions. Global fits to the $b \to s\ell^+\ell^-$ data [24–27, 90–100] suggest that NP contributions to some Wilson coefficients can alleviate some of these tensions. If the anomalies are indeed due to NP, discrepancies will show up in other $b \to s\ell^+\ell^-$ mediated transitions as well such as $B \to K_2^*(1430)\ell^+\ell^-$ which can provide complementary test of NP. While the closely related radiative mode $B \to K_2^*\gamma$ has already been observed in the BaBar [101] and Belle [102] experiments, LHCb has done some studies around the $K_2^*(1430)$ resonance [103]. The measured branching ratio for $B \to K_2^*\gamma$ is comparable to that of $B \to K^*\gamma$. This implies that the mode $B \to K_2^*\ell^+\ell^-$ also has sizeable branching ratio and has been confirmed by direct computations in [104–107].

The short distance physics of $B \to K_2^*\ell^+\ell^-$ is contained in the perturbatively calculable Wilson coefficients. The long-distance physics of $B \to K_2^*$ hadronic matrix elements are parametrized in terms of the form factors and the parametrization is similar to that of $B \to K^*$ [107]. The form factors have been calculated [108] in perturbative QCD approach using light-cone distribution amplitudes [109] and using light-cone sum rules in conjunction with the B meson wave function [110]. Calculations in light-cone QCD sum rule approach is done in [112]. Using different form factors, phenomenological analysis of $B \to K_2^* \ell^+ \ell^-$ has been performed in [104, 107, 113–117]. In most of these works, the focus is on simple observables like decay rate, forward-backward asymmetry of dilepton system, and the polarization fractions of K_2^*. In [104], the four-fold angular distribution of decay products of K_2^* has been analysed in the SM. In [115], the decay $B \to K_2^* (\to K\pi) \ell^+ \ell^-$ is studied in SM as well as in non-universal Z' and vector-like quark models. However, branching fraction of the decay $K_2^* \to K\pi$ was ignored in their analysis.

In this chapter, we have studied the full four-fold angular distribution of $B \to K_2^* (\to K\pi) \ell^+ \ell^-$ decay in the limit of low dilepton invariant mass squared (q^2) or large recoil of the K_2^* meson. In this region, the heavy quark ($m_b \to \infty$) and large recoil ($E_{K_2^*} \to \infty$) imply relations between $B \to K_2^*$ form factors which reduces the number of independent form factors from seven to two. This helps us construct "clean" observables where the form factor dependence cancels at the leading order in $\Lambda_{\rm QCD}/m_b$ and α_s. Due to this cancellation, these observables are excellent probes of NP. We have presented the determinations of the clean observables in the SM and studied the implications of global fits to the present $b \to s \ell^+ \ell^-$ data.

4.1 Theoretical Framework

The low energy effective Hamiltonian for rare $|\Delta B| = |\Delta S| = 1$ transition is given by,

$$\mathcal{H}_{\rm eff} = -\frac{4\,G_F}{\sqrt{2}} V_{tb} V_{ts}^* \frac{\alpha_e}{4\pi} \sum_{i=7,9,10} \Big[\mathcal{C}_i(\mu) \mathcal{O}_i(\mu) + \mathcal{C}_i'(\mu) \mathcal{O}_i'(\mu) \Big] \,, \tag{4.1}$$

The b-quark mass multiplying the dipole operator $\mathcal{O}_7^{(\prime)}$ is assumed to be the running quark mass in the modified minimal-subtraction ($\overline{\rm MS}$) mass scheme. The contributions of the factorizable quark-loop corrections to current-current and penguin operators are absorbed in the effective Wilson coefficients. We have ignored the non-factorizable corrections to the Hamiltonian which are expected to be significant at large recoil [56, 57]. The primed Wilson coefficients are zero in the SM but may be significant in NP models. Moreover, NP contributions to $\mathcal{O}_7$ have not been considered as they are well constrained [118].

We work in the rest frame of B meson and denote the four-momenta of the B-meson, the K_2^*, and the positively and negatively charged leptons by p, k, p_{ℓ^+}, and p_{ℓ^-} respectively. A Tensor meson of spin-2 polarization tensor $\epsilon^{\mu\nu}(n)$, where the helicities are $n = t, 0, \pm 1, \pm 2$, satisfies the relation $\epsilon^{\mu\nu}k_\nu = 0$. For the K_2^* with four momentum $(k_0, 0, 0, \vec{k})$, the polarization tensor $\epsilon^{\mu\nu}(h)$ can be constructed in terms of polarization vectors of spin-1 state i.e. [119]

$$\epsilon_\mu(0) = \frac{1}{m_{K_2^*}}(|\vec{k}|, 0, 0, k_0)\,, \quad \epsilon_\mu(\pm) = \frac{1}{\sqrt{2}}(0, \mp 1, -i, 0)\,, \tag{4.2}$$

in the following way

$$\epsilon_{\mu\nu}(\pm 2) = \epsilon_\mu(\pm 1)\epsilon_\nu(\pm 1)\,, \tag{4.3}$$

$$\epsilon_{\mu\nu}(\pm 1) = \frac{1}{\sqrt{2}}\Big[\epsilon_\nu(\pm)\epsilon_\nu(0) + \epsilon_\nu(\pm)\epsilon_\mu(0)\Big]\,, \tag{4.4}$$

$$\epsilon_{\mu\nu}(0) = \frac{1}{\sqrt{6}}\Big[\epsilon_\mu(+)\epsilon_\nu(-) + \epsilon_\nu(+)\epsilon_\mu(-)\Big] + \sqrt{\frac{2}{3}}\epsilon_\mu(0)\epsilon_\nu(0)\,. \tag{4.5}$$

As the K_2^* meson is partnered with two spin-half leptons in the final state, it can only have helicities $n = t, 0, \pm 1$. It is therefore convenient to introduce a new polarization vector [108]

$$\epsilon_{T\mu}(h) = \frac{\epsilon_{\mu\nu}p^\nu}{m_B} \tag{4.6}$$

where p is the four momentum of B meson. The explicit expressions of polarization vectors are

$$\epsilon_{T\mu}(\pm 1) \;=\; \frac{1}{m_B}\frac{1}{\sqrt{2}}\epsilon(0).p\,\epsilon_\mu(\pm) = \frac{\sqrt{\lambda}}{\sqrt{8}m_B m^*_{K_2}}\epsilon_\mu(\pm)\,, \tag{4.7}$$

$$\epsilon_{T\mu}(0) \;=\; \frac{1}{m_B}\sqrt{\frac{2}{3}}\epsilon(0).p\,\epsilon_\mu(0) = \frac{\sqrt{\lambda}}{\sqrt{6}m_B m^*_{K_2}}\epsilon_\mu(0)\,, \tag{4.8}$$

where $\lambda = m_B^4 + m_{K_2^*}^4 + q^4 - 2(m_B^2 m_{K_2^*}^2 + m_B^2 q^2 + m_{K_2^*}^2 q^2)$. The hadronic matrix elements for $B \to K_2^*$ can be written in terms of $\epsilon_{T\mu}$ as [108]

$$\langle K_2^*(k,n)|\bar{s}\gamma^\mu b|\overline{B}(p)\rangle \;=\; -\frac{2V(q^2)}{m_B + m_{K_2^*}}\epsilon^{\mu\nu\rho\sigma}\epsilon^*_{T\nu}p_\rho k_\sigma,$$

$$\langle K_2^*(k,n)|\bar{s}\gamma^\mu\gamma_5 b|\overline{B}(p)\rangle \;=\; 2im_{K_2^*}A_0(q^2)\frac{\epsilon_T^*\cdot q}{q^2}q^\mu$$

$$
\begin{aligned}
& & +i(m_B + m_{K_2^*})A_1(q^2)\left[\epsilon^*_{T\mu} - \frac{\epsilon^*_T\cdot q}{q^2}q^\mu\right] \qquad (4.9)\\
& & -iA_2(q^2)\frac{\epsilon^*_T\cdot q}{m_B + m_{K_2^*}}\left[P^\mu - \frac{m_B^2 - m_{K_2^*}^2}{q^2}q^\mu\right],\\
\langle K_2^*(k,n)|\bar{s}q_\nu\sigma^{\mu\nu}b|\overline{B}(p)\rangle &=& -2iT_1(q^2)\epsilon^{\mu\nu\rho\sigma}\epsilon^*_{T\nu}p_{B\rho}p_{K\sigma},\\
\langle K_2^*(k,n)|\bar{s}q_\nu\sigma^{\mu\nu}\gamma_5 b|\overline{B}(p)\rangle &=& T_2(q^2)\left[(m_B^2 - m_{K_2^*}^2)\epsilon^*_{T\mu} - \epsilon^*_T\cdot qP^\mu\right]\\
& & +T_3(q^2)\epsilon^*_T\cdot q\left[q^\mu - \frac{q^2(p+k)^\mu}{m_B^2 - m_{K_2^*}^2}\right],
\end{aligned}
$$

where $q = p_{\ell^+} + p_{\ell^-} = p - k$ is the momentum transferred.

4.2 Transversity amplitudes

Using the operators defined in Eq. (4.1), the amplitude of $B \to K_2^*\ell^+\ell^-$ for a given helicity of the K_2^* can be written as

$$
\begin{aligned}
\mathcal{A}(n) &=& -\frac{G_F}{\sqrt{2}}V_{tb}V_{ts}^*\frac{\alpha_e}{\pi}\Bigg(\Bigg[(\mathcal{C}_9 - \mathcal{C}_{10})\langle K_2^*(k,n)|\bar{s}\gamma^\mu P_L b|\overline{B}(p)\rangle\\
& & -i\frac{2\mathcal{C}_7 m_b}{q^2}\langle K_2^*(k,n)|\bar{s}\sigma^{\mu\nu}q_\nu P_R b|\overline{B}(p)\rangle + (\mathcal{C}_9' - \mathcal{C}_{10}')\langle K_2^*(k,n)|\bar{s}\gamma^\mu P_R b|\overline{B}(p)\rangle\Bigg]\\
& & \bar{\ell}\gamma_\mu P_L\ell + \left[\mathcal{C}_{10}\to -\mathcal{C}_{10}, C_{10}'\to -\mathcal{C}_{10}'\right]\bar{\ell}\gamma_\mu P_R\ell\Bigg). \qquad (4.10)
\end{aligned}
$$

The differential distribution for the decay can be calculated using helicity amplitudes $H_\pm^{L,R}$ and $H_0^{L,R}$. These are defined as the projections of the hadronic amplitudes on the polarization vectors of the gauge boson that creates the lepton pair. The superscripts L, R denote to the chiralities of the leptonic current. However, for comparison with the literature we introduce the so called the *transversity amplitudes* which are linear combinations of helicity amplitudes $A_{\parallel L,R} = (H_+^{L,R} + H_-^{L,R})/\sqrt{2}$, $A_{\perp L,R} = (H_+^{L,R} - H_-^{L,R})/\sqrt{2}$, and $A_{0L,R} = H_0^{L,R}$. The expressions of the transversity amplitudes for $B \to K_2^*(\to K\pi)\ell^+\ell^-$ read [115]

$$
\begin{aligned}
A_{0L,R} &=& N\frac{\sqrt{\lambda}}{\sqrt{6}m_B m_{K_2^*}}\frac{1}{2m_{K_2^*}\sqrt{q^2}}\\
& & \Bigg[(\mathcal{C}_{9-} \mp \mathcal{C}_{10-})\left[(m_B^2 - m_{K_2^*}^2 - q^2)(m_B + m_{K_2^*})A_1 - \frac{\lambda}{m_B + m_{K_2^*}}A_2\right]
\end{aligned}
$$

$$+2m_b\mathcal{C}_7[(m_B^2+3m_{K_2^*}^2-q^2)T_2-\frac{\lambda}{m_B^2-m_{K_2^*}^2}T_3]\Bigg], \qquad (4.11)$$

$$A_{\perp L,R} = -\sqrt{2}\frac{\sqrt{\lambda}}{\sqrt{8}m_B m_{K_2^*}}N\left[(\mathcal{C}_{9+}\mp\mathcal{C}_{10+})\frac{\sqrt{\lambda}V}{m_B+m_{K_2^*}}+\frac{2m_b\mathcal{C}_7}{q^2}\sqrt{\lambda}T_1\right], \qquad (4.12)$$

$$A_{||L,R} = \sqrt{2}\frac{\sqrt{\lambda}}{\sqrt{8}m_B m_{K_2^*}}N\Big[(\mathcal{C}_{9-}\mp\mathcal{C}_{10-})(m_B+m_{K_2^*})A_1$$
$$+\frac{2m_b\mathcal{C}_7}{q^2}(m_B^2-m_{K_2^*}^2)T_2\Big], \qquad (4.13)$$

$$A_t = 2\frac{\sqrt{\lambda}}{\sqrt{6}m_B m_{K_2^*}}N[\mathcal{C}_{10-}]A_0\,, \qquad (4.14)$$

where the normalization constant is given by

$$N=\left[\frac{G_F^2\alpha_e^2}{3\cdot 2^{10}\pi^5 m_B^3}|V_{tb}V_{ts}^*|^2\lambda^{1/2}(m_B^2,m_{K_2^*}^2,q^2)\mathcal{B}(K_2^*\to K\pi)\beta_\ell\right]^{\frac{1}{2}}. \qquad (4.15)$$

and $\beta_\ell=\sqrt{1-\frac{4m_\ell^2}{q^2}}$. Here we have defined

$$\mathcal{C}_{9\pm}=\mathcal{C}_9\pm\mathcal{C}_9'\,,\quad \mathcal{C}_{10\pm}=\mathcal{C}_{10}\pm\mathcal{C}_{10}'\,. \qquad (4.16)$$

4.3 Heavy to light form factors at large recoil

The non-perturbative hadronic matrix elements for $B\to K_2^*$ are parametrized in terms of form factors mentioned in Eq. (4.9). They are the source of dominant uncertainty in the theoretical predictions. As the lattice calculations of the form factors are unavailable at present, the uncertainty can be reduced by making use of the relations between the form factors that originate in the limit of heavy quark $m_b\to\infty$ of the initial meson and large energy $E_{K_2^*}$ of the final meson [120, 121]. In these limits, the heavy to light form factors can be expanded in terms of the ratios $\Lambda_{\rm QCD}/m_b$ and $\Lambda_{\rm QCD}/E_{K_2^*}$ which are small numerically. To leading order in $\Lambda_{\rm QCD}/m_b$ and α_s, the large energy symmetry dictates that there are only two independent universal soft form factors ($\xi_{||}(q^2)$ and $\xi_\perp(q^2)$ [121]) in terms of which the rest of the form factors can be written as [107]

$$
\begin{aligned}
A_0(q^2) &= \frac{m_{K_2^*}}{|p_{K_2^*}|}\left[\left(1-\frac{m_{K_2^*}^2}{m_B}\right)\xi_\parallel(q^2)+\frac{m_{K_2^*}}{m_B}\xi_\perp(q^2)\right],\\
A_1(q^2) &= \frac{m_{K_2^*}}{|p_{K_2^*}|}\frac{2E_{K_2^*}}{m_B+m_{K_2^*}}\xi_\perp(q^2),\\
A_2(q^2) &= \frac{m_{K_2^*}}{|p_{K_2^*}|}\left(1+\frac{m_{K_2^*}}{m_B}\right)\left[\xi_\perp(q^2)-\frac{m_{K_2^*}}{E}\xi_\parallel\right],\\
V(q^2) &= \frac{m_{K_2^*}}{|p_{K_2^*}|}\left(1+\frac{m_{K_2^*}}{m_B}\right)\xi_\perp, \\
T_1(q^2) &= \frac{m_{K_2^*}}{|p_{K_2^*}|}\xi_\perp(q^2),\\
T_2(q^2) &= \frac{m_{K_2^*}}{|p_{K_2^*}|}\left(1-\frac{q^2}{m_B^2-m_{K_2^*}^2}\right)\xi_\perp(q^2),\\
T_3(q^2) &= \frac{m_{K_2^*}}{|p_{K_2^*}|}\left[\xi_\perp-\left(1-\frac{m_{K_2^*}^2}{m_B^2}\right)\frac{m_{K_2^*}}{E}\xi_\parallel(q^2)\right].
\end{aligned} \tag{4.17}
$$

Here recoil energy $E_{K_2^*}$ is given by the expression

$$
E_{K_2^*} = \frac{m_B}{2}\left(1-\frac{q^2}{m_B^2}+\frac{m_{K_2^*}^2}{m_B^2}\right). \tag{4.18}
$$

The q^2 dependence of the soft form factors $\xi_\perp(q^2)$ and $\xi_\parallel(q^2)$ is given by [107, 121]

$$
\xi_{\parallel,\perp}(q^2) = \frac{\xi_{\parallel,\perp}(0)}{(1-q^2/m_B^2)^2}. \tag{4.19}
$$

The numerical values of the soft form factors at the zero recoil $q^2 = 0$ have been estimated using Bauer-Stech-Wirbel (BSW) model [122] in Ref. [107]. In Ref. [106] they are also extracted from experimental data on $B \to K^*\gamma$ from BaBar [101] and Belle [102]. For our numerical analysis we have used the values $\xi_\perp(0) = 0.29 \pm 0.09$ and $\xi_\parallel(0) = 0.26 \pm 0.10$ which were obtained in Ref. [108] in perturbative QCD approach utilizing the non-trivial relations realized in the large energy limit. These estimates are consistent with the ones obtained in Refs. [107] and [106] but have large errors. Not to be too conservative in our theory estimates, we choose to use values given above.

Substituting (4.17) in (4.11), we obtain at leading order in Λ_{QCD}/m_b and α_s the simple expressions of the transversity amplitudes in terms of soft form factors $\xi_\parallel$ and $\xi_\perp$ as

$$
A_{0L(R)} = \sqrt{\frac{2}{3}}\frac{N}{\sqrt{q^2}}m_B^2\left(1-\frac{q^2}{m_B^2}\right)\left((\mathcal{C}_{9-}\mp\mathcal{C}_{10+})+2\mathcal{C}_7\frac{m_b}{m_B}\right)\xi_\parallel(q^2), \tag{4.20}
$$

$$A_{\perp L(R)} = -Nm_B\Big(1-\frac{q^2}{m_B^2}\Big)\left((\mathcal{C}_{9+}\mp\mathcal{C}_{10+})+2\mathcal{C}_7\frac{m_b m_B}{q^2}\right)\xi_\perp(q^2)\,, \tag{4.21}$$

$$A_{\parallel L(R)} = Nm_B\Big(1-\frac{q^2}{m_B^2}\Big)\left((\mathcal{C}_{9-}\mp\mathcal{C}_{10-})+2\mathcal{C}_7\frac{m_b m_B}{q^2}\right)\xi_\perp(q^2)\,, \tag{4.22}$$

$$A_t = 2\frac{\sqrt{\lambda}}{\sqrt{6}m_B m_{K_2^*}}N\frac{2m_{K_2^*}m_B}{\sqrt{\lambda}}\left((1-\frac{m_{K_2^*}^2}{m_B E_{K_2^*}})\xi_\parallel+\frac{m_{K_2^*}}{m_B}\xi_\perp\right)\mathcal{C}_{10-} \tag{4.23}$$

One must note that the relations (4.17) are derived in the QCD factorization (QCDF) and soft-collinear-effective theory (SCET) approach wherein the factorization formula for the heavy to light $B \to K_2^*$ form factors is

$$F_i(q^2) = (1+\mathcal{O}(\alpha_s))\xi + \Phi_B \oplus T_i \oplus \Phi_{K_2^*} + \mathcal{O}(\Lambda_{\rm QCD}/m_b)\,. \tag{4.24}$$

In the expression above, T_i are the perturbatively calculable hard scattering kernels and Φ_{B,K^*} are the hadron distribution amplitudes which are non perturbative elements. At present, there are no means to calculate the $\Lambda_{\rm QCD}/m_b$ corrections and therefore the cancellations of soft form factors in the clean observables are valid only at leading order in $\Lambda_{\rm QCD}/m_b$. The higher order terms that are neglected contribute to the uncertainty of our theoretical predictions. We use the ensemble method following Ref. [79] to account for $\Lambda_{\rm QCD}/m_b$ uncertainties in our analysis. This is done by multiplying the transversity amplitudes by correction factors

$$A_{0,\parallel,\perp} \to A_{0,\parallel,\perp}(1+c_{0,\parallel,\perp})\,, \tag{4.25}$$

where $c_{0,\parallel,\perp}$ are the correction factors defined as $c_{0,\parallel,\perp} = |c_{0,\parallel,\perp}|e^{i\theta_{0,\parallel,\perp}}$. We randomly vary $|c_{0,\parallel,\perp}|$ and $\theta_{0,\parallel,\perp}$ using uniform distribution in the ranges $[-0.1, 0.1]$ and $[-\pi, \pi]$ respectively. Other sources of uncertainties are the due to the variation of scale μ between $m_b/2$ and $2m_b$ as well as the ratio m_c/m_b. Some of the inputs and their uncertainties have been listed in Table 4.2.

4.4 Angular distributions and observables

It is assumed that the K_2^* is on the mass shell so that the $B \to K_2^*(\to K\pi)\ell^+\ell^-$ decay can be completely described in terms of only four kinematical variables: q^2 and three angles (θ_ℓ, θ_K and ϕ). The lepton angle θ_ℓ is defined as the angle made by the negatively charged lepton ℓ^- with respect to the direction of the motion of the B meson in the di-lepton rest frame. The angle θ_K is defined as the angle made by the K^- with respect to the opposite of the direction of the B meson in the $K\pi$ rest frame. The angle between the decay planes of the two leptons and the $K\pi$ is denoted by ϕ. In terms of these variables, the four-fold differential distributions is [115],

$$\begin{aligned}
\frac{d^4\Gamma}{dq^2 d\cos\theta_\ell d\cos\theta_K d\phi} &= \frac{15}{128\pi}\Big[I_1^s 3\sin^2 2\theta_K + I_1^c(3\cos^2\theta_K - 1)^2 + I_2^s 3\sin^2 2\theta_K \cos 2\theta_l \\
&+ I_2^c(3\cos^2\theta_K - 1)^2\cos 2\theta_l + I_3 3\sin^2 2\theta_K \sin^2\theta_l \cos 2\phi \\
&+ I_4 2\sqrt{3}(3\cos^2\theta_K - 1)\sin 2\theta_K \sin 2\theta_l \cos\phi \\
&+ I_5 2\sqrt{3}(3\cos^2\theta_K - 1)\sin 2\theta_K \sin\theta_l \cos\phi + I_6 3\sin^2 2\theta_K \cos\theta_l \\
&+ I_7 2\sqrt{3}(3\cos^2\theta_K - 1)\sin 2\theta_K \sin\theta_l \sin\phi \\
&+ I_8 2\sqrt{3}(3\cos^2\theta_K - 1)\sin 2\theta_K \sin 2\theta_l \sin\phi \\
&+ I_9 3\sin^2 2\theta_K \sin^2\theta_l \sin 2\phi \Big]. \qquad (4.26)
\end{aligned}$$

The distribution is similar to the $B \to K^*\ell^+\ell^-$ angular distribution [74, 123] which can be attributed to the fact that $B \to K_2^*\ell^+\ell^-$ decay involves a K_2^* meson with polarization $t, 0, \pm 1$ only, as discussed in Section 4.1. The differences between the two distributions are due to the different spherical harmonics required to describe the strong decays of K^* and K_2^*.

The angular coefficients $I_i(q^2)$ can be written in terms of the transversity amplitudes and are given in Appendix C. The decay rate for the CP-conjugate process is obtained by the replacements $I_{1,2,3,4,7} \to \bar{I}_{1,2,3,4,7}$ and $I_{5,6,8,9} \to -\bar{I}_{5,6,8,9}$, where $\bar{I}$ are equal to I with all the weak phase conjugated. In this chapter we will consider only CP-averaged observables, so that I means $I + \bar{I}$ and total decay width Γ stands for $\Gamma + \bar{\Gamma}$. At leading order in $\Lambda_{\rm QCD}/m_b$ and α_s, the short- and long-distance physics factorize as

$$\begin{aligned}
I_1^c &= \frac{2}{3}\frac{N^2}{q^2} m_B^4 \left(1 - \frac{q^2}{m_B^2}\right)^2 \Big[|\sigma_-|^2 + |\sigma_+|^2 \\
&+ \frac{8\, m_\ell^2}{q^2}\left\{ \mathrm{Re}(\sigma_-\sigma_+^*) + 2|\mathcal{C}_{10-}|^2 \left(1 - \frac{2\, m_{K_2^*}^2}{m_B^2 - q^2} + \frac{m_{K_2^*}}{m_B}\frac{\xi_\perp}{\xi_\parallel}\right)^2 \right\} \Big] \xi_\parallel^2,
\end{aligned}$$

$$
\begin{aligned}
I_1^s &= \frac{3}{4}N^2 m_B^2 \left(1-\frac{q^2}{m_B^2}\right)^2 \Big[\left(1-\frac{4\,m_\ell^2}{3q^2}\right)\left\{(|\rho_-^L|^2+|\rho_+^L|^2)+(L\leftrightarrow R)\right\} \\
&\quad +\frac{m_\ell^2}{3q^2}\,\mathrm{Re}(\rho_-^L\rho_-^{R*}+\rho_+^L\rho_+^{R*})\Big]\xi_\perp^2, \\
I_2^c &= -\frac{2}{3}\frac{N^2}{q^2}m_B^4\,\beta_\ell^2\left(1-\frac{q^2}{m_B^2}\right)^2(|\sigma_-|^2+|\sigma_+|^2)\,\xi_\parallel^2, \\
I_2^s &= \frac{1}{4}N^2 m_B^2\,\beta_\ell^2\left(1-\frac{q^2}{m_B^2}\right)^2\left\{(|\rho_-^L|^2+|\rho_+^L|^2)+(L\leftrightarrow R)\right\}\xi_\perp^2\,, \\
I_3 &= \frac{1}{2}N^2 m_B^2\,\beta_\ell^2\left(1-\frac{q^2}{m_B^2}\right)^2\left\{(|\rho_+^L|^2-|\rho_-^L|^2)+(L\leftrightarrow R)\right\}\xi_\perp^2\,, \\
I_4 &= \frac{1}{\sqrt{3}}\frac{N^2}{\sqrt{q^2}}m_B^3\,\beta_\ell^2\left(1-\frac{q^2}{m_B^2}\right)^2\mathrm{Re}[\sigma_-\rho_-^{L*}+\sigma_+\rho_-^{R*}]\xi_\perp\xi_\parallel\,, \qquad (4.27) \\
I_5 &= -\frac{2}{\sqrt{3}}\frac{N^2}{\sqrt{q^2}}m_B^3\,\beta_\ell\left(1-\frac{q^2}{m_B^2}\right)^2\mathrm{Re}[\sigma_-\rho_+^{L*}-\sigma_+\rho_+^{R*}]\,\xi_\perp\xi_\parallel\,, \\
I_6 &= -2N^2 m_B^2\,\beta_\ell\left(1-\frac{q^2}{m_B^2}\right)^2\mathrm{Re}[(\rho_-^L\rho_+^{L*})-(L\leftrightarrow R)]\,\xi_\perp^2\,, \\
I_7 &= \frac{2}{\sqrt{3}}\frac{N^2}{\sqrt{q^2}}m_B^3\,\beta_\ell\left(1-\frac{q^2}{m_B^2}\right)^2\mathrm{Im}[\sigma_-\rho_-^{L*}-\sigma_+\rho_-^{R*}]\,\xi_\perp\xi_\parallel\,, \\
I_8 &= -\frac{1}{\sqrt{3}}\frac{N^2}{\sqrt{q^2}}m_B^3\,\beta_\ell^2\left(1-\frac{q^2}{m_B^2}\right)^2\mathrm{Im}[\sigma_-\rho_+^{L*}+\sigma_+\rho_+^{R*}]\,\xi_\perp\xi_\parallel\,, \\
I_9 &= -N^2 m_B^2\,\beta_\ell^2\left(1-\frac{q^2}{m_B^2}\right)^2\mathrm{Im}[(\rho_-^L\rho_+^{L*})+(L\leftrightarrow R)]\,\xi_\perp^2\,.
\end{aligned}
$$

Here we have introduced the following combinations of short-distance Wilson coefficients

$$\rho_\mp^L(q^2) = \mathcal{C}_{9\mp}-\mathcal{C}_{10\mp}+\frac{2\,m_b m_B}{q^2}\mathcal{C}_7, \qquad (4.28)$$

$$\rho_\mp^R(q^2) = \mathcal{C}_{9\mp}+\mathcal{C}_{10\mp}+\frac{2\,m_b m_B}{q^2}\mathcal{C}_7, \qquad (4.29)$$

$$\sigma_\mp(q^2) = \mathcal{C}_{9-}\mp\mathcal{C}_{10+}+\frac{2\,m_b}{m_B}\mathcal{C}_7. \qquad (4.30)$$

One must note that in Eq. (4.27), the q^2-dependence of form factors $\xi_{\perp,\parallel}(q^2)$ and the Wilson coefficients $\rho_\mp^{L,R}(q^2)$ is not displayed for brevity. In the SM basis, one has $\rho_-^L=\rho_+^L$ and $\rho_-^R=\rho_+^R$.

From the angular distribution (4.26) one can construct observables such as the forward-backward asymmetry A_{FB}, the longitudinal polarization fraction F_L, and the differential decay width $d\Gamma/dq^2$ as functions of q^2. This can be done by weighted angular integrals of the four fold differential distribution given in Eq. (4.26) as following

$$\mathcal{O}_i(q^2) = \int d\cos\theta_\ell \; d\cos\theta_K \; d\phi \; \mathcal{W}_i(\theta_\ell, \theta_K, \phi) \, \frac{d^4\Gamma}{dq^2 d\cos\theta_\ell d\cos\theta_K d\phi}\,, \tag{4.31}$$

from which various angular observables can be extracted by the suitable choices for weight function $\mathcal{W}_i(\theta_\ell, \theta_K, \phi)$. The full differential decay width $d\Gamma/dq^2$ is simply obtained by choosing $\mathcal{W}_\Gamma = 1$ and given as

$$\frac{d\Gamma}{dq^2} \;=\; \frac{1}{4}(3I_1^c + 6I_1^s - I_2^c - 2I_2^s)\,. \tag{4.32}$$

The observable $A_{\rm FB}$ (normalized by differential decay width) is obtained using $\mathcal{W}_{A_{\rm FB}} = {\rm sgn}[\cos\theta_\ell]/(d\Gamma/dq^2)$ which gives,

$$A_{\rm FB}(q^2) \;=\; \frac{3I_6}{3I_1^c + 6I_1^s - I_2^c - 2I_2^s}\,. \tag{4.33}$$

The longitudinal polarization fraction F_L (normalized by differential decay width) is extracted with $\mathcal{W}_{F_L} = (3/2)(-3 + 7\cos^2\theta_K)/(d\Gamma/dq^2)$ and gives,

$$F_L(q^2) \;=\; \frac{3I_1^c - I_2^c}{3I_1^c + 6I_1^s - I_2^c - 2I_2^s}\,. \tag{4.34}$$

The transverse polarization fraction is $F_T = 1 - F_L$ by definition.

In Table 4.1 we present our q^2-bin averaged estimates of the observables mentioned above for $B \to K_2^* \mu^+\mu^-$ in different bins in the SM. The uncertainties come from $\Lambda_{\rm QCD}/m_b$ corrections, variation of renormalization scale μ, form factors and other numerical inputs. In Figure 4.1, the dependence of these three observables on dilepton invariant mass q^2 is shown. One can see that the branching ratio for the mode $B \to K_2^* \mu^+\mu^-$ is only one order of magnitude smaller than the one for $B \to K^* \mu^+\mu^-$. Therefore, $B \to K_2^* \mu^+\mu^-$ can be a viable search at LHCb in future. However, due to large uncertainties branching ratio, $A_{\rm FB}$ and F_L are not suitable for searches of new physics.

The study of the four-fold angular distribution allows you to construct numerous observables that can be measured by the LHCb. Due to factorization of long

q^2 (GeV^2)	$10^7 \times \langle \mathrm{BR}(B \to K_2^*\mu\mu)\rangle$	$\langle F_L\rangle$	$\langle A_{FB}\rangle$
$[0.1 - 1.0]$	0.204 ± 0.093	0.350 ± 0.199	0.092 ± 0.028
$[1.0 - 2.0]$	0.104 ± 0.056	0.691 ± 0.205	0.193 ± 0.127
$[2.0 - 4.0]$	0.197 ± 0.113	0.764 ± 0.188	0.066 ± 0.056
$[4.0 - 6.0]$	0.233 ± 0.124	0.684 ± 0.207	-0.135 ± 0.089
$[1.0 - 6.0]$	0.534 ± 0.292	0.714 ± 0.201	0.001 ± 0.018

Table 4.1: Our predictions for $\mathrm{BR}(B \to K_2^*\mu^+\mu^-)$, F_L, and A_{FB} in the SM.

and short-distance physics at large recoil Eq. (4.27), one can construct observables in terms of ratios where the form factors cancel. This makes them highly sensitive to NP. For the decay $B \to K^*(\to K\pi)\mu^+\mu^-$, such observables have been constructed (see, for example, [81] and references therein). from $B \to K^*\ell^+\ell^-$ [75, 78, 81], we consider following set of observables,

$$\langle P_1\rangle = \frac{1}{2}\frac{\int_{\rm bin} dq^2 I_3}{\int_{\rm bin} dq^2 I_2^s}, \qquad \langle P_4\rangle = \frac{\int_{\rm bin} dq^2 I_4}{\sqrt{-\int_{\rm bin} dq^2 I_2^c \int_{\rm bin} dq^2 I_2^s}}, \tag{4.35}$$

$$\langle P_2\rangle = \frac{1}{8}\frac{\int_{\rm bin} dq^2 I_6}{\int_{\rm bin} dq^2 I_2^s}, \qquad \langle P_5\rangle = \frac{\int_{\rm bin} dq^2 I_5}{2\sqrt{-\int_{\rm bin} dq^2 I_2^c \int_{\rm bin} dq^2 I_2^s}}, \tag{4.36}$$

$$\langle P_3\rangle = -\frac{1}{4}\frac{\int_{\rm bin} dq^2 I_9}{\int_{\rm bin} dq^2 I_2^s}, \qquad \langle P_6\rangle = \frac{\int_{\rm bin} dq^2 I_7}{2\sqrt{-\int_{\rm bin} dq^2 I_2^c \int_{\rm bin} dq^2 I_2^s}}. \tag{4.37}$$

where the soft form factor cancel at leading order in α_s and $\Lambda_{\rm QCD}/m_b$ making them suitable probe for new physics. The subleading corrections to them will be estimated following the discussions in section 4.3.

In the recent measurements of $B \to K(K^*)\ell^+\ell^-$ from LHCb [11, 19], the branching ratios of di-muon over di-electrons known as R_{K,K^*} shows significant deviation from their SM predictions $R_{K,K^*} \sim 1$ [18]. This hints towards violation of lepton flavor universality. Observation of the same pattern of deviation in the K and K^* mode is quite intriguing and has attracted a lot of attention recently.

A model independent analysis can be found in Ref. [124]. If NP is to account for these, such deviations should be seen in $B \to K_2^* \ell^+ \ell^-$ as well and needs to be studied. We define similar ratio for $B \to K_2^* \ell^+ \ell^-$,

$$R_{K_2^*} = \frac{\mathcal{B}(B \to K_2^* \mu\mu)}{\mathcal{B}(B \to K_2^* ee)} \,. \tag{4.38}$$

Having discussed all the observables, we now proceed with the numerical analysis of these observables in the SM and NP scenarios in the next section.

4.5 Numerical Analysis

In light of the recent flavor anomalies, several studies of global fits of Wilson coefficients to $b \to s\ell^+\ell^-$ data have been performed to understand the pattern of NP [24, 26, 27, 90–94]. These fits indicate that a negative contribution to the Wilson coefficient $\mathcal{C}_9^\mu$ can alleviate the tension. There are other scenarios as well which lead to similar fits. Following Ref. [100] we consider three of them (called S1, S2, S3) having largest pull $\left(\sqrt{\Delta\chi^2}\right)$,

1. S1 (NP in $\mathcal{C}_9$ only): $\mathcal{C}_9^{\mu,\mathrm{NP}} = -1.02$ for which the pull is 5.8σ.

2. S2 (NP in $\mathcal{C}_9$ and $\mathcal{C}_{10}$): $\mathcal{C}_9^{\mu,\mathrm{NP}} = -\mathcal{C}_{10}^{\mu,\mathrm{NP}} = -0.49$ for which the pull is 5.4σ.

3. S3 (NP in $\mathcal{C}_9$ and $\mathcal{C}_9'$): $\mathcal{C}_9^{\mu,\mathrm{NP}} = -\mathcal{C}_9'^{\,\mu,\mathrm{NP}} = -1.02$ for which the pull is 5.7σ.

where the numerical values of the WCs are the best fit value.

The main numerical results for SM and the three NP scenarios for all the angular observables considered in this work are collected in Section 4.6. The binned predictions for clean observables are displayed in Figure 4.2. To make binned average predictions of these observables, we have simultaneously varied the form factors, $\Lambda_{\mathrm{QCD}}/m_b$ corrections, and other inputs within their 1σ range. The resultant uncertainty on the observables corresponds to the union of uncertainties from all sources. For the observables defined in terms of ratios, we have performed the integration in numerator and denominator separately before taking ratio. Our analysis is restricted to low dilepton invariant mass region and we have considered q^2 bins lying in range $0.1 - 6.0$ GeV^2. This region is sufficiently below the radiative tail of the charmonium resonances $J/\psi, \psi'$. Therefore, apart from the perturbative $c\bar{c}$ contributions to the Wilson coefficients, the contributions from the charmonium resonances are not taken into account.

The branching fraction for $B \to K_2^* \mu^+ \mu^-$ in the SM is $\sim \mathcal{O}(10^{-7})$ (see Table 4.1). In all three NP scenarios, we have found consistently smaller central values for branching fraction compared to the SM value. This is attributed to the fact that the global analysis of $b \to s\ell^+\ell^-$ suggests destructive NP contribution to $\mathcal{C}_9^\mu$. For $A_{\rm FB}$ (F_L) we find slightly larger (smaller) central value in NP cases compared to the central SM value. However, as these observables ($d\Gamma/dq^2$, F_L and A_{FB}) at present have large theoretical errors, no striking deviation from the SM value is found. On the other hand, prospects for testing NP hypothesis in $b \to s\ell^+\ell^-$ in some clean observables $P_i(q^2)$ are promising.

The clean observable P_1, which depends on the angular coefficients I_3 and I_2, is of special interest due to its remarkable sensitivity to right-handed currents. The $(V - A)$ structure of the SM interactions implies that the $H_\pm$ helicities of the $B \to K_2^* \ell^+ \ell^-$ are suppressed leading to $|A_\parallel| \simeq |A_\perp|$. Therefore, P_1 is predicted to be zero in the SM. Similar characteristic is also shared by its $B \to K^*$ counterpart [26]. As shown in Figure 4.2, P_1 is consistent with zero in the SM and in two scenarios S1 and S2 (which assume NP in the left-handed currents only), while large deviation is found in S3 (which has nonzero $\mathcal{C}_9'$). The bands correspond to various uncertainties in theory. Since form factors cancel in the ratio, uncertainties are dominated by $\Lambda_{\rm QCD}/m_b$ corrections which are modelled by Eq. (4.25).

The observable P_2 is similar to forward-backward asymmetry $A_{\rm FB}$ but is much cleaner. We noted that the uncertainty is largely dominated by parametric errors including the scale μ. Similar to $A_{\rm FB}$, P_2 has significantly larger values in all three NP scenarios. The zero-crossing of P_2 are same as of A_{FB} since their numerators are same. They lie in the [2,4] GeV^2 and at the leading order is given by

$$q_0^2(P_2) \simeq -\frac{2\,\mathcal{C}_7}{\mathcal{C}_9 - (\mathcal{C}'_{10}/\mathcal{C}_{10})\,\mathcal{C}'_9}\,m_b\,m_B. \tag{4.39}$$

In order to obtain the above relation, we have used transversity amplitudes given in Eqs. (4.20)-(4.23) and assumed the WCs to be real. The expression is identical to the corresponding observable for $B \to K^*$ case. Note that the zero crossing $q_0^2(P_2)$ depends on $\mathcal{C}_9^{\ell(\prime)}$ and $\mathcal{C}_{10}^{\ell(\prime)}$ while it has no dependence on the mass of lepton in final state. Consequently, in the SM it has the same value for all three decay modes $B \to K_2^*\ell^+\ell^-$ $(\ell = e, \mu, \tau)$. Therefore the zero crossing $q_0^2(P_2)$ is a good test of lepton flavor universality (LFU) violating NP.

For P'_4 and P'_5, the largest deviations from the SM prediction are seen in S3, thereby showing sensitivity to NP contribution to right-handed currents. On the other hand, P_3 and P'_6 depend on $I_9(q^2)$ and $I_7(q^2)$ respectively. These two observables depend on imaginary part of $\rho_{\mp}^{L,R}(q^2)$ and $\sigma_{\mp}(q^2)$. The imaginary part of $\mathcal{C}_{9,7}^{\text{eff}}$ in SM is very tiny, and therefore the SM predictions for P_3 and P'_6 are highly suppressed. Since we consider only real WC from NP, these observables remain suppressed in all scenarios we have considered. Any deviation in these observables, if seen in experiments, will be a sign of CP-violating NP. Furthermore, the dominant uncertainty in P_3 comes from Λ_{QCD}/m_b. The errors in $P'_{4,5,6}$ are dominated by Λ_{QCD}/m_b corrections we well as parametric uncertainties.

Finally, in Figure 4.3 we present our determinations of the ratio $R_{K_2^*}$. Similar observables for $B \to K^{(*)}\ell^+\ell^-$ are predicted to be ~ 1 in the SM [18]. These ratios are exceptionally clean observables and the theoretical errors are at $\sim 1\%$ level only. This makes them an ideal candidate to probe NP. As mentioned earlier, the experimental determination of R_K and R_{K^*} are lower than the SM value, which could be interpreted as sign of NP. The measurement of $R_{K_2^*}$ can corroborate the deviations seen in R_K and R_K^*. In all three NP scenarios, $R_{K_2^*}$ is suppressed compared to the SM value. For S2, the deviations are largest while for S3 the suppression is relatively smaller as this scenario has a mixture of left-handed and right-handed currents. The bin averaged predictions for $R_{K_2^*}$ in the SM and NP cases are given in Section 4.6.

Parameter	Value	Source
m_B	5.279 GeV	[7]
$m_{K_2^*}$	1432.4 ± 1.3 MeV	[7]
$m_b^{\overline{\text{MS}}}$	4.20 GeV	[111]
m_b^{pole}	4.7417 GeV	[111]
m_c^{pole}	1.5953 GeV	[111]
$\lvert V_{ts}^* V_{tb}\rvert$	0.04088 ± 0.00055	[125]
$\alpha_s(\mu = 4.2\ \text{GeV})$	0.2233	[111]
$\alpha_e(\mu = 4.2\ \text{GeV})$	1/133.28	[111]
$Br(K_2^* \to K\pi)$	$(49.9 \pm 1.2)\%$	[7]

Table 4.2: The numerical inputs used in our analysis. The values of α_s, α_e, and $m_b^{\overline{\text{MS}}}$ at low scale $\mu = 2.1$ GeV and high scale $\mu = 8.4$ GeV are also used from Ref. [111].

	$\mu = 2.1$ GeV	$\mu = 4.2$ GeV	$\mu = 8.4$ GeV
$\mathcal{C}_1$	-0.4965	-0.2877	-0.1488
$\mathcal{C}_2$	1.0246	1.0101	1.0036
$\mathcal{C}_3$	-0.0143	-0.0060	-0.0027
$\mathcal{C}_4$	-0.1500	-0.0860	-0.0543
$\mathcal{C}_5$	0.0010	0.0004	0.0002
$\mathcal{C}_6$	0.0032	0.0011	0.0004
$\mathcal{C}_7$	-0.3782	-0.3361	-0.3036
$\mathcal{C}_8$	-0.2133	-0.1821	-0.1629
$\mathcal{C}_9$	4.5692	4.2745	3.8698
$\mathcal{C}_{10}$	-4.1602	-4.1602	-4.1602

Table 4.3: Values of SM Wilson coefficients taken from Ref. [111]

4.6 Results

4.6.1 Prediction of observables in the SM

Bin	P_1	P_2	P_3
$[0.1, 1]$	-0.001 ± 0.058	0.125 ± 0.004	0.0 ± 0.029
$[1, 2]$	-0.001 ± 0.058	0.431 ± 0.010	0.0 ± 0.029
$[2, 4]$	-0.001 ± 0.058	0.186 ± 0.041	0.0 ± 0.029
$[4, 6]$	-0.001 ± 0.058	-0.284 ± 0.028	0.0 ± 0.029
$[1, 6]$	-0.001 ± 0.058	0.001 ± 0.035	0.0 ± 0.029
Bin	P_4'	P_5'	P_6'
$[0.1, 1]$	-0.530 ± 0.016	0.615 ± 0.020	0.036 ± 0.039
$[1, 2]$	-0.178 ± 0.021	$0.235 \pm 0.0.031$	0.044 ± 0.021
$[2, 4]$	0.533 ± 0.037	-0.493 ± 0.048	0.039 ± 0.033
$[4, 6]$	0.886 ± 0.028	-0.869 ± 0.033	0.023 ± 0.053
$[1, 6]$	0.551 ± 0.033	-0.519 ± 0.041	0.033 ± 0.034
Bin	$BR\ (10^{-7})$	A_{FB}	F_L
$[0.1, 1]$	0.204 ± 0.093	0.092 ± 0.028	0.350 ± 0.199
$[1, 2]$	0.104 ± 0.056	0.193 ± 0.127	0.691 ± 0.205
$[2, 4]$	0.197 ± 0.113	0.066 ± 0.056	0.764 ± 0.188
$[4, 6]$	0.233 ± 0.124	-0.135 ± 0.089	0.684 ± 0.207
$[1, 6]$	0.534 ± 0.292	0.001 ± 0.018	0.714 ± 0.201

4.6.2 Prediction of observables in the NP scenario S1

Bin	P_1	P_2	P_3
$[0.1, 1]$	-0.001 ± 0.058	0.123 ± 0.004	0.0 ± 0.029
$[1, 2]$	-0.001 ± 0.058	0.409 ± 0.011	0.0 ± 0.029
$[2, 4]$	-0.001 ± 0.058	0.355 ± 0.026	0.0 ± 0.029
$[4, 6]$	-0.001 ± 0.058	-0.069 ± 0.036	0.0 ± 0.029

$[1, 6]$	-0.001 ± 0.058	0.181 ± 0.029	0.0 ± 0.029

Bin	P_4'	P_5'	P_6'
$[0.1, 1]$	-0.421 ± 0.012	0.731 ± 0.023	0.039 ± 0.046
$[1, 2]$	-0.101 ± 0.014	0.434 ± 0.028	0.045 ± 0.031
$[2, 4]$	0.478 ± 0.031	-0.165 ± 0.048	0.041 ± 0.018
$[4, 6]$	0.843 ± 0.028	-0.628 ± 0.041	0.027 ± 0.039
$[1, 6]$	0.509 ± 0.029	-0.236 ± 0.045	0.036 ± 0.020

Bin	$BR\ (10^{-7})$	A_{FB}	F_L
$[0.1, 1]$	0.197 ± 0.092	0.099 ± 0.026	0.298 ± 0.186
$[1, 2]$	0.094 ± 0.046	0.230 ± 0.127	0.610 ± 0.216
$[2, 4]$	0.167 ± 0.091	0.156 ± 0.109	0.706 ± 0.202
$[4, 6]$	0.191 ± 0.099	-0.035 ± 0.031	0.657 ± 0.211
$[1, 6]$	0.452 ± 0.235	0.091 ± 0.059	0.665 ± 0.210

4.6.3 Prediction of observables in the NP scenario S2

Bin	P_1	P_2	P_3
$[0.1, 1]$	-0.001 ± 0.058	0.110 ± 0.004	0.0 ± 0.029
$[1, 2]$	-0.001 ± 0.058	0.394 ± 0.011	0.0 ± 0.029
$[2, 4]$	-0.001 ± 0.058	0.300 ± 0.035	0.0 ± 0.029
$[4, 6]$	-0.001 ± 0.058	-0.210 ± 0.036	0.0 ± 0.029
$[1, 6]$	-0.001 ± 0.058	0.096 ± 0.035	0.0 ± 0.029

Bin	P_4'	P_5'	P_6'
$[0.1, 1]$	-0.544 ± 0.016	0.635 ± 0.020	0.035 ± 0.040
$[1, 2]$	-0.258 ± 0.017	0.321 ± 0.028	0.043 ± 0.025
$[2, 4]$	0.410 ± 0.039	-0.359 ± 0.052	0.042 ± 0.027
$[4, 6]$	0.845 ± 0.030	-0.821 ± 0.037	0.027 ± 0.050
$[1, 6]$	0.449 ± 0.035	-0.408 ± 0.046	0.036 ± 0.028

Bin	$BR\ (10^{-7})$	A_{FB}	F_L

$[0.1, 1]$	0.191 ± 0.090	0.087 ± 0.023	0.299 ± 0.187
$[1, 2]$	0.088 ± 0.044	0.206 ± 0.121	0.637 ± 0.213
$[2, 4]$	0.155 ± 0.088	0.112 ± 0.088	0.749 ± 0.192
$[4, 6]$	0.179 ± 0.096	-0.098 ± 0.068	0.690 ± 0.206
$[1, 6]$	0.422 ± 0.227	0.043 ± 0.035	0.699 ± 0.204

4.6.4 Prediction of observables in the NP scenario S3

Bin	P_1	P_2	P_3
$[0.1, 1]$	0.056 ± 0.058	0.123 ± 0.004	0.001 ± 0.029
$[1, 2]$	0.194 ± 0.056	0.404 ± 0.011	0.005 ± 0.028
$[2, 4]$	0.164 ± 0.058	0.339 ± 0.025	0.007 ± 0.026
$[4, 6]$	-0.033 ± 0.060	-0.065 ± 0.034	0.004 ± 0.026
$[1, 6]$	0.083 ± 0.059	0.174 ± 0.028	0.005 ± 0.026
Bin	P_4'	P_5'	P_6'
$[0.1, 1]$	-0.247 ± 0.008	0.876 ± 0.026	0.043 ± 0.052
$[1, 2]$	0.127 ± 0.016	0.694 ± 0.026	0.049 ± 0.034
$[2, 4]$	0.699 ± 0.035	0.207 ± 0.047	0.045 ± 0.020
$[4, 6]$	0.997 ± 0.030	-0.251 ± 0.045	0.030 ± 0.042
$[1, 6]$	0.704 ± 0.032	0.110 ± 0.046	0.039 ± 0.021
Bin	$BR\ (10^{-7})$	A_{FB}	F_L
$[0.1, 1]$	0.187 ± 0.090	0.103 ± 0.025	0.262 ± 0.174
$[1, 2]$	0.083 ± 0.039	0.252 ± 0.127	0.566 ± 0.218
$[2, 4]$	0.145 ± 0.075	0.172 ± 0.108	0.661 ± 0.210
$[4, 6]$	0.168 ± 0.083	-0.038 ± 0.031	0.607 ± 0.217
$[1, 6]$	0.396 ± 0.196	0.099 ± 0.059	0.617 ± 0.215

4.6.5 Prediction of $R_{K_2^*}$

Bin	SM	S1	S2	S3
$[0.1, 1]$	0.984 ± 0.005	0.945 ± 0.056	0.920 ± 0.051	0.963 ± 0.050
$[1, 2]$	0.997 ± 0.003	0.922 ± 0.092	0.855 ± 0.057	0.954 ± 0.090
$[2, 4]$	0.996 ± 0.002	0.868 ± 0.067	0.790 ± 0.015	0.898 ± 0.065
$[4, 6]$	0.996 ± 0.002	0.823 ± 0.026	0.762 ± 0.007	0.845 ± 0.024
$[1, 6]$	0.996 ± 0.002	0.859 ± 0.052	0.790 ± 0.014	0.885 ± 0.050

4.7 Summary and Discussion

In this chapter, we have performed an angular analysis of exclusive semileptonic decay $B \to K_2^*(\to K\pi)\mu^+\mu^-$. This decay is governed by the $b \to s\ell^+\ell^-$ FCNC transition at the quark level. Recently, about $2-3\ \sigma$ discrepancies in $b \to s\ell^+\ell^-$ transitions have recently been observed in $B \to K(K^*)\ell^+\ell^-$ decays. If these discrepancies are in fact due to NP, then similar anomalies are expected in $B \to K_2^*(\to K\pi)\mu^+\mu^-$ transitions as well.

The full angular distribution of $B \to K_2^*(\to K\pi)\mu^+\mu^-$ in the transversity basis, similar to $B \to K^*(\to K\pi)\mu^+\mu^-$, offers a large number of observables. In this study, we have worked in the limit of heavy quark $m_b \to \infty$ and large energy $E_{K_2^*} \to \infty$ where symmetry relations reduce the number of independent form factors from seven to two($\xi_\perp(q^2)$ and $\xi_\|(q^2)$). Using these symmetry relations, we have provided expressions for transversity amplitudes and have constructed new clean angular observables. The form factor dependence for these clean observables cancel at leading order in α_s and $\Lambda_{\rm QCD}/m_b$. The uncertainties due to the sub-leading corrections have also been included.

We have presented determinations of $B \to K_2^*(\to K\pi)\mu^+\mu^-$ decay rate, forward-backward asymmetry, longitudinal polarization fractions, and clean observables in the SM and several NP cases . The NP scenarios are motivated by the recent global fits to the $b \to s\ell^+\ell^-$ data. We have also considered the LFU violation sensitive observable $R_{K_2^*}$. The $B \to K_2^*(\to K\pi)\mu^+\mu^-$ decay may provide new and complementary information to $B \to K^*(K)\mu^+\mu^-$ in searches of NP.

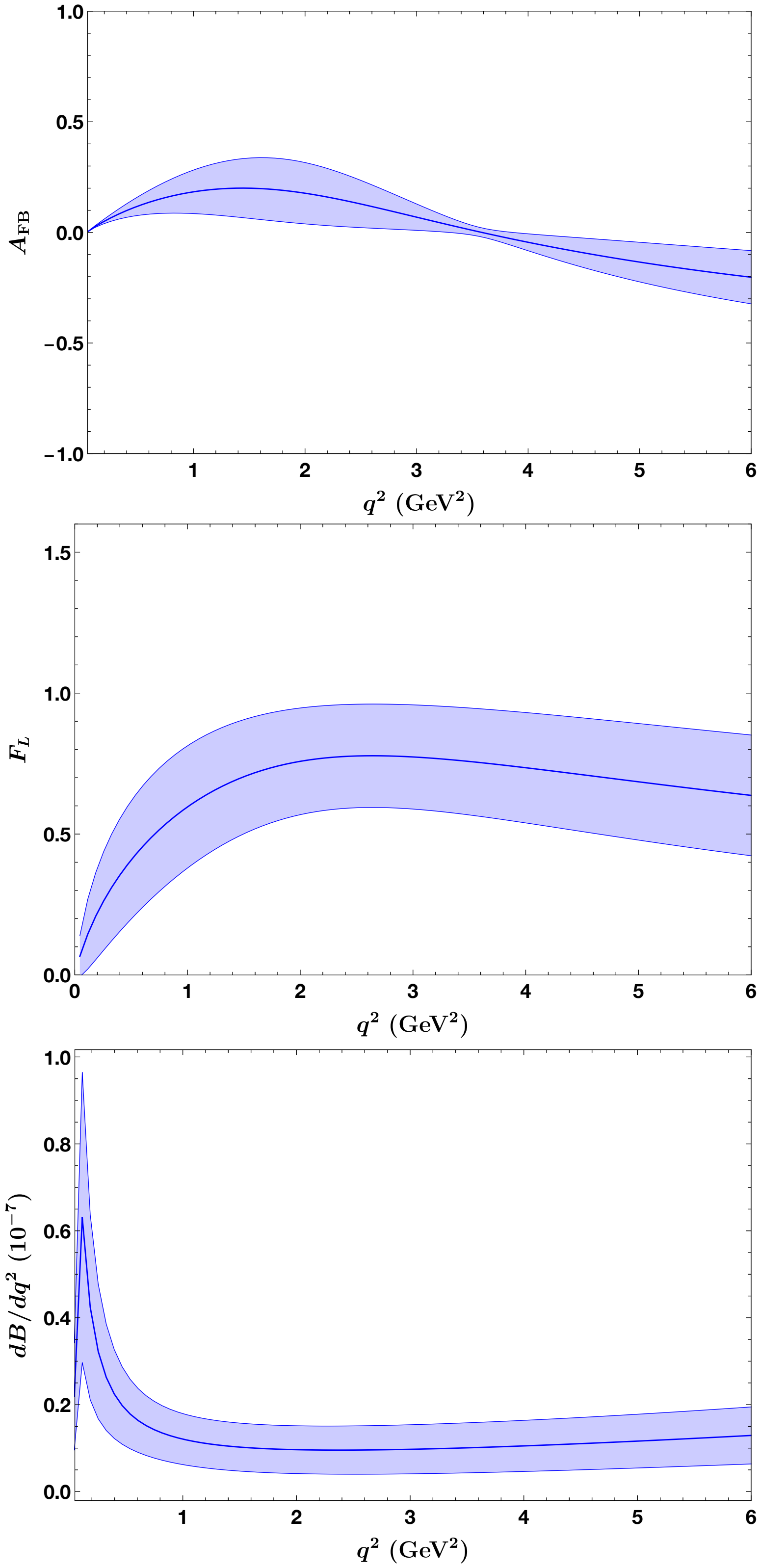

Figure 4.1: For $B \to K_2^* \mu^+ \mu^-$ in SM, the variation of $d\mathcal{B}/dq^2$, $A_{\rm FB}$, and F_L with q^2 is shown. The bands show estimates of uncertainties due to errors in various inputs (discussed in the text).

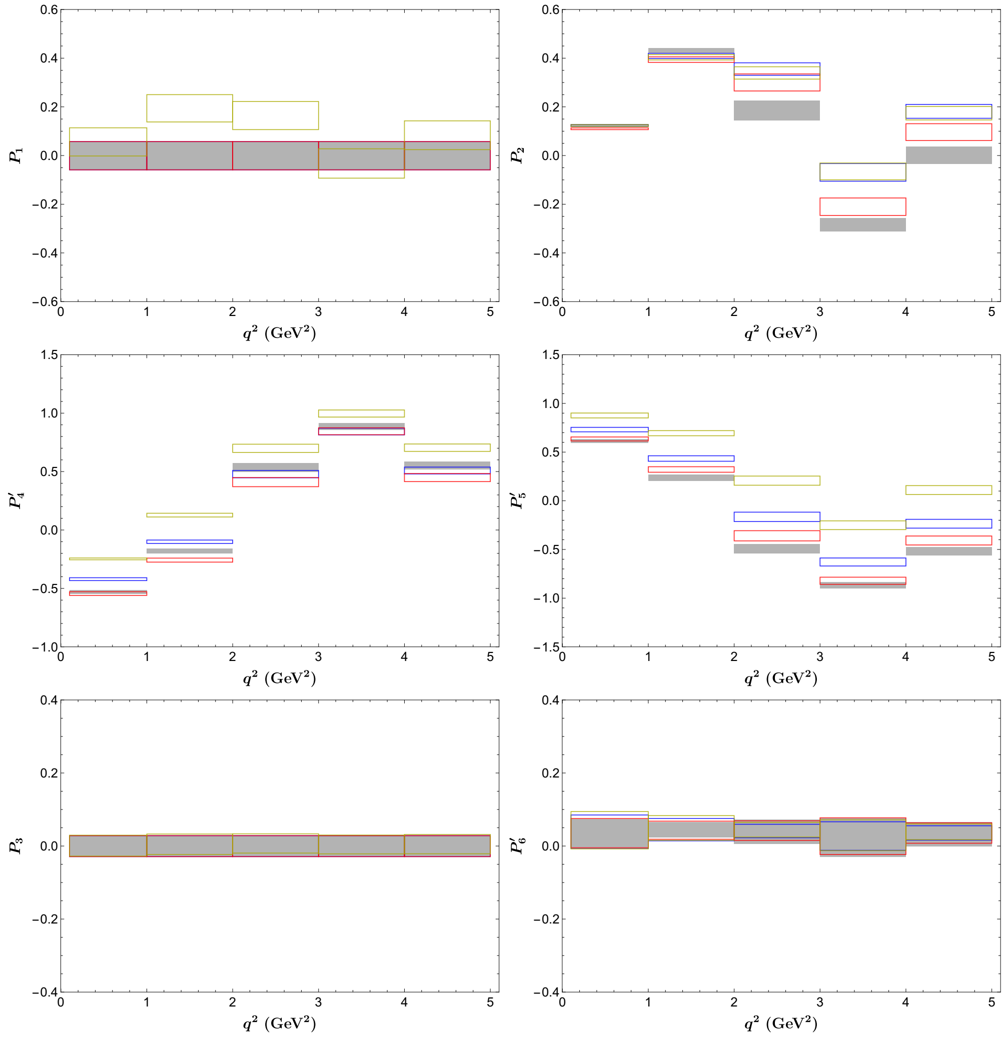

Figure 4.2: The clean observables $P_i^{(\prime)}(q^2)$ $(i = 1, 2, 3, 4, 5, 6)$ in different q^2 bins in the SM (grey shaded), S1 (blue), S2 (red), and S3 (yellow) are shown. The width of boxes denote the bin size, and height gives estimate of uncertainties.

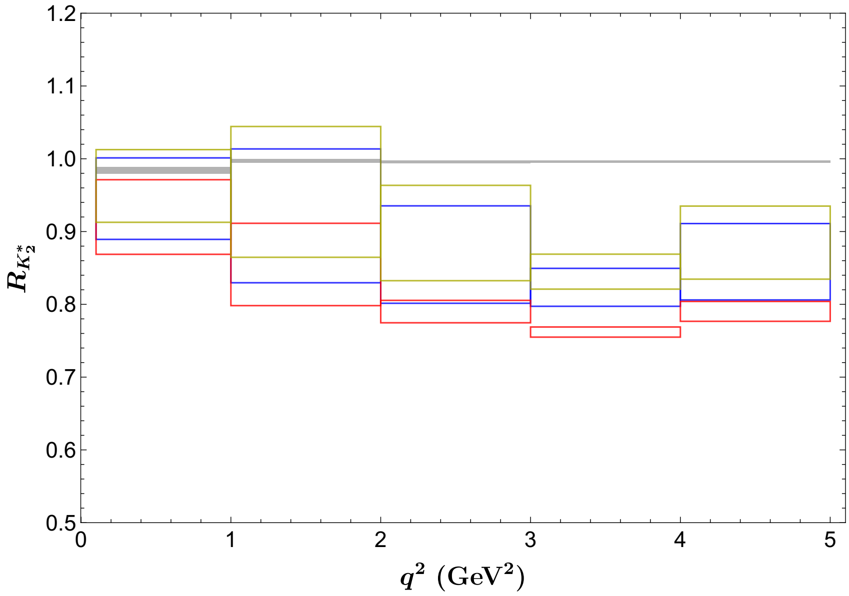

Figure 4.3: Binned predictions for $R_{K_2^*}$ in the SM (grey) and NP scenarios S1 (blue), S2 (red), and S3 (yellow).

Chapter 5

Four-lepton decay of charged B meson

Purely leptonic two body decays of B-mesons (for example $B^+ \to \ell^+\nu_\ell$ and $B_{s,d} \to \ell^+\ell^-$) occupy a very special place in the quest of probing physics beyond the standard model. This is due to the fact that these decays depend very minimally on the hadronic inputs. Unlike the semi-leptonic and non-leptonic decays which require a detailed knowledge of form factors and delicate non-factorizable contributions, these purely leptonic two body modes only depend on the B-meson decay constant, generically denoted by f_B. The charged current mediated decays $B^+ \to \ell^+\nu_\ell$ are especially simple as they proceed at the tree level and apart from the decay constant, are proportional to the CKM element V_{ub}, making them a good laboratory for extracting it. These modes however suffer from the helicity suppression:

$$\mathcal{BR}(B^+ \to \ell^+\nu_\ell) = \frac{G_F^2 m_B m_\ell^2}{8\pi}\left(1 - \frac{m_\ell^2}{m_B^2}\right)^2 f_B^2\,|V_{ub}|^2\,\tau_B \tag{5.1}$$

where G_F is the Fermi coupling constant, m_ℓ is the mass of lepton, m_B is the mass of B meson, τ_B and f_B is the lifetime and decay constant of B^+ meson respectively. Experimentally, $B^+ \to \tau^+\nu_\tau$ is measured to be $(1.09 \pm 0.24) \times 10^{-4}$ [126–129] which is in good agreement with the standard model expectation. The situation for the lighter leptons is more merky with the muon mode having an upper limit as measured by BaBar collaboration [130],

$$\mathcal{BR}(B^+ \to \mu^+\nu) < 1.0 \pm 10^{-6} \tag{5.2}$$

which is larger than the standard model predictions,

$$\mathcal{BR}(B^+ \to \mu^+\nu)|_{\rm SM} = (5.6 \pm 0.4) \times 10^{-7}. \tag{5.3}$$

Recent measurement by Belle suggests, $\mathcal{BR}(B^- \to \mu^-\bar{\nu}) \in [2.9, 10.7] \times 10^{-7}$ at 90% which is consistent with SM [131]. The electron mode seems rather difficult, at least at the moment.

A similar process with extra photon in the final state i.e., $B^+ \to \ell^+\nu_\ell\gamma$ can help since there is no longer the disadvantage of helicity suppression. At present, the Belle collaboration has provided the upper limit [132],

$$\mathcal{BR}(B^+ \to e^+\nu_e\gamma) < 4.3 \times 10^{-6}, \tag{5.4}$$

$$\mathcal{BR}(B^+ \to \mu^+\nu_\mu\gamma) < 3.4 \times 10^{-6}, \tag{5.5}$$

at 90% confidence limit. Theoretically, this decay mode has caught much attention as it can be used to probe a particular hadronic parameter, λ_B in the limit when energy of photon is very large in comparison to the scale of strong interactions [59, 133, 134]. Here, λ_B is the inverse moment of the B-meson light-cone distribution element and defined as,

$$\lambda_B^{-1}(\mu) = \int_0^\infty \frac{dk}{k}\phi_B^+(k,\mu) \tag{5.6}$$

where ϕ_B^+ is the distribution amplitude of B meson. λ_B is one of most important parameters used to define amplitude of hadronic decays. However, its value is very uncertain with estimates ranging from 200 MeV obtained using non-leptonic decays [72, 135] to 460 ± 110 MeV obtained from QCD sum rules [136]. On the experimental side, BaBar collaboration has provided two analyses which provides a lower limit as $\lambda_B > 699$ MeV [137] and $\lambda_B > 300$ MeV [138].

As Belle has already provided upper limits on the radiative decay, more precise results are expected after run of Belle II. However, it is tough to measure this decay at LHCb as it involves two neutral particles. On the other hand, if photon were to be on-shell and emits a lepton pair, then a final state of three charged leptons and a neutrino is measurable at LHCb. Infact, an upper limit has already been provided by LHCb in the region where the lowest of the muon pair mass combination is below 980 MeV [139],

$$\mathcal{BR}(B^+ \to \mu^+\mu^-\mu^+\nu_\mu) < 1.6 \times 10^{-8} \tag{5.7}$$

There exists only one study of this mode which is based on vector meson dominance (VMD) approach and predicts the branching ratio to be $\sim 3 \times 10^{-7}$ which is larger than the experimental limit [140]. In this chapter, a systematic study of four lepton decays of B mesons has been undertaken.

5.1 The Effective Amplitude

We consider the decay of charged B meson into 4 leptons i.e,

$$B^-(P_B) \to \ell^+(k_1)\ell^-(k_2)\ell'(p_1)\bar{\nu}_{\ell'}(p_2)$$

. The process can be approximated as $B \to \ell'\bar{\nu}_{\ell'}\gamma^*, \gamma^* \to \ell\ell$, where the contribution due to Z boson as propagator has been neglected. Under this approximation, the amplitude of decay of B meson to four leptons is given as:

$$\mathcal{A}(B^- \to \ell^+\ell^-\ell'\bar{\nu}_{\ell'}) = \mathcal{A}(B^- \to \ell'\bar{\nu}(p)\gamma^*(q)) \otimes \mathcal{A}(\gamma^*(q) \to \ell^+\ell^-). \tag{5.8}$$

Here, $p = p_1 + p_2$ and $q = k_1 + k_2$. The corresponding Feynman diagrams are given in Figure 5.1

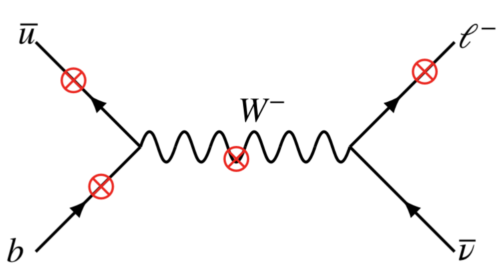

Figure 5.1: Feynman diagram for $B^- \to \ell^-\nu$ at tree level. The red circled-cross marks the possible emission of photon which further decays into a lepton pair

Theoretically, the extra photon can be emitted from any of the charged lines: the two quarks in the initial state, the charged lepton in the final state or from the W-propagator. Very clearly, the emission from the W-propagator will be suppressed by the W-boson mass and thus this contribution can be trivially neglected. Next consider the emission from the b-quark. This brings an additional b-quark propagator and for a hard photon emission, such a diagram is subleading in $1/m_b$. Thus working in the leading order in the heavy quark expansion, it is safe to ignore emission from the initial b-quark. We are thus left with only two possibilities: emission from the light up-quark and from the final state charged lepton. The emission from the final state charged lepton can be very easily written and is proportional to f_B.

Using [141] to write the amplitude corresponding to the radiative part in Eq. (5.8) followed by a lepton pair production,

$$\begin{aligned}\mathcal{A}(B \to \ell^+\ell^-(p)\ell'\nu(q)) = \frac{G_F}{\sqrt{2}} V_{ub} \frac{ie^2}{q^2} g^{\mu\nu} (\bar{\ell}\gamma^\nu \ell) \big[(\bar{\ell}'\Gamma_\rho \nu) \\ \int d^4x e^{iqx} \left\langle 0 | T\left\{ j_\mu^{em}(x) \bar{u}\Gamma^\rho b(0) \right\} | B(p+q) \right\rangle - \\ \int d^4x e^{iqx} \left\langle \ell'\bar{\nu}(p) | T\left\{ j_\mu^{em}(x) \bar{\ell}'\Gamma^\rho \nu(0) \right\} | 0 \right\rangle i f_B (p+q)^\rho \big]\end{aligned} \tag{5.9}$$

with $\Gamma^\mu = \gamma^\mu(1-\gamma_5)$ and $j_\mu^{em} = \sum_\psi Q_\psi \bar{\psi}\gamma_\mu \psi$ and Q_ψ is the electromagnetic charge of the corresponding Dirac field. The first term in Eq (5.9) is the contribution due to photon emission from the B meson while second term corresponds to photon emission from the charged lepton.

The second term can be calculated the solving the Feynman diagram which simplifies to,

$$-\frac{G_F}{\sqrt{2}} V_{ub} \frac{ie^2}{q^2} (\bar{\ell}\gamma^\mu \ell)(\bar{\ell}'\Gamma^\rho \nu) f_B \tag{5.10}$$

For the first term, the hadronic part doesn't factorize out trivially. Thus, it is written in terms of most generic form and then solved using conservation of the em current and equation of motion. Let us define,

$$T_{\mu\rho}(p,q) = i\int d^4x e^{iqx} \left\langle 0 | T\left\{ j_\mu^{em}(x)\bar{u}\Gamma_\rho b(0)\right\} | B^-(p+q) \right\rangle . \tag{5.11}$$

The most general form of $T_{\mu\rho}$ is terms of p and q is given as,

$$T_{\mu\rho}(p,q) = a g_{\mu\rho} + b p_\mu q_\rho + c q_\mu p_\rho + d p_\mu p_\rho + e q_\mu q_\rho + F_V \epsilon_{\rho\mu\lambda\sigma} p^\lambda q^\sigma . \tag{5.12}$$

Constraints on $T_{\mu\rho}$ can be obtained using the current conservation of em current i.e, $\partial^\mu j_\mu^{em} = 0$. This is done by differentiating the correlation function in the definition of $T_{\mu\rho}$, which gives,

$$q^\mu T_{\mu\rho} = i(p+q)_\rho f_B \tag{5.13}$$

Using the form of $T_{\mu\rho}$ from Eq. (5.12) in Eq. (5.13) implies,

$$a + b\ p.q + e\ q^2 = i f_B \tag{5.14}$$

$$c\ p.q + d\ p^2 = i f_B \tag{5.15}$$

Using these relations, $T_{\mu\rho}$ can be written in a general form,

$$T_{\mu\rho} = iF_A(g_{\mu\rho}\ p.q - p_\mu q_\rho) + \alpha\ g_{\mu\rho}\ p.q + \beta\ p_\mu q_\rho + F_e\ q^2\ g_{\mu\rho} \tag{5.16}$$

$$+ F_V\ \epsilon_{\rho\mu\lambda\sigma}\ p^\lambda q^\sigma + p_\rho \text{ terms..} \tag{5.17}$$

Again using the condition in Eq. (5.13) and comparing the coefficients of q_ρ,

$$F_e q^2 = i f_B - \alpha p.q. \tag{5.18}$$

Thus, $T_{\mu\rho}$ is reduced to,

$$\begin{aligned} T_{\mu\rho} =& iF_A(g_{\mu\rho}\ p.q - p_\mu q_\rho) + F_V\ \epsilon_{\rho\mu\lambda\sigma}\ p^\lambda q^\sigma + i f_B g_{\mu\rho} \\ & - (\alpha+\beta)\ g_{\mu\rho}\ p.q + \beta\ p_\mu q_\rho + p_\rho \text{ terms..} \end{aligned} \tag{5.19}$$

Redefining $F_A \to F_A + \beta$, the amplitude can be written as,

$$\mathcal{A} = \frac{G_F}{\sqrt{2}} V_{ub} \frac{e^2}{q^2} (\bar{\ell}\gamma^\mu \ell)(\bar{\ell}'\Gamma^\rho \nu) \Big[iF_A(g_{\mu\rho}\ p.q - p_\mu q_\rho) + F_V\ \epsilon_{\rho\mu\lambda\sigma}\ p^\lambda q^\sigma \Big], \tag{5.20}$$

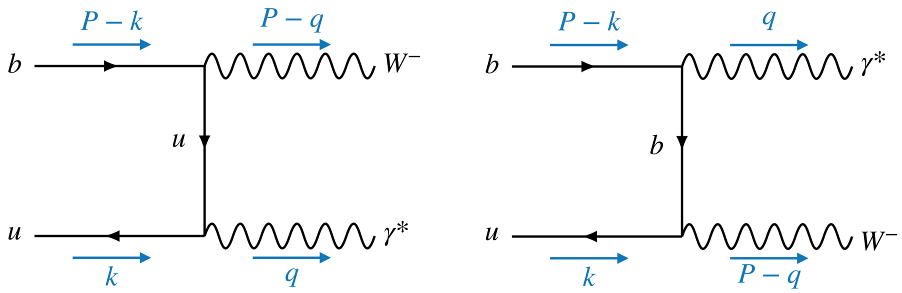

Figure 5.2: (a): photon emission from u quark, (b): photon emission from b quark

The term $if_B g_{\mu\rho}$ in the expression of $T_{\mu\rho}$ is the contact term and cancels the contribution of photon emission from charged lepton. Also, p_ρ terms when acted on the weak current gives contribution proportional to $m_{\ell'}$, and hence, these terms have been neglected since in this work ℓ' is considered to be either a muon or electron. In case of tau, the additional form factors which appear with p_ρ term in Eq. (5.16) need to be calculated. This is beyond the scope of the present study and will be studied in near future.

5.2 Form Factor

The form factors have been calculated for the process $B \to \gamma\ell\bar{\nu}_\ell$ [142]. The same procedure can now be used for the present purpose while keeping the q^2 non-zero. At the leading order, the two diagrams in Figure 5.2 contribute to the form factors. The second diagram in Figure 5.2 is suppressed due to the heavy quark as propagator and hence is not considered in this calculation. The amplitude corresponding to the first diagram is given by,

$$\mathcal{M} = -Q_u \bar{v}^s(k)\gamma_\mu \frac{1}{\not{q} - \not{k}}\gamma_\nu(1-\gamma_5)u^s(p-k), \tag{5.21}$$

where u and v are the spinor wave functions of the b and $\bar{u}$ quarks respectively; and Q_u is the electric charge of the u-quark. It is convenient to use light-cone coordinates ($l = (l_+, l_-, l_\perp)$) where,

$$l_\pm = \frac{l_0 \pm l_3}{\sqrt{2}}, \qquad\qquad l_\perp = (l_1, l_2). \tag{5.22}$$

The spectator quark is a soft-particle which implies that the components of momentum of u-quark scale as $k = (k_+, k_-, k_\perp) \sim (\lambda, \lambda, \lambda)$, while the momentum of the virtual photon scale as $q = (q_+, q_-, q_\perp = (\lambda, 1, \lambda^{1/2}))$. This implies,

$$(q-k)^2 \sim q^2 - 2q_- k_+ \tag{5.23}$$

while rest of the terms are suppressed by higher powers of λ. Consider the four-momentum of photon by $q^\mu = (E, q_\perp, -q_3)$. In the light-cone coordinates, photon momentum is defined as, $(q_+, q_-, q_\perp)$, where,

$$q_+ = \frac{1}{\sqrt{2}}(E - q_3) \qquad\qquad q_- = \frac{1}{\sqrt{2}}(E + q_3) \tag{5.24}$$

For hard-collinear photon, $q_- \sim \frac{1}{\sqrt{2}} E$ in the leading order. Thus, $2q_- k_+ \simeq 2Ek_+ + \mathcal{O}(1/E)$. Using this and following [142], the form factor at the leading order and in tree approximation reads,

$$F_{B\to\gamma^*}(q^2, p^2) = Q_u m_B f_B \int_0^\infty \frac{dk_+}{2\pi} \frac{\phi_B^+(k_+)}{2Ek_+ - q^2 - i\epsilon} \tag{5.25}$$

where, ϕ_B^+ is the light-cone distribution amplitude (LCDA) of the B-meson. Using the general dispersion relation for form factors and utilizing quark-hadron duality, the two form factors F_A and F_V at the leading order read,

$$\begin{aligned} F_V(p^2, q^2) = F_A(p^2, q^2) &= Q_u m_B f_B \int_{s_0/2E}^\infty dk_+ \frac{\phi_B^+(k_+)}{2Ek_+ - q^2 - i\epsilon} \\ &+ Q_u m_B f_B \int_0^{s_0/2E} dk_+ \frac{e^{-(2Ek_+ - m_\rho^2)/M^2}}{m_\rho^2 - q^2 - i\epsilon} \phi_B^+(k_+) \end{aligned} \tag{5.26}$$

where s_0 is a certain effective threshold, m_ρ is the mass of ρ meson, and M is the Borel parameter. The second term contains the soft contribution to the form factors, while the first one is the hard contribution. These terms are explicitly evaluated, carefully keeping the track of $i\epsilon$ and only at the very end, we set $\epsilon \to 0$.

We also consider the effect of symmetry breaking term which is large for the case of $B \to l\bar{\nu}\gamma$ when energy of photon (E_γ) is very small (~ 1.5 GeV). It is given by,

$$\Delta F_V = -\Delta F_A = \frac{Q_u f_B m_B}{(2E_\gamma)^2} \tag{5.27}$$

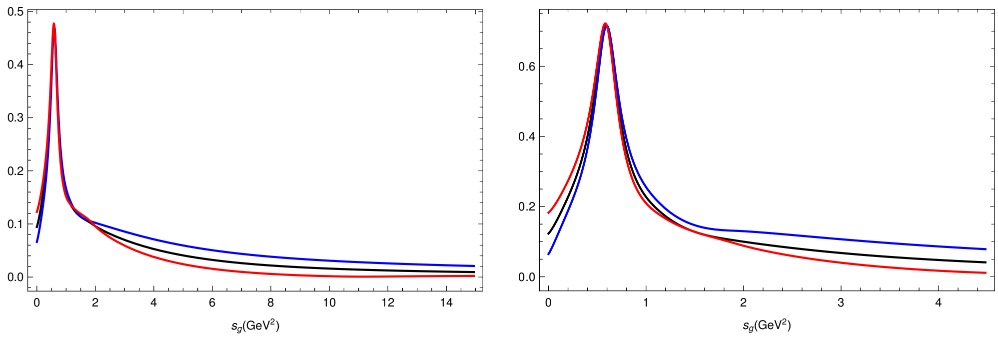

Figure 5.3: Black:Real part of $F_{A,V}$ at tree level, Blue: Real part of F_A including the symmetry breaking correction, Red: Real part of F_V including the symmetry breaking correction.The plots are shown for a fixed value of s_W,(a):s_W =1 GeV^2,(b): s_W =10 GeV^2

The form factors have been plotted in Figure 5.3 with and without the correction specified in Eq. (5.27). It is apparent from Figure 5.3 that contribution of this correction is very small for small values of $s_\gamma(< 2\ \text{GeV}^2)$ which is the region that actually contributes to the branching ratio. Thus, not much deviations are expected in the predictions of branching ratio even when this correction is included.

5.3 Numerical estimates and results

In this section, we discuss the kinematics and relations used for the process,

$$B^-(P_B) \to l^+(k_1)l^-(k_2)l'(p_1)\bar{\nu}_{l'}(p_2) \tag{5.28}$$

It is useful to introduce following combinations of the four momenta of final state particles;

$$P = k_1 + k_2; \qquad Q = k_1 - k_2 \qquad L = p_1 + p_2 \qquad M = p_1 - p_2 \tag{5.29}$$

The full kinematics of the decay can be described by five independent variables. The variables used in this word are defined as,

1. s_W, the effective mass squared of the $\ell'\bar{\nu}$ system.

$$s_W = (p_1 + p_2)^2 = L^2 \tag{5.30}$$

2. s_γ, the effective mass squared of the $\ell^+\ell^-$ system.

$$s_\gamma = (k_1 + k_2)^2 = P^2 \tag{5.31}$$

3. θ_γ is the angle of the ℓ^+ in the $\ell^+\ell^-$ center-of-mass system with respect to the $\ell^+\ell^-$ line of flight in B^- rest frame.

$$\cos\theta_\gamma = -\frac{\vec{Q}.\vec{L}}{|\vec{Q}|\;|\vec{L}|} \tag{5.32}$$

4. θ_W is the angle of the ℓ'^- in the $\ell'^-\bar{\nu}$ center-of-mass system with respect to the $\ell'^-\bar{\nu}$ line of flight in B^- rest frame.

$$\cos\theta_W = -\frac{\vec{M}.\vec{P}}{|\vec{M}|\;|\vec{P}|} \tag{5.33}$$

5. ϕ, the angle formed by the two lepton pairs.

$$\sin\phi = \frac{(\vec{P}\times\vec{M})\times(\vec{L}\times\vec{Q})}{|\vec{P}\times\vec{M}|\;|\vec{L}\times\vec{Q}|} \tag{5.34}$$

The range of these variables is,

$$4m_\ell^2 \leq s_\gamma \leq (M_B - m_{\ell'})^2 \tag{5.35}$$

$$m_{\ell'}^2 \leq s_W \leq (M_B - \sqrt{s_\gamma})^2 \tag{5.36}$$

$$0 \leq \theta_\gamma, \theta_W \leq \pi,\;\; 0 \leq \phi \leq 2\pi \tag{5.37}$$

The partial decay rate for the four body decay is given by,

$$d^5\Gamma = \frac{\pi\lambda(m_B^2, s_\gamma, s_W)^{1/2}}{(4\pi)^7} m_B^5 |\mathcal{M}|^2 d\Phi \tag{5.38}$$

where,

$$d\Phi = ds_\gamma\; ds_W\; d(\cos\theta_\gamma)\; d(\cos\theta_W)\; d\phi \tag{5.39}$$

is the phase space,

$$\lambda[a,b,c] = a^4 + b^4 + c^4 - 2(a^2b^2 + b^2c^2 + c^2a^2), \tag{5.40}$$

and A is the amplitude of the process defined in Eq. (5.20) for the case when $\ell \neq \ell'$. For $\ell = \ell'$, the amplitude gets modified to $A \to A - A'$, where A' is obtained from A through the substitution $p_1 \leftrightarrow k_2$, resulting in,

$$|\mathcal{M}|^2 = \frac{1}{2}\Big[\,|A|^2\, d\Phi + |A'|^2\, d\Phi' - (AA'^\dagger + A^\dagger A')d\Phi\Big] \tag{5.41}$$

[7]		
$m_B = 5279.25 \pm 0.17$ MeV	$f_B = 192.0 \pm 4.3$ MeV	$\lvert V_{ub}\rvert = (3.94 \pm 0.36)10^{-3}$
$G_F = 1.166 \times 10^{-5}$ GeV^{-2}	$\alpha_{em} = 1/137$	$M_\rho = 775.45 \pm 0.04$ MeV
$m_e = 0.511 \times 10^{-3}$ GeV	$m_\mu = 0.105$ GeV	$\tau_B = (1.641 \pm 0.008) \times 10^{-12}$ s
[142]		
$\lambda_B = [300 - 600]$ MeV	$s_0 = 1.5$ GeV^2	$M^2 = $ [1.0-2.0] GeV^2

Table 5.1: Values of input parameters

where Φ' corresponds to the phase space of final particles corresponding to amplitude A' and again is obtained through Φ with the modification $p_1 \leftrightarrow k_2$. The partial decay rate in Eq. (5.38) is valid for massless particles in the final states. To calculate the branching ratio, we consider B-meson distribution amplitudes (DAs) to be,

$$\phi_B^+(k) = \frac{k}{\lambda_B^2} e^{-k/\lambda_B} \tag{5.42}$$

where, λ_B is the first inverse moment of the B-meson. The input values used for the numerical estimates are given in Table 5.1. The total branching ratio for the process is obtained by integrating $d^5\Gamma$ over the full range (Table 5.2). The

	$e\bar{\nu}\mu\mu$ (10^{-11})	$e\bar{\nu}ee$ (10^{-8})	$\mu\bar{\nu}ee$ (10^{-9})	$\mu\bar{\nu}\mu\mu$ (10^{-11})
$\lambda_B = 0.2$	3.134 ± 0.649	1.027 ± 0.213	5.348 ± 1.149	6.171 ± 1.316
$\lambda_B = 0.4$	0.685 ± 0.142	0.386 ± 0.080	2.118 ± 0.452	1.331 ± 0.284
$\lambda_B = 0.6$	0.251 ± 0.052	0.199 ± 0.041	1.150 ± 0.245	0.479 ± 0.102

Table 5.2: Branching ratios for different values of λ_B for $M^2 = 1.5$ GeV^2. The error is due to errors is due to the input parameters.

profile of differential branching ratio of the mode $(B \to \mu\bar{\nu}ee)$ is shown in Figure

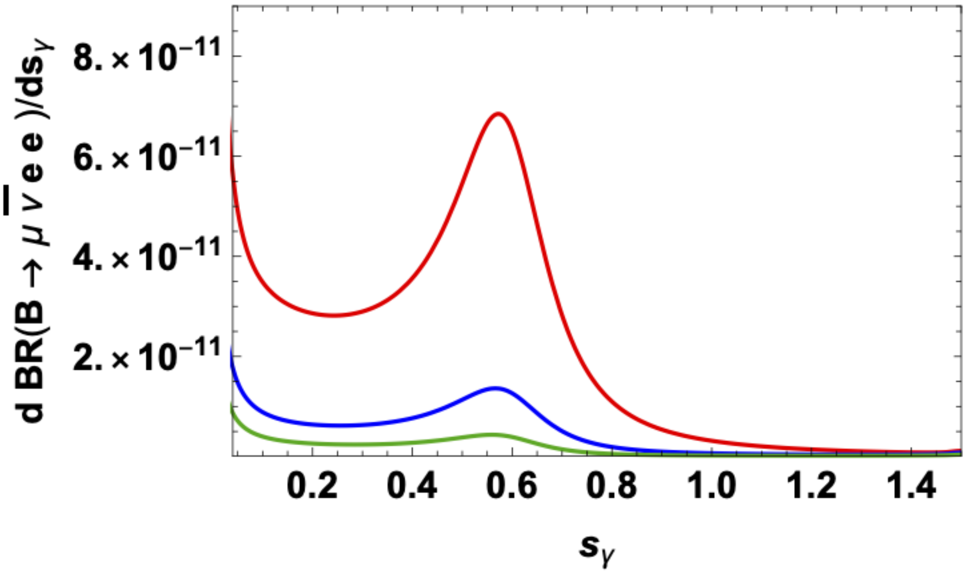

Figure 5.4: Red, Blue, and Green curves show the differential branching ratio corresponding to $\lambda_B = 200, 400, 600$ MeV and for $M^2 = 1.5$ GeV^2. The peak around M_ρ is because of the contribution of ρ meson to the form factor.

5.4. The contribution due to ρ meson produces a small peak and unlike a purely resonant contribution, the peak is tamed due to exponential weight factor is Eq. (5.26).

5.4 Conclusion

In this chapter, I have studied purely leptonic decay mode $B^- \to \ell^-\ell^+\ell'^-\bar{\nu}_{\ell'}$. LHCb collaboration has already provided the first upper limit on the branching ratio. A systematic study of such modes is lacking and first step towards achieving this goal has been taken. Employing the method of light cone sum rules, the relevant form factors, assuming all leptons in the final state to be massless, have been computed at the leading order. The results obtained are consistent with the experimental upper limit. A lot more work is required to have a better and precise theoretical prediction. In particular, higher twist contributions and inclusion of α_s corrections are called for. Also, additional form factors will be needed for massive leptons. In the absence of such calculations, the first steps taken in this chapter are important to have any meaningful comparison with the experimental numbers.

Chapter 6

Summary and Future Directions

Flavor physics provides a probe to test and improve our present knowledge of elementary particles and their interactions. Historically, the study of flavor transitions has played a crucial role in development of the Standard model (SM) as we study it today. One of the interesting and important features of SM is the Cabbibo-Kobayashi-Masakawa (CKM) matrix which governs the dynamics of quark interactions. The CKM matrix is also the source of CP violation within SM. Thus, the study of CKM matrix is important. Since there are no rules or theoretical constraints on the CKM elements, the best way is to measure it experimentally. For example, the measurement of strangely prolonged kaon lifetime lead to the idea of quark mixing in the first two generations. Later, the idea of unitarity of CKM matrix (for two generations at that time) led to the prediction of charm quark. Another historic milestone was the discovery of CP violation in kaon system. It was shown later that minimum three generations are required for CKM to have a CP violating phase. Thus, two new quarks as a doublet were proposed (t, b') which were later discovered in colliders. In the last 90's, CP violation was also measured in B meson system, which was much larger in comparison to that of kaon system making it experimentally more interesting. The recent discovery of the Higgs boson marks the completion of SM.

On the theoretical side, CP violation in B system has potential impact on study of baryon asymmetry in the universe, baryogenesis, and other cosmological data. However, it needed copious productions of B mesons which led to emergence of dedicated experiments to study B mesons. This includes B factories like Belle and BaBar which are based on e^-e^+ collisions at center of mass energy equal to the mass of $\Upsilon(4S)$, and colliders based on pp collisions like LHC. These experiments have accumulated large data over years and given interesting results. In this thesis I have focused on the recent anomalies in the semileptonic decays based on two channels, $b \to s\ell^+\ell^-$ and $b \to c\ell\nu_\ell$ at quark level.

A lot of theoretical work has been done on semileptonic B decays in last two decays. The four-body decay provides a plethora of observables which can be used to verify the SM and to understand the nature of new physics otherwise. The study of B decays is usually done in the domain of Heavy Quark Effective Theory (HQET). Using the effective theory, the long-distance and short-distance part of the dynamics is separated making the theoretical study cleaner and easier. The short-distance part contains the contribution of heavy particles (heavier than electroweak scale) as well as any potential contribution of new heavy particle. The long-distance part forms the hadronic matrix elements and their computation require non-perturbative QCD methods. The hadronic matrix elements can be parameterized in terms of form factors. In case of semileptonic decays, there are seven independent form factors which are functions of q^2, the invariant mass squared of the lepton pair. These form factors are computed using Light Cone Sum rules (LCSR) in low$-q^2$ region and lattice QCD in high$-q^2$ region. These QCD approaches generally rely on many assumptions and non-perturbative calculations which lead to large uncertainties in the theoretical predictions. A lot of work has been done in constructing observables such that they are less sensitive to hadronic uncertainties. The construction depends on the fact that in the large recoil limit (low q^2), the seven form factors can be expressed in terms of only two independent form factors which can be canceled by taking appropriate ratios. However, it is known that the corrections to these two form factors bring back the uncertainties in the definition of observables. Other useful observables are the ratios of branching ratio of different lepton pairs. Since hadronic inputs are same, they cancel to a large extent. Also, the ratio is a test of Lepton Flavour Universality (LFU). These observables have been studied by various experiments for processes, $B^+ \to K^+\ell^+\ell^-$, $B \to K^*\ell^+\ell^-$, $B_s \to \phi\mu^+\mu^-$, $\Lambda_b \to \Lambda_c\ell^+\ell^-$, $B \to D^{(*)}\ell^+\ell^-$, and $B_c \to J/\psi\ell^+\ell^-$. The LFU violating observables corresponding to all these modes show deviation with respect to SM. Other consistent anomaly is in P_5' in the decay channel $B \to K^*\ell^+\ell^-$. Global fits of the data for all $b \to s\ell\ell$ based channels point towards a degenerate new physics contribution. There are various combinations of values of WCs which can explain the data and exhibit almost same pull.

To understand the nature of new physics, better measurements are required on experimental side and improvement in the calculation of hadronic parameters on the theoretical side. In this thesis, one of the work aims in giving SM predictions for other semileptonic decay based on $b \to s\ell\ell$ transition, given by $B \to K_2^*\mu^+\mu^-$. Since this is also induced by $b \to s\ell\ell$ transition at quark level, the Wilson coefficients remain same. However, K_2^* is a tensor particle, thus the hadronic parameters are different in comparison to already studied semileptonic decays. As a result of it, the impact of the various global fit solutions is different on the observables of this mode and it can be used to break the degeneracy. In the work done during thesis, detailed predictions of all angular observables for the decay channel $B \to K_2^*\mu^+\mu^-$ have been provided for SM as well as new other new physics scenarios favoured by current global fits. Non-factorizable contributions have also been added systematically.

As there are deviations in the Flavour Changing Neutral Current (FCNC) $b \to s$, it is important to study $b \to d\ell\ell$ channel as well. Not much theoretical or experimental attention has been given to this channel as the branching ratio is CKM suppressed, it is very hard to measure it with the current experimental facilities. However, they should be measurable at Belle-II and LHCb run 3. At present, experimental value of branching ratio of two decay modes is available,

$$\mathcal{BR}(B \to \pi\mu^+\mu^-) = (2.3 \pm 0.6 \pm 0.1) \times 10^{-8} \tag{6.1}$$

$$\mathcal{BR}(B_s \to \bar{K}^*\mu^+\mu^-) = (3.0 \pm 1.0 \pm 0.2 \pm 0.3) \times 10^{-8} \tag{6.2}$$

Theoretically, the predictions of the decay $B \to \pi\ell^+\ell^-$ are available only. In the work done in the thesis, SM predictions of two decay modes based on $b \to d\ell\ell$ transition have been given, which are $B_s \to \bar{K}^*\ell^+\ell^-$ and $B \to \rho\ell^+\ell^-$ in the region $0.1 \leq q^2(\text{GeV}^2) \leq 6$. Detailed predictions for these two decay modes, including the non-factorizable contributions are given for the first time. For $B_s \to \bar{K}^*\mu^+\mu^-$ a comparison has been made in the predictions of observables for two sets of form factors. One set is based on LCSR calculation while other is based on an interpolation between LCSR calculation in low$-q^2$ region and lattice QCD calculation in high$-q^2$ region. The prediction of branching ratio for both the cases is in agreement with the LHCb results.

One important feature of the decays induced by $b \to d\ell\ell$ channel is that the CKM phase enters in the amplitude at leading order and thus some of the CP violating observables are expected to be measurable. There is another interesting and important feature in the case of $B \to \rho\ell\ell$. Since ρ is a CP eigenstate, the flavor of the decaying B meson can not be tagged. As a result, one has to take into account the $B^0 - \bar{B}^0$ mixing effects. This leads to a study of time dependent observables. In this work, tie-integrated observables have been considered only. Since the productions and tagging mechanism is different at B factories and LHC, the integration limit over time are different leading to somewhat different theoretical dependence on parameters defining $B - \bar{B}$ meson system. Taking this into account, predictions of observables for the mode $B \to \rho\ell\ell$ have been given separately for LHCb and B-factories.

Another channel under study is four lepton decay of charged B meson, $B^- \to \ell^-\ell^+\ell'^-\bar{\nu}$, where ℓ and ℓ' can be electron or muon. The leptonic and radiative B^- decays are known to be relevant to probe new physics and hadronic parameters respectively. Since the four lepton decay channels are potentially large background for such decays, its study is important. Such decays have not been measured yet, LHCb has provided an upper limit on one of the decays,

$$\mathcal{BR}(B^+ \to \mu^+\mu^-\mu^+\bar{\nu}) < 1.6 \times 10^{-8} \tag{6.3}$$

To date there is only one study of such modes which is based on an approximated calculation, which is already at odds with experimental limit. In this ongoing work, LCSR have been used to compute the relevant form factors at tree level. Using these, predictions for branching ratios for all of the decays with $\ell, \ell' \in \{e, \mu\}$ have been given. However, α_s corrections to form factors are yet to be calculated which are expected to be important.

Calculation of one more form factors is still required for the process $B^- \to \ell^+\ell^-\tau^-\bar{\nu}$. In the case of electron or muon, the extra form factor does not play any role as it is suppressed by a factor of m_ℓ/m_B. However, for τ it will be important and hence needs to be calculated.

There are several other directions that one can make progress in context of semileptonic B decays. The study of semileptonic channels where the final state hadron is a CP eigenstate is interesting and can be used to constrain several parameters related to $B_q - \bar{B}_q$ system. Another possibility is to look at the q^2 profiles of the angular observables of semileptonic decays. It has been pointed out in literature that zeroes of these observables are less sensitive to hadronic uncertainty. Similarly, the points (q^2) where profile of two observable cross each other can be used to extract information. These crossing points are equivalent to zeroes of linear combination of two observables and hence it should be measurable in experiments.

LHCb and Belle II are expected to collect a much larger data in future, allowing a precise study of different channels and observables. This would shed clear light on the discrepancies and deviations, if any. These measurements, in conjunction with measurements from Kaon, charm and tau experiments, coupled with direct searches at LHC would provide an unambiguous answer to many of the current puzzles. B-decays, particularly the leptonic and semileptonic decays, are expected to play an important role and one expects interesting times ahead.

Appendix

A Operators for Semileptonic B decays

The full operator basis for $b \to s\ell\ell$ transition is given as [51] ,

$$
\begin{aligned}
\mathcal{O}_1^u &= (\bar{s}_L \gamma_\mu T^a u_L)\,(\bar{u}_L \gamma^\mu T^a b_L) \\
\mathcal{O}_2^u &= (\bar{s}_L \gamma_\mu u_L)\,(\bar{u}_L \gamma^\mu b_L) \\
\mathcal{O}_1^c &= (\bar{s}_L \gamma_\mu T^a c_L)\,(\bar{c}_L \gamma^\mu T^a b_L) \\
\mathcal{O}_2^c &= (\bar{s}_L \gamma_\mu c_L)\,(\bar{c}_L \gamma^\mu b_L) \\
\mathcal{O}_3 &= (\bar{s}_L \gamma_\mu b_L) \sum_q (\bar{q} \gamma^\mu q) \\
\mathcal{O}_4 &= (\bar{s}_L \gamma_\mu T^a b_L) \sum_q (\bar{q} \gamma^\mu T^a q) \\
\mathcal{O}_5 &= (\bar{s}_L \gamma_{\mu_1} \gamma_{\mu_2} \gamma_{\mu_3} b_L) \sum_q (\bar{q} \gamma^{\mu_1} \gamma^{\mu_2} \gamma^{\mu_3} q) \\
\mathcal{O}_6 &= (\bar{s}_L \gamma_{\mu_1} \gamma_{\mu_2} \gamma_{\mu_3} T^a b_L) \sum_q (\bar{q} \gamma^{\mu_1} \gamma^{\mu_2} \gamma^{\mu_3} T^a q) \\
\mathcal{O}_7 &= \frac{e}{g_s^2} m_b\,(\bar{s}_L \sigma^{\mu\nu} b_R)\,F_{\mu\nu} \\
\mathcal{O}_8 &= \frac{1}{g_s} m_b\,(\bar{s}_L \sigma^{\mu\nu} T^a b_R)\,G^a_{\mu\nu} \\
\mathcal{O}_9 &= \frac{e^2}{g_s^2} (\bar{s}_L \gamma_\mu b_L) \sum_l \left(\bar{l} \gamma^\mu l\right) \\
\mathcal{O}_{10} &= \frac{e^2}{g_s^2} (\bar{s}_L \gamma_\mu b_L) \sum_l \left(\bar{l} \gamma^\mu \gamma_5 l\right) \\
\mathcal{O}_S &= \frac{e^2}{16\pi^2} m_b\,(\bar{s} P_R b)\,(\bar{\mu}\mu) \\
\mathcal{O}_S' &= \frac{e^2}{16\pi^2} m_b\,(\bar{s} P_L b)\,(\bar{\mu}\mu) \\
\mathcal{O}_P &= \frac{e^2}{16\pi^2} m_b\,(\bar{s} P_R b)\,(\bar{\mu}\gamma_5\mu) \\
\mathcal{O}_P' &= \frac{e^2}{16\pi^2} m_b\,(\bar{s} P_L b)\,(\bar{\mu}\gamma_5\mu)
\end{aligned}
\tag{A.4}
$$

B Auxiliary functions for Wilson Coefficients

Auxiliary functions used in the definitions of effective Wilson coefficients are given by [49],

$$
\begin{aligned}
A_7 =& \frac{4\pi}{\alpha_s(\mu)}\mathcal{C}_7(\mu) - \frac{1}{3}\mathcal{C}_3(\mu) - \frac{4}{9}\mathcal{C}_4(\mu) - \frac{20}{3}\mathcal{C}_5(\mu) - \frac{80}{9}\mathcal{C}_6(\mu) \\
A_8 =& \frac{4\pi}{\alpha_s(\mu)}\mathcal{C}_8(\mu) + \mathcal{C}_3(\mu) - \frac{1}{6}\mathcal{C}_4(\mu) + 20\mathcal{C}_5(\mu) - \frac{10}{3}\mathcal{C}_6(\mu) \\
A_9 =& \frac{4\pi}{\alpha_s(\mu)}\mathcal{C}_9(\mu) + \frac{4}{3}\mathcal{C}_3(\mu) + \frac{64}{9}\mathcal{C}_5(\mu) + \frac{64}{27}\mathcal{C}_6(\mu) \\
&+ \left[\frac{\xi_u + \xi_c}{-\xi_t}\left(\mathcal{C}_1(\mu)\gamma_{19}^{(0)} + \mathcal{C}_2(\mu)\gamma_{29}^{(0)}\right) + \sum_{i=3}^{6}\mathcal{C}_i(\mu)\gamma_{i9}^{(0)}\right]\ln\left(\frac{m_b}{\mu}\right) \\
A_{10} =& \frac{4\pi}{\alpha_s(\mu)}\mathcal{C}_{10}(\mu) \\
T_{9a} =& \frac{4}{3}\mathcal{C}_1(\mu) + \mathcal{C}_2(\mu) \\
T_{9b} =& 6\mathcal{C}_3(\mu) + 60\mathcal{C}_5(\mu) \\
U_9 =& -\frac{7}{2}\mathcal{C}_3(\mu) - \frac{2}{3}\mathcal{C}_4(\mu) - 38\mathcal{C}_5(\mu) - \frac{32}{3}\mathcal{C}_6(\mu) \\
W_9 =& -\frac{1}{2}\mathcal{C}_3(\mu) - \frac{2}{3}\mathcal{C}_4(\mu) - 8\mathcal{C}_5(\mu) - \frac{32}{3}\mathcal{C}_6(\mu)
\end{aligned}
\tag{B.5}
$$

C Angular Coefficients $I_i(q^2)$

The expressions of the angular coefficients in terms of transversity amplitudes are given as [74],

$$
\begin{aligned}
I_1^c &= (|A_{0L}|^2 + |A_{0R}|^2) + 8\frac{m_\ell^2}{q^2}\mathrm{Re}[A_{0L}A_{0R}^*] + 4\frac{m_\ell^2}{q^2}|A_t|^2, \\
I_1^s &= \frac{3}{4}\left(1 - \frac{4m_\ell^2}{3q^2}\right)[|A_{\perp L}|^2 + |A_{||L}|^2 + |A_{\perp R}|^2 + |A_{||R}|^2] + \frac{4m_\ell^2}{q^2}\mathrm{Re}[A_{\perp L}A_{\perp R}^* + A_{||L}A_{||R}^*], \\
I_2^c &= -\beta_\ell^2(|A_{0L}|^2 + |A_{0R}|^2), \quad I_2^s = \frac{1}{4}\beta_l^2(|A_{\perp L}|^2 + |A_{||L}|^2 + |A_{\perp R}|^2 + |A_{||R}|^2), \\
I_3 &= \frac{1}{2}\beta_l^2(|A_{\perp L}|^2 - |A_{||L}|^2 + |A_{\perp R}|^2 - |A_{||R}|^2) \\
I_4 &= \frac{1}{\sqrt{2}}\beta_\ell^2[\mathrm{Re}(A_{0L}A_{||L}^*) + \mathrm{Re}(A_{0R}A_{||R}^*], \quad I_5 = \sqrt{2}\beta_l[\mathrm{Re}(A_{0L}A_{\perp L}^*) - \mathrm{Re}(A_{0R}A_{\perp R}^*)], \\
I_6 &= 2\beta_\ell[\mathrm{Re}(A_{||L}A_{\perp L}^*) - \mathrm{Re}(A_{||R}A_{\perp R}^*)], \quad I_7 = \sqrt{2}\beta_\ell[\mathrm{Im}(A_{0L}A_{||L}^*) - \mathrm{Im}(A_{0R}A_{||R}^*)], \\
I_8 &= \frac{1}{\sqrt{2}}\beta_\ell^2[\mathrm{Im}(A_{0L}A_{\perp L}^*) + \mathrm{Im}(A_{0R}A_{\perp R}^*)], \quad I_9 = \beta_\ell^2[\mathrm{Im}(A_{||L}A_{\perp L}^*) + \mathrm{Im}(A_{||R}A_{\perp R}^*)],
\end{aligned}
\tag{C.6}
$$

where $\beta_\ell = \sqrt{1 - \frac{4m_\ell^2}{q^2}}$.

Bibliography

[1] S. L. Glashow, "*Partial-symmetries of weak interactions*," Nuclear Physics **22** (1961) no. 4, 579 – 588. http://www.sciencedirect.com/science/article/pii/0029558261904692.

[2] S. Weinberg, "*A Model of Leptons*,"Phys. Rev. Lett. **19** (Nov, 1967) 1264–1266. https://link.aps.org/doi/10.1103/PhysRevLett.19.1264.

[3] A. Salam, "*Weak and Electromagnetic Interactions*," Conf. Proc. **C680519** (1968) 367–377.

[4] P. W. Higgs, "*Broken Symmetries and the Masses of Gauge Bosons*," Phys. Rev. Lett. **13** (1964) 508–509. [,160(1964)].

[5] N. Cabibbo, "*Unitary Symmetry and Leptonic Decays*,"Phys. Rev. Lett. **10** (Jun, 1963) 531–533. https://link.aps.org/doi/10.1103/PhysRevLett.10.531.

[6] M. Kobayashi and T. Maskawa, "*CP-Violation in the Renormalizable Theory of Weak Interaction*,"Progress of Theoretical Physics **49** (02, 1973) 652–657, http://oup.prod.sis.lan/ptp/article-pdf/49/2/652/5257692/49-2-6 https://doi.org/10.1143/PTP.49.652.

[7] **Particle Data Group**, M. Tanabashi *et al.*, "*Review of Particle Physics*,"Phys. Rev. D **98** (Aug, 2018) 030001. https://link.aps.org/doi/10.1103/PhysRevD.98.030001.

[8] L. Wolfenstein, "*Parametrization of the Kobayashi-Maskawa Matrix*,"Phys.

Rev. Lett. **51** (Nov, 1983) 1945–1947.
https://link.aps.org/doi/10.1103/PhysRevLett.51.1945.

[9] C. Jarlskog, "*Commutator of the Quark Mass Matrices in the Standard Electroweak Model and a Measure of Maximal* CP *Nonconservation*," Phys. Rev. Lett. **55** (Sep, 1985) 1039–1042.
https://link.aps.org/doi/10.1103/PhysRevLett.55.1039.

[10] L. V. Silva, "*CP violation and the CKM matrix*,".
https://indico.cern.ch/event/684284/contributions/2952455/attachments/1719296/2774804/Vale_Silva_3.pdf.

[11] **LHCb**, R. Aaij *et al.*, "*Test of lepton universality using* $B^+ \to K^+\ell^+\ell^-$ *decays*," Phys. Rev. Lett. **113** (2014) 151601, arXiv:1406.6482.

[12] **LHCb**, R. Aaij *et al.*, "*Measurement of Form-Factor-Independent Observables in the Decay* $B^0 \to K^{*0}\mu^+\mu^-$," Phys. Rev. Lett. **111** (2013) 191801, arXiv:1308.1707.

[13] **LHCb**, R. Aaij *et al.*, "*Angular analysis of the* $B^0 \to K^{*0}\mu^+\mu^-$ *decay using 3 fb*$^{-1}$ *of integrated luminosity*," JHEP **02** (2016) 104, arXiv:1512.04442.

[14] **Belle**, A. Abdesselam *et al.*, "*Angular analysis of* $B^0 \to K^*(892)^0\ell^+\ell^-$," in *Proceedings, LHCSki 2016 - A First Discussion of 13 TeV Results: Obergurgl, Austria, April 10-15, 2016*. 2016. arXiv:1604.04042.

[15] **Belle**, S. Wehle *et al.*, "*Lepton-Flavor-Dependent Angular Analysis of* $B \to K^*\ell^+\ell^-$," Phys. Rev. Lett. **118** (2017) no. 11, 111801, arXiv:1612.05014.

[16] **ATLAS**, T. A. collaboration, "*Angular analysis of* $B_d^0 \to K^*\mu^+\mu^-$ *decays in* pp *collisions at* $\sqrt{s} = 8$ *TeV with the ATLAS detector*,".

[17] **CMS**, C. Collaboration, "*Measurement of the* P_1 *and* P_5' *angular parameters of the decay* $\mathrm{B}^0 \to \mathrm{K}^{*0}\mu^+\mu^-$ *in proton-proton collisions at* $\sqrt{s} = 8$ TeV,".

[18] M. Bordone, G. Isidori, and A. Pattori, "*On the Standard Model predictions for R_K and R_{K^*}*," Eur. Phys. J. **C76** (2016) no. 8, 440, arXiv:1605.07633.

[19] **LHCb**, R. Aaij *et al.*, "*Test of lepton universality with $B^0 \to K^{*0}\ell^+\ell^-$ decays*," JHEP **08** (2017) 055, arXiv:1705.05802.

[20] **Belle**, A. Abdesselam *et al.*, "*Test of lepton flavor universality in $B \to K^*\ell^+\ell^-$ decays at Belle*," arXiv:1904.02440.

[21] **LHCb**, R. Aaij *et al.*, "*Differential branching fraction and angular analysis of the decay $B_s^0 \to \phi\mu^+\mu^-$*," JHEP **07** (2013) 084, arXiv:1305.2168.

[22] **LHCb**, R. Aaij *et al.*, "*Angular analysis and differential branching fraction of the decay $B_s^0 \to \phi\mu^+\mu^-$*," JHEP **09** (2015) 179, arXiv:1506.08777.

[23] **LHCb**, R. Aaij *et al.*, "*Differential branching fraction and angular analysis of $\Lambda_b^0 \to \Lambda\mu^+\mu^-$ decays*," JHEP **06** (2015) 115, arXiv:1503.07138. [Erratum: JHEP09,145(2018)].

[24] W. Altmannshofer and D. M. Straub, "*Implications of $b \to s$ measurements*," in *Proceedings, 50th Rencontres de Moriond Electroweak Interactions and Unified Theories: La Thuile, Italy, March 14-21, 2015*, pp. 333–338. 2015. arXiv:1503.06199.

[25] B. Capdevila, A. Crivellin, S. Descotes-Genon, J. Matias, and J. Virto, "*Patterns of New Physics in $b \to s\ell^+\ell^-$ transitions in the light of recent data*," JHEP **01** (2018) 093, arXiv:1704.05340.

[26] S. Descotes-Genon, L. Hofer, J. Matias, and J. Virto, "*Global analysis of $b \to s\ell\ell$ anomalies*," JHEP **06** (2016) 092, arXiv:1510.04239.

[27] T. Hurth, F. Mahmoudi, and S. Neshatpour, "*On the anomalies in the latest LHCb data*," Nucl. Phys. **B909** (2016) 737–777, arXiv:1603.00865.

[28] D. Bigi, P. Gambino, and S. Schacht, "*$R(D^*)$, $|V_{cb}|$, and the Heavy Quark Symmetry relations between form factors*," JHEP **11** (2017) 061, arXiv:1707.09509.

[29] S. Jaiswal, S. Nandi, and S. K. Patra, "*Extraction of $|V_{cb}|$ from $B \to D^{(*)}\ell\nu_\ell$ and the Standard Model predictions of $R(D^{(*)})$*," JHEP **12** (2017) 060, arXiv:1707.09977.

[30] **ATLAS, CMS, LHCb**, E. Graverini, "*Flavour anomalies: a review*," J. Phys. Conf. Ser. **1137** (2019) no. 1, 012025, arXiv:1807.11373.

[31] **BaBar**, J. P. Lees *et al.*, "*Evidence for an excess of $\bar{B} \to D^{(*)}\tau^-\bar{\nu}_\tau$ decays*," Phys. Rev. Lett. **109** (2012) 101802, arXiv:1205.5442.

[32] **BaBar**, J. P. Lees *et al.*, "*Measurement of an Excess of $\bar{B} \to D^{(*)}\tau^-\bar{\nu}_\tau$ Decays and Implications for Charged Higgs Bosons*," Phys. Rev. **D88** (2013) no. 7, 072012, arXiv:1303.0571.

[33] **Belle**, M. Huschle *et al.*, "*Measurement of the branching ratio of $\bar{B} \to D^{(*)}\tau^-\bar{\nu}_\tau$ relative to $\bar{B} \to D^{(*)}\ell^-\bar{\nu}_\ell$ decays with hadronic tagging at Belle*," Phys. Rev. **D92** (2015) no. 7, 072014, arXiv:1507.03233.

[34] **Belle**, A. Abdesselam *et al.*, "*Measurement of the branching ratio of $\bar{B}^0 \to D^{*+}\tau^-\bar{\nu}_\tau$ relative to $\bar{B}^0 \to D^{*+}\ell^-\bar{\nu}_\ell$ decays with a semileptonic tagging method*," in *Proceedings, 51st Rencontres de Moriond on Electroweak Interactions and Unified Theories: La Thuile, Italy, March 12-19, 2016*. 2016. arXiv:1603.06711.

[35] **LHCb**, R. Aaij *et al.*, "*Measurement of the ratio of branching fractions $\mathcal{B}(\bar{B}^0 \to D^{*+}\tau^-\bar{\nu}_\tau)/\mathcal{B}(\bar{B}^0 \to D^{*+}\mu^-\bar{\nu}_\mu)$*," Phys. Rev. Lett. **115** (2015) no. 11, 111803, arXiv:1506.08614. [Erratum: Phys. Rev. Lett.115,no.15,159901(2015)].

[36] **Belle**, S. Hirose *et al.*, "*Measurement of the τ lepton polarization and $R(D^*)$ in the decay $\bar{B} \to D^*\tau^-\bar{\nu}_\tau$*," Phys. Rev. Lett. **118** (2017) no. 21, 211801, arXiv:1612.00529.

[37] **LHCb**, R. Aaij *et al.*, "*Measurement of the ratio of the $B^0 \to D^{*-}\tau^+\nu_\tau$ and $B^0 \to D^{*-}\mu^+\nu_\mu$ branching fractions using three-prong τ-lepton decays*," Phys. Rev. Lett. **120** (2018) no. 17, 171802, arXiv:1708.08856.

[38] **LHCb**, R. Aaij *et al.*, "*Measurement of the ratio of branching fractions $\mathcal{B}(B_c^+ \to J/\psi\tau^+\nu_\tau)/\mathcal{B}(B_c^+ \to J/\psi\mu^+\nu_\mu)$*," Phys. Rev. Lett. **120** (2018) no. 12, 121801, arXiv:1711.05623.

[39] A. Yu. Anisimov, I. M. Narodetsky, C. Semay, and B. Silvestre-Brac, "*The B_c meson lifetime in the light front constituent quark model*," Phys. Lett. **B452** (1999) 129–136, arXiv:hep-ph/9812514.

[40] V. V. Kiselev, "*Exclusive decays and lifetime of B_c meson in QCD sum rules*," arXiv:hep-ph/0211021.

[41] M. A. Ivanov, J. G. Korner, and P. Santorelli, "*Exclusive semileptonic and nonleptonic decays of the B_c meson*," Phys. Rev. **D73** (2006) 054024, arXiv:hep-ph/0602050.

[42] E. Hernandez, J. Nieves, and J. M. Verde-Velasco, "*Study of exclusive semileptonic and non-leptonic decays of B_c - in a nonrelativistic quark model*," Phys. Rev. **D74** (2006) 074008, arXiv:hep-ph/0607150.

[43] **Belle-II**, W. Altmannshofer *et al.*, "*The Belle II Physics Book*," arXiv:1808.10567.

[44] K. G. Wilson, "*Non-Lagrangian Models of Current Algebra*,"Phys. Rev. **179** (Mar, 1969) 1499–1512. https://link.aps.org/doi/10.1103/PhysRev.179.1499.

[45] K. G. Wilson and W. Zimmermann, "*Operator product expansions and composite field operators in the general framework of quantum field theory*," Commun. Math. Phys. **24** (1972) 87–106.

[46] W. Zimmermann, "*Normal products and the short distance expansion in the perturbation theory of renormalizable interactions*," Annals of Physics **77** (1973) no. 1, 570 – 601. http://www.sciencedirect.com/science/article/pii/0003491673904302.

[47] A. J. Buras, "*Weak Hamiltonian, CP violation and rare decays*," in *Probing the standard model of particle interactions. Proceedings, Summer School in*

Theoretical Physics, NATO Advanced Study Institute, 68th session, Les Houches, France, July 28-September 5, 1997. Pt. 1, 2, pp. 281–539. 1998. arXiv:hep-ph/9806471.

[48] H. H. Asatrian, H. M. Asatrian, C. Greub, and M. Walker, "*Two loop virtual corrections to $B \to X_s l^+ l^-$ in the standard model*," Phys. Lett. **B507** (2001) 162–172, arXiv:hep-ph/0103087.

[49] H. M. Asatrian, K. Bieri, C. Greub, and M. Walker, "*Virtual corrections and bremsstrahlung corrections to $b \to d l^+ l^-$ in the standard model*," Phys. Rev. **D69** (2004) 074007, arXiv:hep-ph/0312063.

[50] M. Gorbahn and U. Haisch, "*Effective Hamiltonian for non-leptonic $|\Delta F| = 1$ decays at NNLO in QCD*," Nucl. Phys. **B713** (2005) 291–332, arXiv:hep-ph/0411071.

[51] C. Bobeth, M. Misiak, and J. Urban, "*Photonic penguins at two loops and m_t dependence of $BR[B \to X_s l^+ l^-]$*," Nucl. Phys. **B574** (2000) 291–330, arXiv:hep-ph/9910220.

[52] H. H. Asatryan, H. M. Asatrian, C. Greub, and M. Walker, "*Calculation of two loop virtual corrections to $b \to s l^+ l^-$ in the standard model*," Phys. Rev. **D65** (2002) 074004, arXiv:hep-ph/0109140.

[53] S. Jäger and J. Martin Camalich, "*On $B \to V\ell\ell$ at small dilepton invariant mass, power corrections, and new physics*," JHEP **05** (2013) 043, arXiv:1212.2263.

[54] P. Ball and R. Zwicky, "*$B_{d,s} \to \rho, \omega, K^*, \phi$ decay form-factors from light-cone sum rules revisited*," Phys. Rev. **D71** (2005) 014029, arXiv:hep-ph/0412079.

[55] A. Bharucha, D. M. Straub, and R. Zwicky, "*$B \to V\ell^+\ell^-$ in the Standard Model from light-cone sum rules*," JHEP **08** (2016) 098, arXiv:1503.05534.

[56] M. Beneke, T. Feldmann, and D. Seidel, "*Systematic approach to exclusive $B \to V l^+ l^-$, $V\gamma$ decays*," Nucl. Phys. **B612** (2001) 25–58, arXiv:hep-ph/0106067.

[57] M. Beneke, T. Feldmann, and D. Seidel, "*Exclusive radiative and electroweak $b \to d$ and $b \to s$ penguin decays at NLO*," Eur. Phys. J. **C41** (2005) 173–188, arXiv:hep-ph/0412400.

[58] A. Khodjamirian, T. Mannel, A. A. Pivovarov, and Y. M. Wang, "*Charm-loop effect in $B \to K^{(*)}\ell^+\ell^-$ and $B \to K^*\gamma$*," JHEP **09** (2010) 089, arXiv:1006.4945.

[59] M. Beneke and T. Feldmann, "*Symmetry breaking corrections to heavy to light B meson form-factors at large recoil*," Nucl. Phys. **B592** (2001) 3–34, arXiv:hep-ph/0008255.

[60] **Belle**, Y. Sato *et al.*, "*Measurement of the branching ratio of $\bar{B}^0 \to D^{*+}\tau^-\bar{\nu}_\tau$ relative to $\bar{B}^0 \to D^{*+}\ell^-\bar{\nu}_\ell$ decays with a semileptonic tagging method*," Phys. Rev. **D94** (2016) no. 7, 072007, arXiv:1607.07923.

[61] A. Abdesselam *et al.*, "*Measurement of the τ lepton polarization in the decay $\bar{B} \to D^*\tau^-\bar{\nu}_\tau$*," arXiv:1608.06391.

[62] **LHCb**, R. Aaij *et al.*, "*First observation of the decay $B^+ \to \pi^+\mu^+\mu^-$*," JHEP **12** (2012) 125, arXiv:1210.2645.

[63] J.-J. Wang, R.-M. Wang, Y.-G. Xu, and Y.-D. Yang, "*The Rare decays $B^+(u) \to \pi^+ l^+ l^-, \rho^+ l^+ l^-, B^0(d) \to l^+ l^-$ in the R-parity violating supersymmetry*," Phys. Rev. **D77** (2008) 014017, arXiv:0711.0321.

[64] W.-S. Hou, M. Kohda, and F. Xu, "*Rates and asymmetries of $B \to \pi\ell^+\ell^-$ decays*," Phys. Rev. **D90** (2014) no. 1, 013002, arXiv:1403.7410.

[65] **LHCb**, R. Aaij *et al.*, "*Study of the rare B_s^0 and B^0 decays into the $\pi^+\pi^-\mu^+\mu^-$ final state*," Phys. Lett. **B743** (2015) 46–55, arXiv:1412.6433.

[66] F. Kruger, L. M. Sehgal, N. Sinha, and R. Sinha, "*Angular distribution and CP asymmetries in the decays $\bar{B} \to K^- \pi^+ e^- e^+$ and $\bar{B} \to \pi^- \pi^+ e^- e^+$*," Phys. Rev. **D61** (2000) 114028, arXiv:hep-ph/9907386. [Erratum: Phys. Rev.D63,019901(2001)].

[67] T. M. Aliev and M. Savci, "*Exclusive $B \to \pi e^+ e^-$ and $B \to \rho e^+ e^-$ decays in two Higgs doublet model*," Phys. Rev. **D60** (1999) 014005, arXiv:hep-ph/9812272.

[68] S. R. Choudhury and N. Gaur, "*SUSY effects on the exclusive semileptonic decays $B \to \pi \tau^+ \tau^-$ and $B \to \rho \tau^+ \tau^-$*," Phys. Rev. **D66** (2002) 094015, arXiv:hep-ph/0206128.

[69] R. N. Faustov and V. O. Galkin, "*Rare $B \to \pi l \bar{l}$ and $B \to \rho l \bar{l}$ decays in the relativistic quark model*," Eur. Phys. J. **C74** (2014) no. 6, 2911, arXiv:1403.4466.

[70] R. N. Faustov and V. O. Galkin, "*Rare B_s decays in the relativistic quark model*," Eur. Phys. J. **C73** (2013) no. 10, 2593, arXiv:1309.2160.

[71] Y.-L. Wu, M. Zhong, and Y.-B. Zuo, "*$B_s, D_s \to \pi, K, \eta, \rho, K^*, \omega, \phi$ Transition Form Factors and Decay Rates with Extraction of the CKM parameters $|V_{ub}|, |V_{cs}|, |V_{cd}|$*," Int. J. Mod. Phys. **A21** (2006) 6125–6172, arXiv:hep-ph/0604007.

[72] M. Beneke and M. Neubert, "*QCD factorization for $B \to PP$ and $B \to PV$ decays*," Nucl. Phys. **B675** (2003) 333–415, arXiv:hep-ph/0308039.

[73] P. Ball and V. M. Braun, "*Handbook of higher twist distribution amplitudes of vector mesons in QCD*," in *Continuous advances in QCD. Proceedings, 3rd Workshop, QCD'98, Minneapolis, USA, April 16-19, 1998*, pp. 125–141. 1998. arXiv:hep-ph/9808229.

[74] W. Altmannshofer, P. Ball, A. Bharucha, A. J. Buras, D. M. Straub, and M. Wick, "*Symmetries and Asymmetries of $B \to K^* \mu^+ \mu^-$ Decays in the Standard Model and Beyond*," JHEP **01** (2009) 019, arXiv:0811.1214.

[75] S. Descotes-Genon, J. Matias, M. Ramon, and J. Virto, "*Implications from clean observables for the binned analysis of $B \to K * \mu^+\mu^-$ at large recoil*," JHEP **01** (2013) 048, arXiv:1207.2753.

[76] F. Kruger and J. Matias, "*Probing new physics via the transverse amplitudes of $B^0 \to K^{*0}(\to K^-\pi^+)l^+l^-$ at large recoil*," Phys. Rev. **D71** (2005) 094009, arXiv:hep-ph/0502060.

[77] U. Egede, T. Hurth, J. Matias, M. Ramon, and W. Reece, "*New observables in the decay mode $\bar{B}_d \to \bar{K}^{*0}l^+l^-$*," JHEP **11** (2008) 032, arXiv:0807.2589.

[78] J. Matias, F. Mescia, M. Ramon, and J. Virto, "*Complete Anatomy of $\bar{B}_d \to \bar{K}^{*0}(\to K\pi)l^+l^-$ and its angular distribution*," JHEP **04** (2012) 104, arXiv:1202.4266.

[79] U. Egede, T. Hurth, J. Matias, M. Ramon, and W. Reece, "*New physics reach of the decay mode $\bar{B} \to \bar{K}^{*0}\ell^+\ell^-$*," JHEP **10** (2010) 056, arXiv:1005.0571.

[80] D. Becirevic and E. Schneider, "*On transverse asymmetries in $B \to K^*l^+l^-$*," Nucl. Phys. **B854** (2012) 321–339, arXiv:1106.3283.

[81] S. Descotes-Genon, T. Hurth, J. Matias, and J. Virto, "*Optimizing the basis of $B \to K^*ll$ observables in the full kinematic range*," JHEP **05** (2013) 137, arXiv:1303.5794.

[82] A. Ali, P. Ball, L. T. Handoko, and G. Hiller, "*A Comparative study of the decays $B \to (K, K^{*)}\ell^+\ell^-$ in standard model and supersymmetric theories*," Phys. Rev. **D61** (2000) 074024, arXiv:hep-ph/9910221.

[83] G. Kumar and N. Mahajan, "*$B \to K^*l^+l^-$: Zeroes of angular observables as test of standard model*," Phys. Rev. **D93** (2016) no. 5, 054041, arXiv:1412.2955.

[84] S. Descotes-Genon and J. Virto, "*Time dependence in $B \to V\ell\ell$ decays*," JHEP **04** (2015) 045, arXiv:1502.05509. [Erratum: JHEP07,049(2015)].

[85] **BaBar**, D. Boutigny *et al.*, "*The BABAR physics book: Physics at an asymmetric B factory*," in *Workshop on Physics at an Asymmetric B Factory (BaBar Collaboration Meeting) Pasadena, California, September 22-24, 1997*. 1998. http://www-public.slac.stanford.edu/sciDoc/docMeta.aspx?slacPubNumber=SLAC-R-504.

[86] **LHCb**, R. Aaij *et al.*, "*A new algorithm for identifying the flavour of B_s^0 mesons at LHCb*," JINST **11** (2016) no. 05, P05010, arXiv:1602.07252.

[87] **LHCb**, R. Aaij *et al.*, "*New algorithms for identifying the flavour of* B^0 *mesons using pions and protons*," Eur. Phys. J. **C77** (2017) no. 4, 238, arXiv:1610.06019.

[88] **LHCb**, R. Aaij *et al.*, "*Evidence for the decay $B_S^0 \to \overline{K}^{*0}\mu^+\mu^-$*," JHEP **07** (2018) 020, arXiv:1804.07167.

[89] S. Cheng, A. Khodjamirian, and J. Virto, "*$B \to \pi\pi$ Form Factors from Light-Cone Sum Rules with B-meson Distribution Amplitudes*," JHEP **05** (2017) 157, arXiv:1701.01633.

[90] S. Descotes-Genon, J. Matias, and J. Virto, "*Understanding the $B \to K^*\mu^+\mu^-$ Anomaly*," Phys. Rev. **D88** (2013) 074002, arXiv:1307.5683.

[91] W. Altmannshofer and D. M. Straub, "*New physics in $b \to s$ transitions after LHC run 1*," Eur. Phys. J. **C75** (2015) no. 8, 382, arXiv:1411.3161.

[92] W. Altmannshofer and D. M. Straub, "*New Physics in $B \to K^*\mu\mu$?*," Eur. Phys. J. **C73** (2013) 2646, arXiv:1308.1501.

[93] F. Beaujean, C. Bobeth, and D. van Dyk, "*Comprehensive Bayesian analysis of rare (semi)leptonic and radiative B decays*," Eur. Phys. J. **C74**

(2014) 2897, arXiv:1310.2478. [Erratum: Eur. Phys. J.C74,3179(2014)].

[94] T. Hurth and F. Mahmoudi, "*On the LHCb anomaly in B* $\to K^*\ell^+\ell^-$," JHEP **04** (2014) 097, arXiv:1312.5267.

[95] A. K. Alok, A. Dighe, S. Gangal, and D. Kumar, "*Continuing search for new physics in* $b \to s\mu\mu$ *decays: two operators at a time*," arXiv:1903.09617.

[96] M. Ciuchini, A. M. Coutinho, M. Fedele, E. Franco, A. Paul, L. Silvestrini, and M. Valli, "*New Physics in* $b \to s\ell^+\ell^-$ *confronts new data on Lepton Universality*," arXiv:1903.09632.

[97] G. D'Amico, M. Nardecchia, P. Panci, F. Sannino, A. Strumia, R. Torre, and A. Urbano, "*Flavour anomalies after the* R_{K^*} *measurement*," JHEP **09** (2017) 010, arXiv:1704.05438.

[98] A. Datta, J. Kumar, and D. London, "*The B Anomalies and New Physics in* $b \to se^+e^-$," arXiv:1903.10086.

[99] J. Aebischer, W. Altmannshofer, D. Guadagnoli, M. Reboud, P. Stangl, and D. M. Straub, "*B-decay discrepancies after Moriond 2019*," arXiv:1903.10434.

[100] M. Algueró, B. Capdevila, A. Crivellin, S. Descotes-Genon, P. Masjuan, J. Matias, and J. Virto, "*Addendum: "Patterns of New Physics in* $b \to s\ell^+\ell^-$ *transitions in the light of recent data" and "Are we overlooking Lepton Flavour Universal New Physics in* $b \to s\ell\ell$ *?"*," arXiv:1903.09578.

[101] **BaBar**, B. Aubert *et al.*, "*Measurement of the* $B^0 \to K_2^*(1430)^0\gamma$ *and* $B^+ \to K_2^*(1430)^+\gamma$ *branching fractions*," Phys. Rev. **D70** (2004) 091105, arXiv:hep-ex/0409035.

[102] **Belle**, S. Nishida *et al.*, "*Radiative B meson decays into* $K\pi\gamma$ *and* $K\pi\pi\gamma$ *final states*," Phys. Rev. Lett. **89** (2002) 231801, arXiv:hep-ex/0205025.

[103] **LHCb**, R. Aaij *et al.*, "*Differential branching fraction and angular moments analysis of the decay $B^0 \to K^+\pi^-\mu^+\mu^-$ in the $K^*_{0,2}(1430)^0$ region*," JHEP **12** (2016) 065, arXiv:1609.04736.

[104] S. Rai Choudhury, A. S. Cornell, G. C. Joshi, and B. H. J. McKellar, " *Analysis of the B $\to K_2^*(\to K\pi)l^+l^-$ decay*," Phys. Rev. **D74** (2006) 054031, arXiv:hep-ph/0607289.

[105] S. R. Choudhury, A. S. Cornell, and N. Gaur, "*Analysis of the $\bar{B} \to \bar{K}_2(1430)l^+l^-$ decay*," Phys. Rev. **D81** (2010) 094018, arXiv:0911.4783.

[106] H. Hatanaka and K.-C. Yang, "*Radiative and Semileptonic B Decays Involving the Tensor Meson K_2^*(1430) in the Standard Model and Beyond*," Phys. Rev. **D79** (2009) 114008, arXiv:0903.1917.

[107] H. Hatanaka and K.-C. Yang, "*Radiative and Semileptonic B Decays Involving Higher K-Resonances in the Final States*," Eur. Phys. J. **C67** (2010) 149–162, arXiv:0907.1496.

[108] W. Wang, "*B to tensor meson form factors in the perturbative QCD approach*," Phys. Rev. **D83** (2011) 014008, arXiv:1008.5326.

[109] H.-Y. Cheng, Y. Koike, and K.-C. Yang, "*Two-parton Light-cone Distribution Amplitudes of Tensor Mesons*," Phys. Rev. **D82** (2010) 054019, arXiv:1007.3541.

[110] Z.-G. Wang, "*Analysis of the $B \to K_2^*(1430), a_2(1320), f_2(1270)$ form-factors with light-cone QCD sum rules*," Mod. Phys. Lett. **A26** (2011) 2761–2782, arXiv:1011.3200.

[111] W. Detmold and S. Meinel, "*$\Lambda_b \to \Lambda\ell^+\ell^-$ form factors, differential branching fraction, and angular observables from lattice QCD with relativistic b quarks*," Phys. Rev. **D93** (2016) no. 7, 074501, arXiv:1602.01399.

[112] K.-C. Yang, "*B to Light Tensor Meson Form Factors Derived from Light-Cone Sum Rules*," Phys. Lett. **B695** (2011) 444–448, arXiv:1010.2944.

[113] I. Ahmed, M. J. Aslam, M. Junaid, and S. Shafaq, "*Model independent analysis of $B \to K_2^*(1430)\mu^+\mu^-$ decay*," JHEP **02** (2012) 045.

[114] M. Junaid, M. J. Aslam, and I. Ahmed, "*Complementarity of Semileptonic B to $K_2^*(1430)$ and $K^*(892)$ Decays in the Standard Model with Fourth Generation*," Int. J. Mod. Phys. **A27** (2012) 1250149, arXiv:1103.3934.

[115] R.-H. Li, C.-D. Lu, and W. Wang, "*Branching ratios, forward-backward asymmetries and angular distributions of $B \to K_2^* l^+ l^-$ in the standard model and new physics scenarios*," Phys. Rev. **D83** (2011) 034034, arXiv:1012.2129.

[116] C.-D. Lu and W. Wang, "*Analysis of $B \to K_J^*(\to K\pi)\mu^+\mu^-$ in the higher kaon resonance region*," Phys. Rev. **D85** (2012) 034014, arXiv:1111.1513.

[117] T. M. Aliev and M. Savci, "*$B \to K_2 \ell^+ \ell^-$ decay beyond the Standard Model*," Phys. Rev. **D85** (2012) 015007, arXiv:1109.2738.

[118] A. Paul and D. M. Straub, "*Constraints on new physics from radiative B decays*," JHEP **04** (2017) 027, arXiv:1608.02556.

[119] E. R. Berger, A. Donnachie, H. G. Dosch, and O. Nachtmann, "*Observing the odderon: Tensor meson photoproduction*," Eur. Phys. J. **C14** (2000) 673–682, arXiv:hep-ph/0001270.

[120] M. J. Dugan and B. Grinstein, "*QCD basis for factorization in decays of heavy mesons*," Phys. Lett. **B255** (1991) 583–588.

[121] J. Charles, A. Le Yaouanc, L. Oliver, O. Pene, and J. C. Raynal, "*Heavy to light form-factors in the heavy mass to large energy limit of QCD*," Phys. Rev. **D60** (1999) 014001, arXiv:hep-ph/9812358.

[122] M. Wirbel, B. Stech, and M. Bauer, "*Exclusive Semileptonic Decays of Heavy Mesons*," Z. Phys. **C29** (1985) 637.

[123] J. Gratrex, M. Hopfer, and R. Zwicky, "*Generalised helicity formalism, higher moments and the $B \to K_{J_K}(\to K\pi)\bar{\ell}_1\ell_2$ angular distributions*," Phys. Rev. **D93** (2016) no. 5, 054008, arXiv:1506.03970.

[124] G. Hiller and I. Nisandzic, "*R_K and R_{K^*} beyond the standard model*," Phys. Rev. **D96** (2017) no. 3, 035003, arXiv:1704.05444.

[125] **UTfit**. http://www.utfit.org/UTfit/ResultsSummer2014PostMoriondSM.

[126] **Belle Collaboration**, B. Kronenbitter *et al.*, "*Measurement of the branching fraction of $B^+ \to \tau^+\nu_\tau$ decays with the semileptonic tagging method*,"Phys. Rev. D **92** (Sep, 2015) 051102. https://link.aps.org/doi/10.1103/PhysRevD.92.051102.

[127] **Belle Collaboration**, K. Hara *et al.*, "*Evidence for $B^- \to \tau^-\overline{\nu}_\tau$ with a Hadronic Tagging Method Using the Full Data Sample of Belle*,"Phys. Rev. Lett. **110** (Mar, 2013) 131801. https://link.aps.org/doi/10.1103/PhysRevLett.110.131801.

[128] **BABAR Collaboration**, J. P. Lees *et al.*, "*Evidence of $B^+ \to \tau^+\nu$ decays with hadronic B tags*,"Phys. Rev. D **88** (Aug, 2013) 031102. https://link.aps.org/doi/10.1103/PhysRevD.88.031102.

[129] **BABAR Collaboration**, B. Aubert *et al.*, "*Search for $B^+ \to \ell^+\nu_\ell$ recoiling against $B^- \to D^0\ell^-\overline{\nu}X$*,"Phys. Rev. D **81** (Mar, 2010) 051101. https://link.aps.org/doi/10.1103/PhysRevD.81.051101.

[130] **BABAR Collaboration**, B. Aubert *et al.*, "*Search for the rare leptonic decays $B^+ \to l^+\nu_l$ ($l = e, \mu$)*,"Phys. Rev. D **79** (May, 2009) 091101. https://link.aps.org/doi/10.1103/PhysRevD.79.091101.

[131] **The Belle Collaboration**, A. Sibidanov *et al.*, "*Search for $B^- \to \mu^-\overline{\nu}_\mu$ Decays at the Belle Experiment*,"Phys. Rev. Lett. **121** (Jul, 2018) 031801. https://link.aps.org/doi/10.1103/PhysRevLett.121.031801.

[132] M. Gelb, "*$B \to l\nu\gamma$ at Belle*,". 20 min.

[133] A. G. Grozin and M. Neubert, "*Asymptotics of heavy meson form-factors*," Phys. Rev. **D55** (1997) 272–290, arXiv:hep-ph/9607366.

[134] S. W. Bosch, R. J. Hill, B. O. Lange, and M. Neubert, "*Factorization and Sudakov resummation in leptonic radiative B decay*," Phys. Rev. **D67** (2003) 094014, arXiv:hep-ph/0301123.

[135] M. Beneke, T. Huber, and X.-Q. Li, "*NNLO vertex corrections to non-leptonic B decays: Tree amplitudes*," Nucl. Phys. **B832** (2010) 109–151, arXiv:0911.3655.

[136] V. M. Braun, D. Yu. Ivanov, and G. P. Korchemsky, "*The B meson distribution amplitude in QCD*," Phys. Rev. **D69** (2004) 034014, arXiv:hep-ph/0309330.

[137] **BaBar**, B. Aubert *et al.*, "*Search for the radiative leptonic decay $B^+ \to \gamma\ell^+\nu_l$*," arXiv:0704.1478.

[138] **BaBar**, B. Aubert *et al.*, "*A Model-independent search for the decay $B^+ \to l^+\nu_l\gamma$*," Phys. Rev. **D80** (2009) 111105, arXiv:0907.1681.

[139] **LHCb**, R. Aaij *et al.*, "*Search for the rare decay $B^+ \to \mu^+\mu^-\mu^+\nu_\mu$*," Submitted to: Eur. Phys. J. (2018) , arXiv:1812.06004.

[140] A. V. Danilina and N. V. Nikitin, "*Four-Leptonic Decays of Charged and Neutral B Mesons within the Standard Model*," Phys. Atom. Nucl. **81** (2018) no. 3, 347–359. [Yad. Fiz.81,no.3,331(2018)].

[141] A. Khodjamirian and D. Wyler, "*Counting contact terms in $B \to V\gamma$ decays*," arXiv:hep-ph/0111249.

[142] V. M. Braun and A. Khodjamirian, "*Soft contribution to $B \to \gamma\ell\nu_\ell$ and the B-meson distribution amplitude*," Phys. Lett. **B718** (2013) 1014–1019, arXiv:1210.4453.